中央研究院
天文及天文物理研究所
ACADEMIA SINICA
Institute of Astronomy and Astrophysics

The splashback radius and the radial velocity profiles of galaxy clusters in IllustrisTNG

Expanding the boundaries of dark matter halo

Shanghai Jiaotong University

Michele Pizzardo

May 26th, 2025

Dynamical regimes of galaxy clusters

- Turnaround
- Infall
- Orbiting

Dynamical regimes of galaxy clusters

- Turnaround
- Infall
- Orbiting

Average $\mathrm{v}_{\mathrm{rad}}$ of the 1697 TNG clusters with $M_{200c} > 10^{14}\mathrm{M}_{\odot}$ and $0.01 \leq z \leq 1.04$

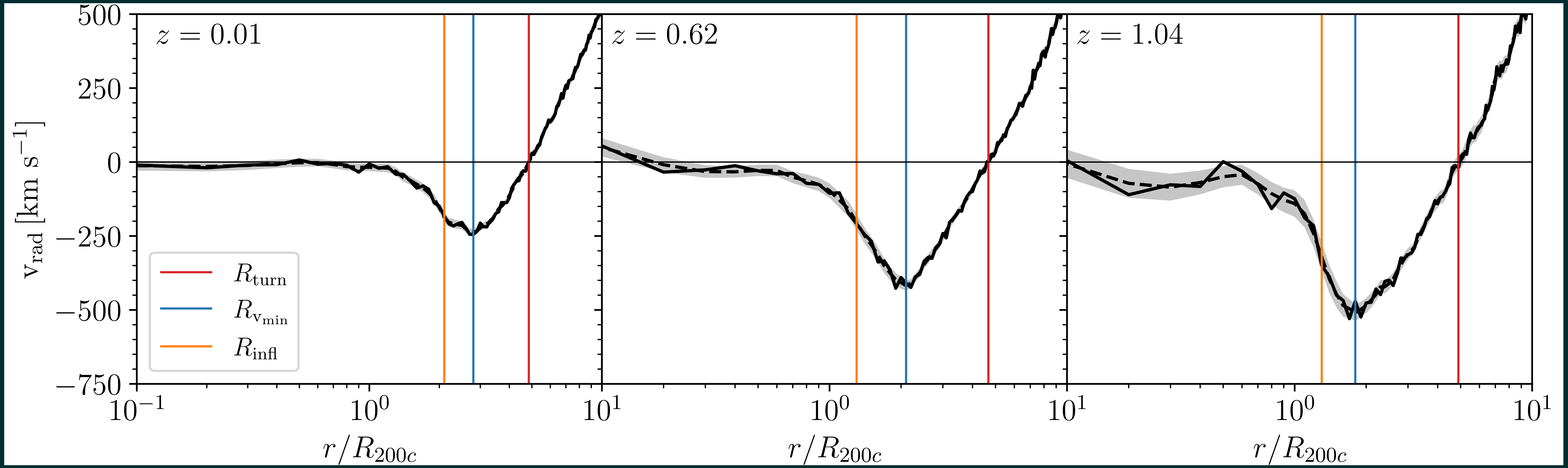

Dynamical regimes of galaxy clusters

- Turnaround
- Infall
- Orbiting

Average $\mathrm{v_{rad}}$ of the 1697 TNG clusters with $M_{200c} > 10^{14}\mathrm{M_\odot}$ and $0.01 \leq z \leq 1.04$

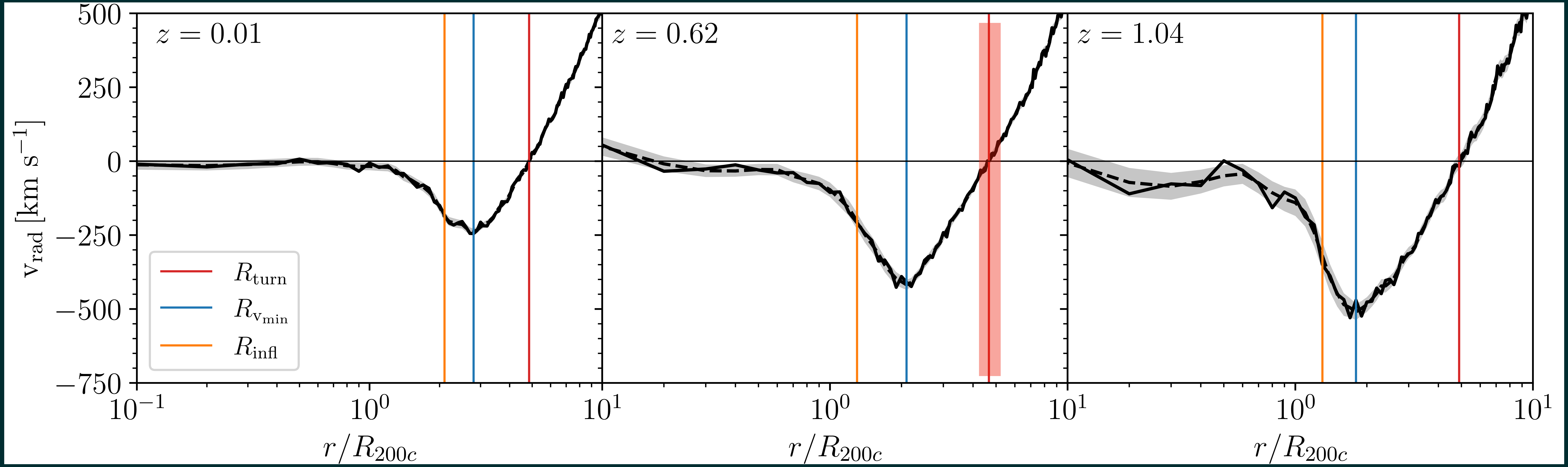

Dynamical regimes of galaxy clusters

- Turnaround
- Infall
- Orbiting

Average $\mathrm{v_{rad}}$ of the 1697 TNG clusters with $M_{200c} > 10^{14}\mathrm{M}_\odot$ and $0.01 \leq z \leq 1.04$

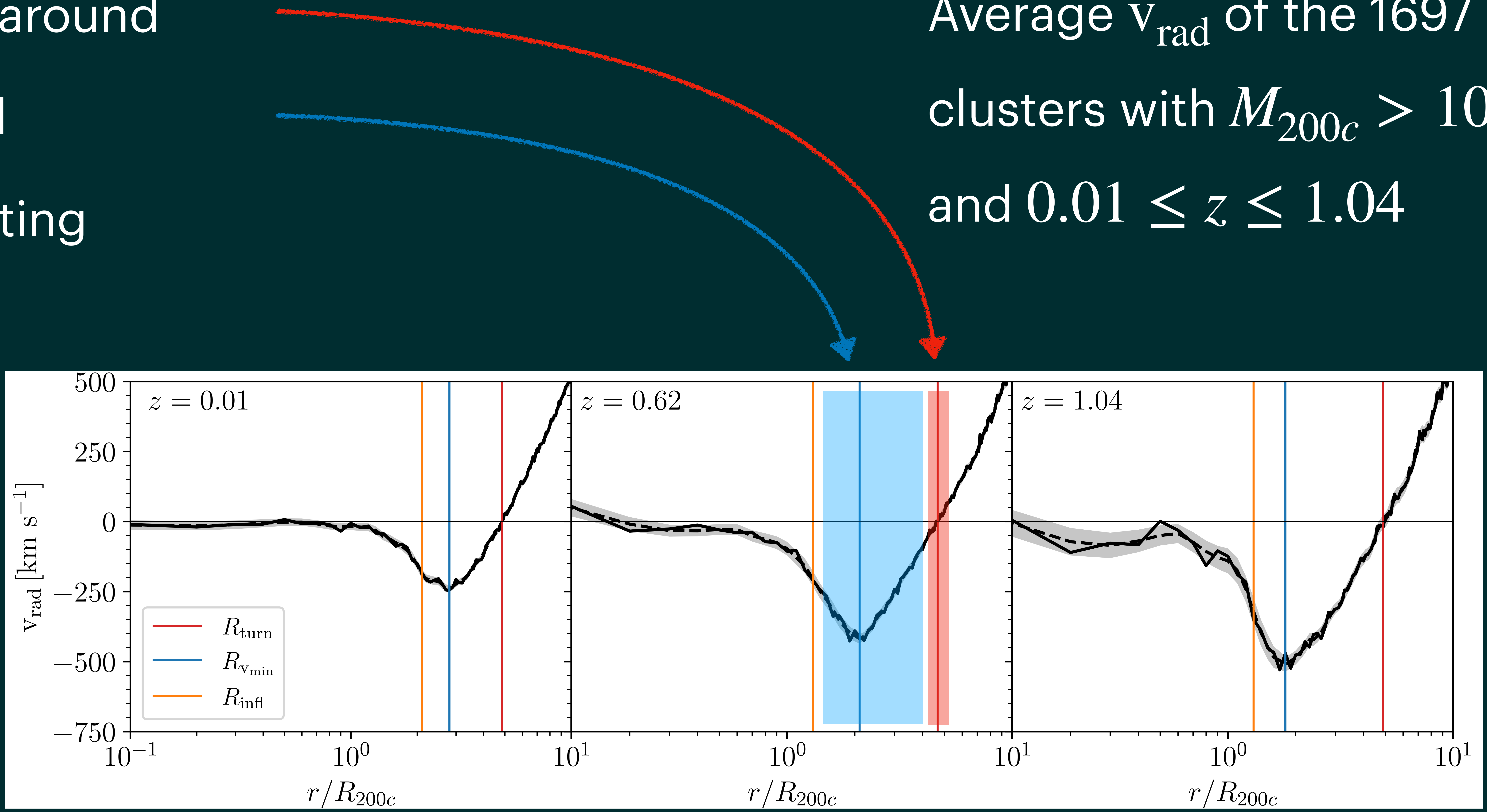

Dynamical regimes of galaxy clusters

- Turnaround
- Infall
- Orbiting

Average $\mathrm{v_{rad}}$ of the 1697 TNG clusters with $M_{200c} > 10^{14}\mathrm{M}_\odot$ and $0.01 \leq z \leq 1.04$

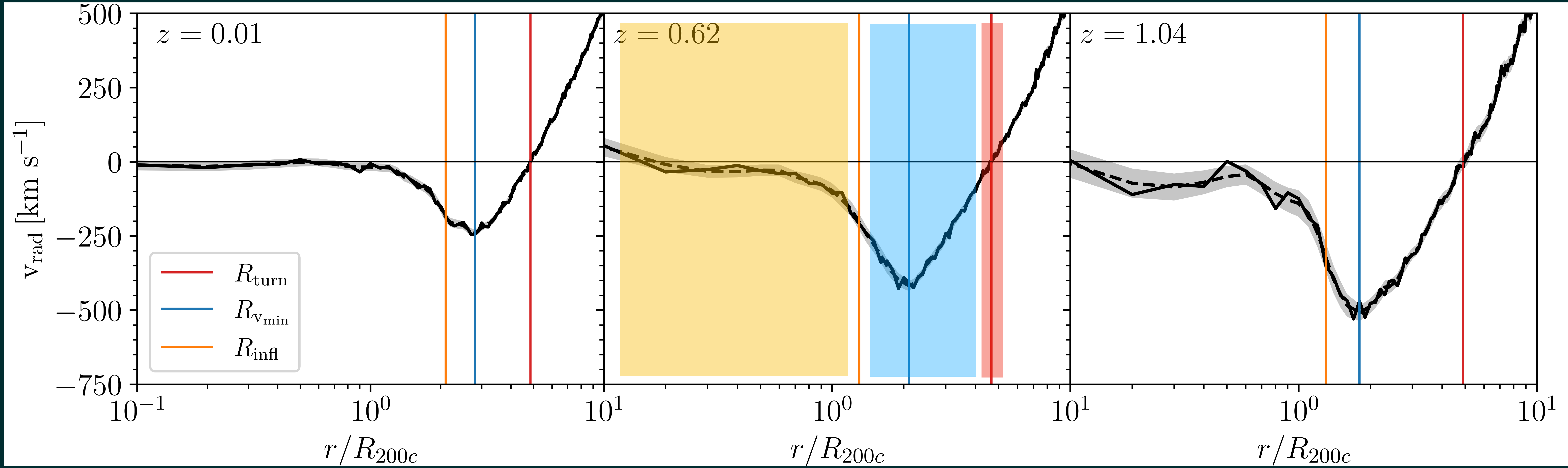

The splashback radius

The splashback radius

Inner boundary of the infall region?

The splashback radius

Inner boundary of the infall region?

R_{vir}

R_{200m}, R_{200c}

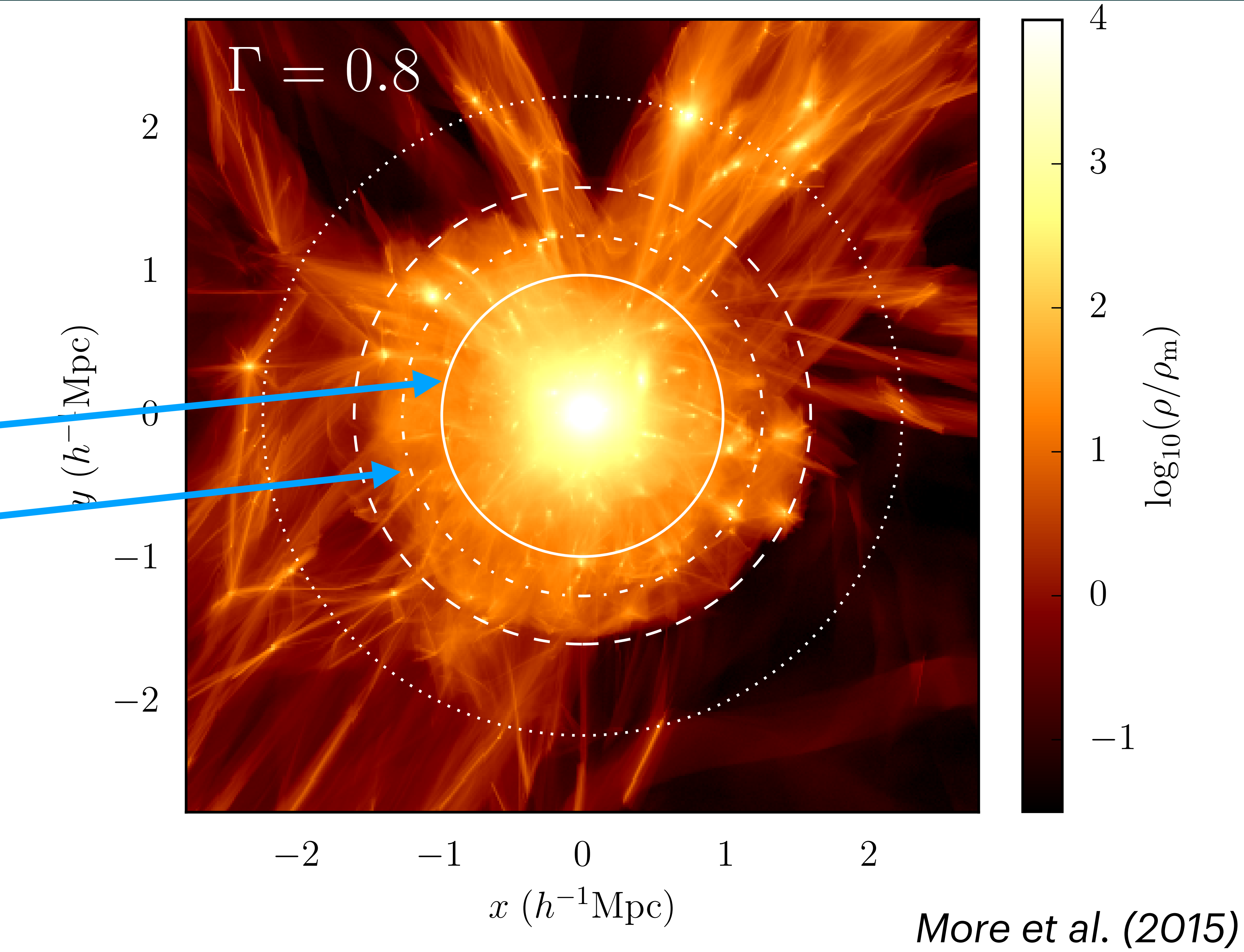

More et al. (2015)

The splashback radius

Inner boundary of the infall region?

R_{vir}

R_{200m}, R_{200c}

Splashback radius
(Adhikari et al. 2014, Diemer & Kravtsov 2015)

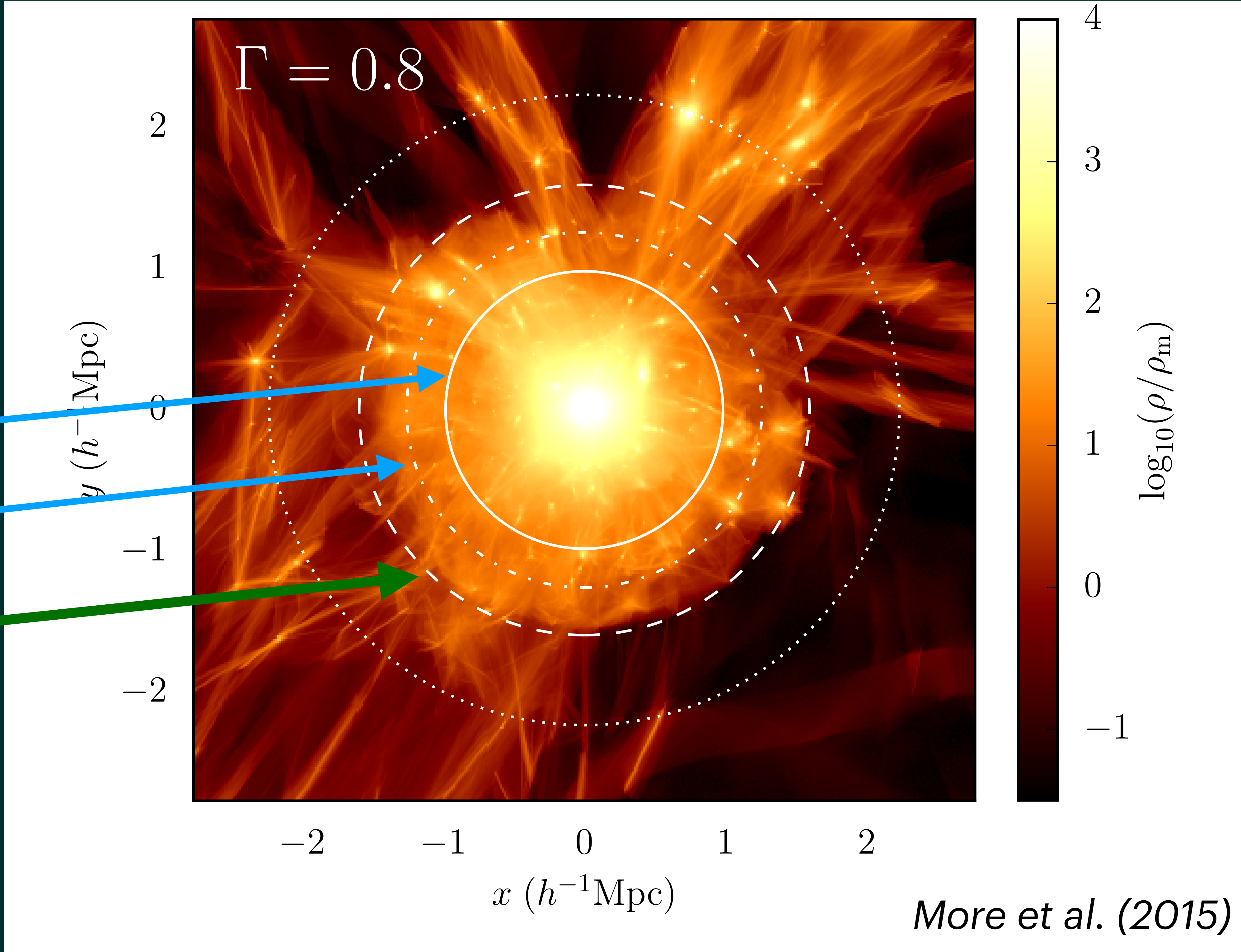

More et al. (2015)

The splashback radius

Inner boundary of the infall region?

R_{vir}

R_{200m}, R_{200c}

Splashback radius

(Adhikari et al. 2014, Diemer & Kravtsov 2015)

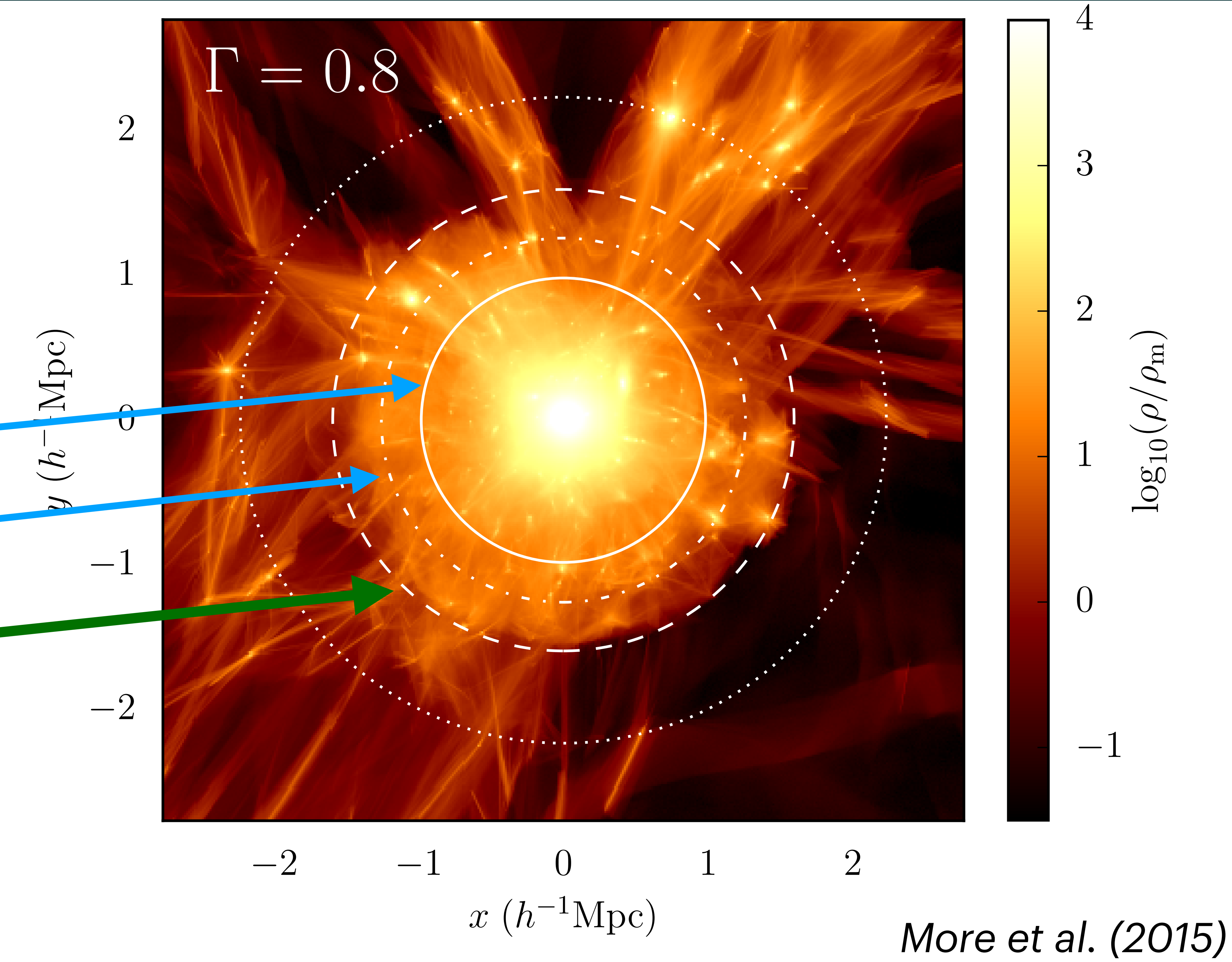

More et al. (2015)

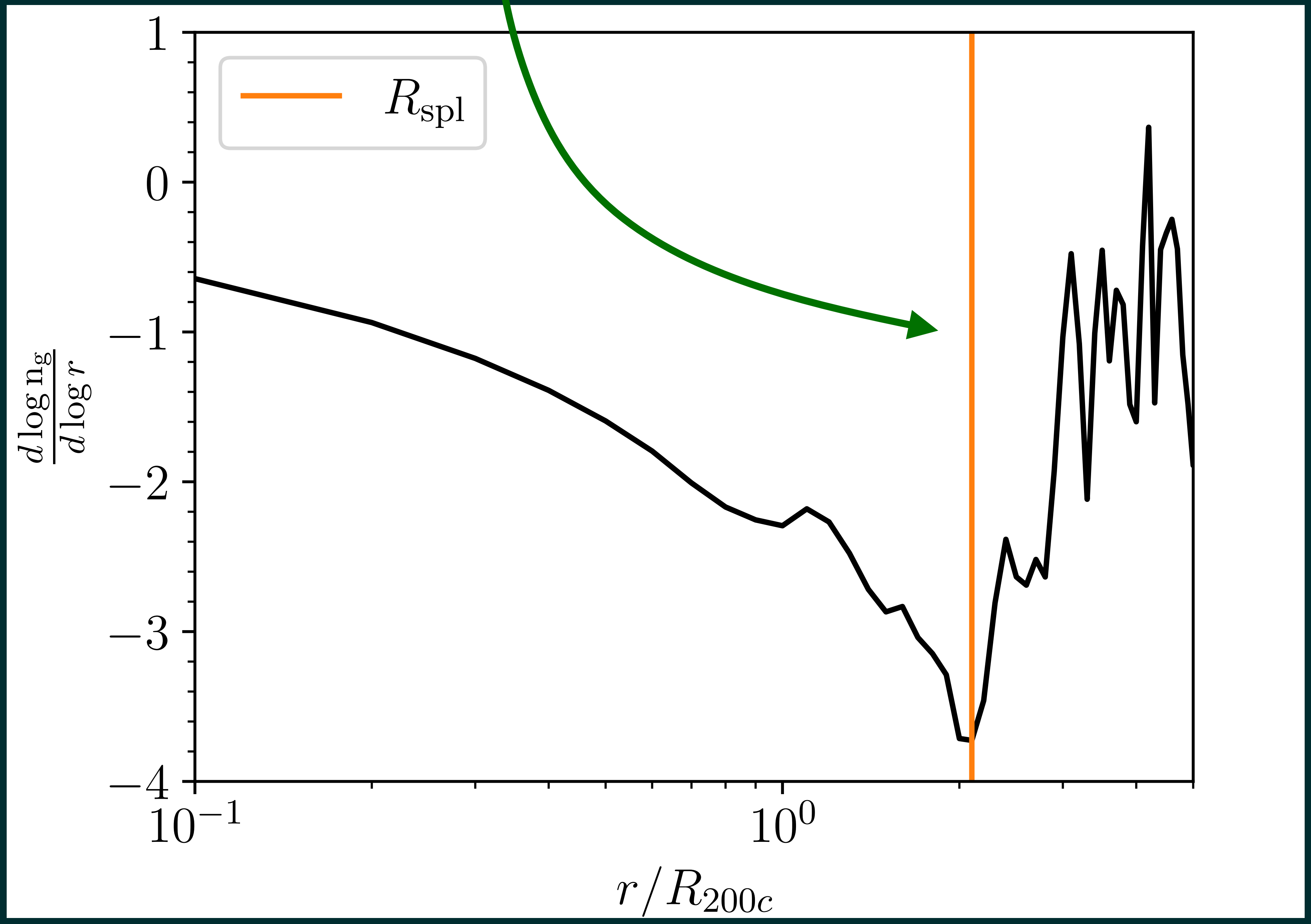

The splashback radius

Inner boundary of the infall region?

R_{vir}

R_{200m}, R_{200c}

Splashback radius

(Adhikari et al. 2014, Diemer & Kravtsov 2015)

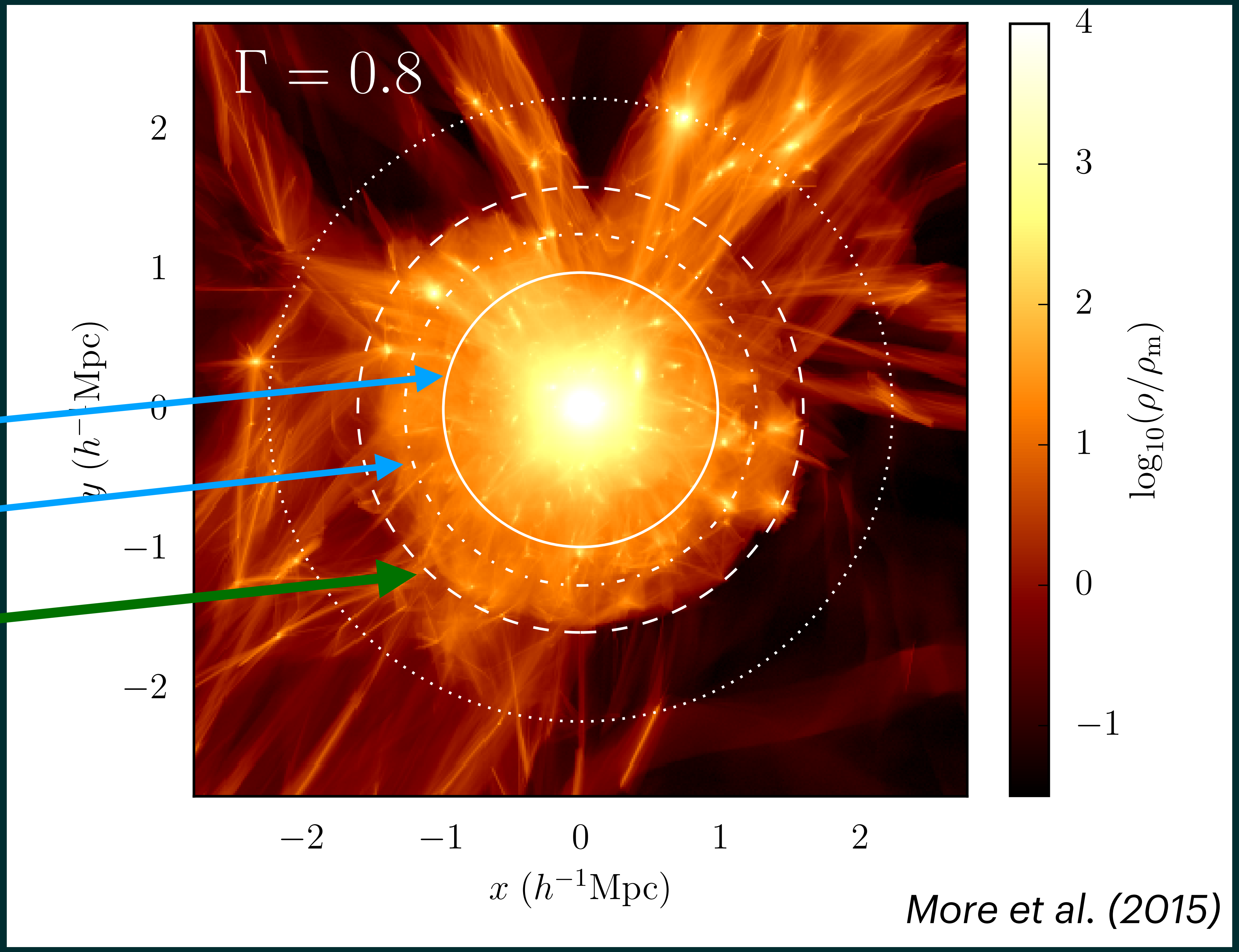

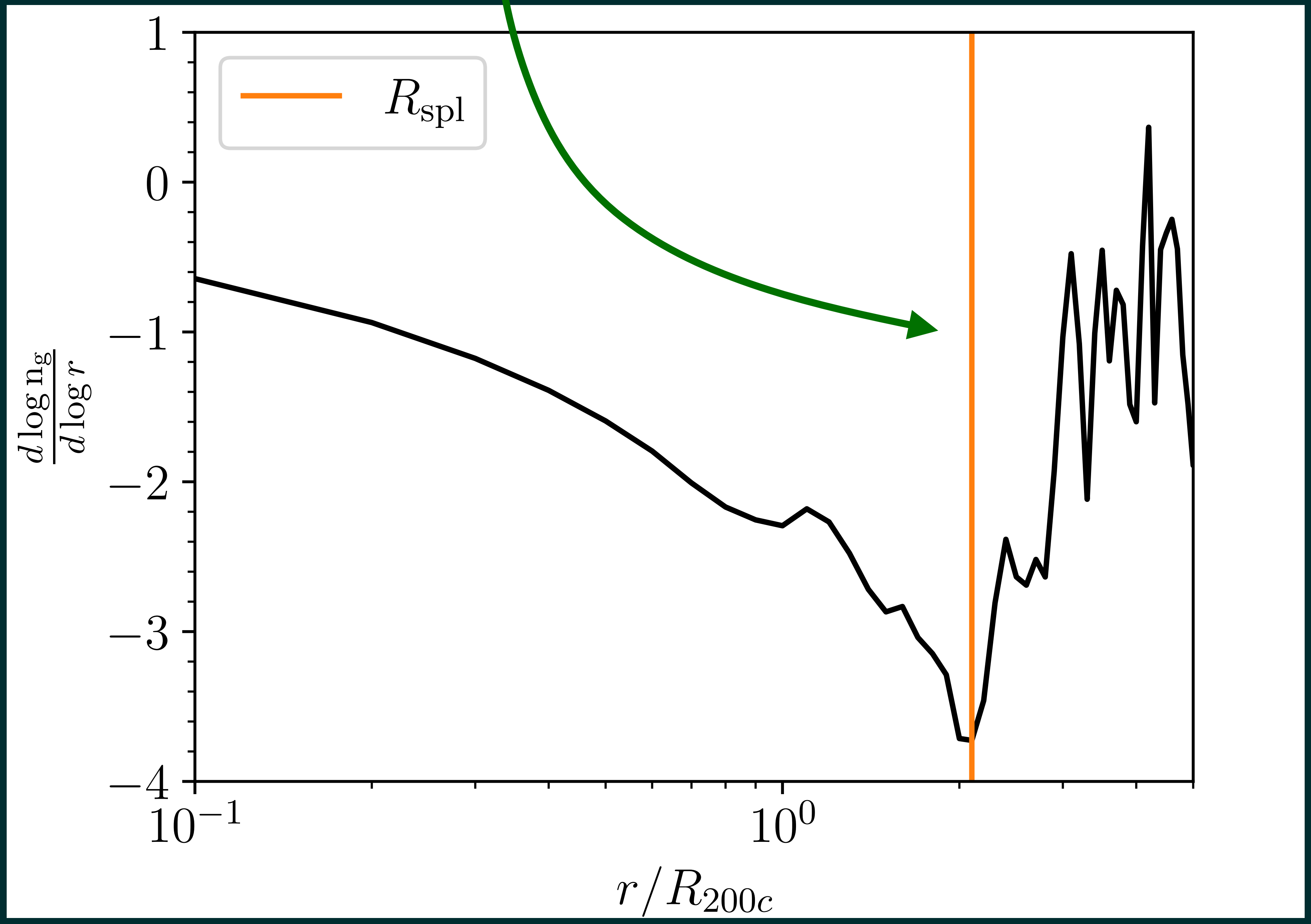

- Physical meaning studied with ***CDM only simulations*** *(Diemer et al. 2014+)*
- Signatures from ***galaxies***?

The inflection point of $\mathrm{v}_{\mathrm{rad}}(r)$

The inflection point of $\mathrm{v}_{\mathrm{rad}}(r)$

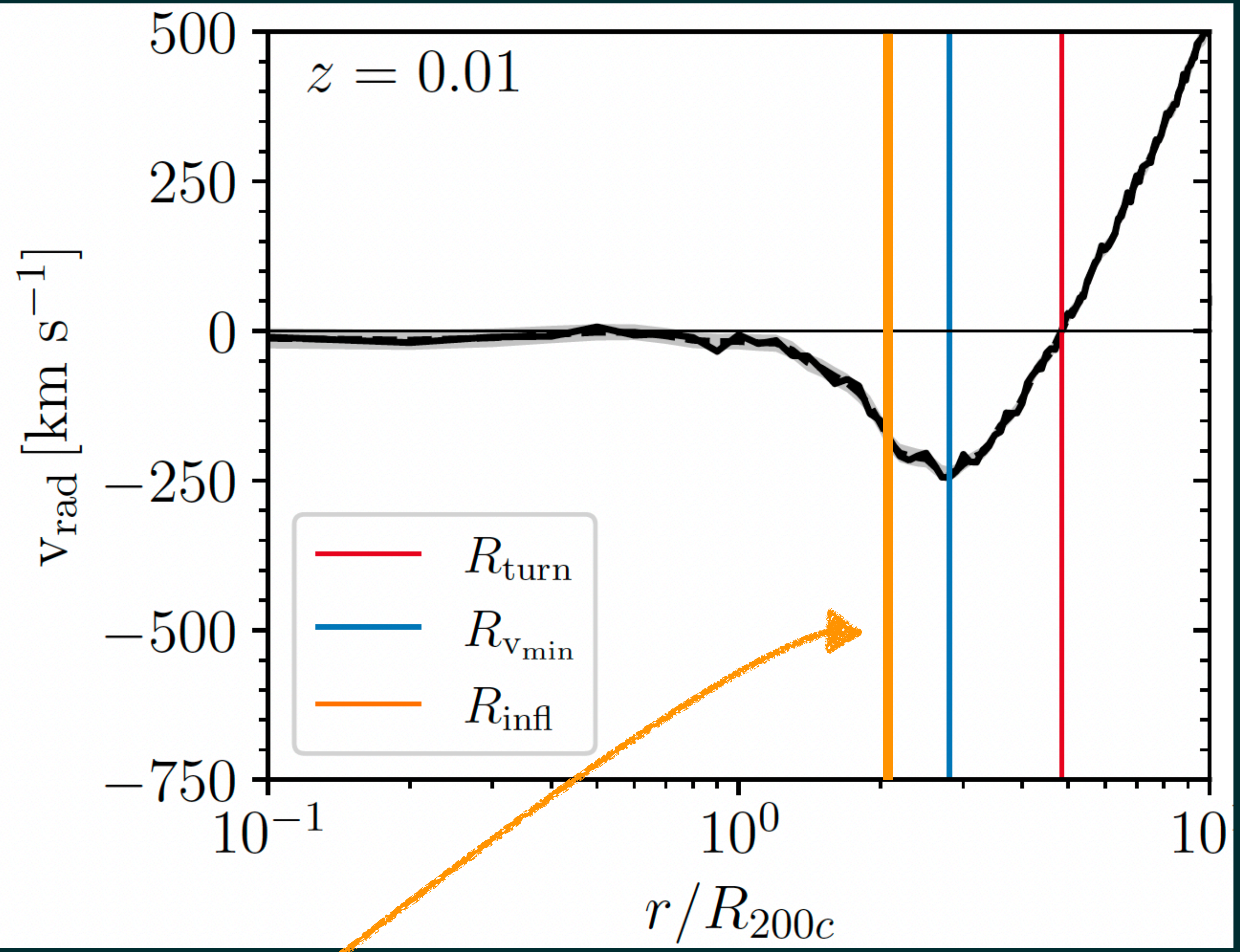

At R_{infl} $\longrightarrow$ ***maximum***

radial change of $\mathrm{v}_{\mathrm{rad}}(r)$

$\sim$

infall $\longrightarrow$ orbits

The inflection point of $v_{rad}(r)$

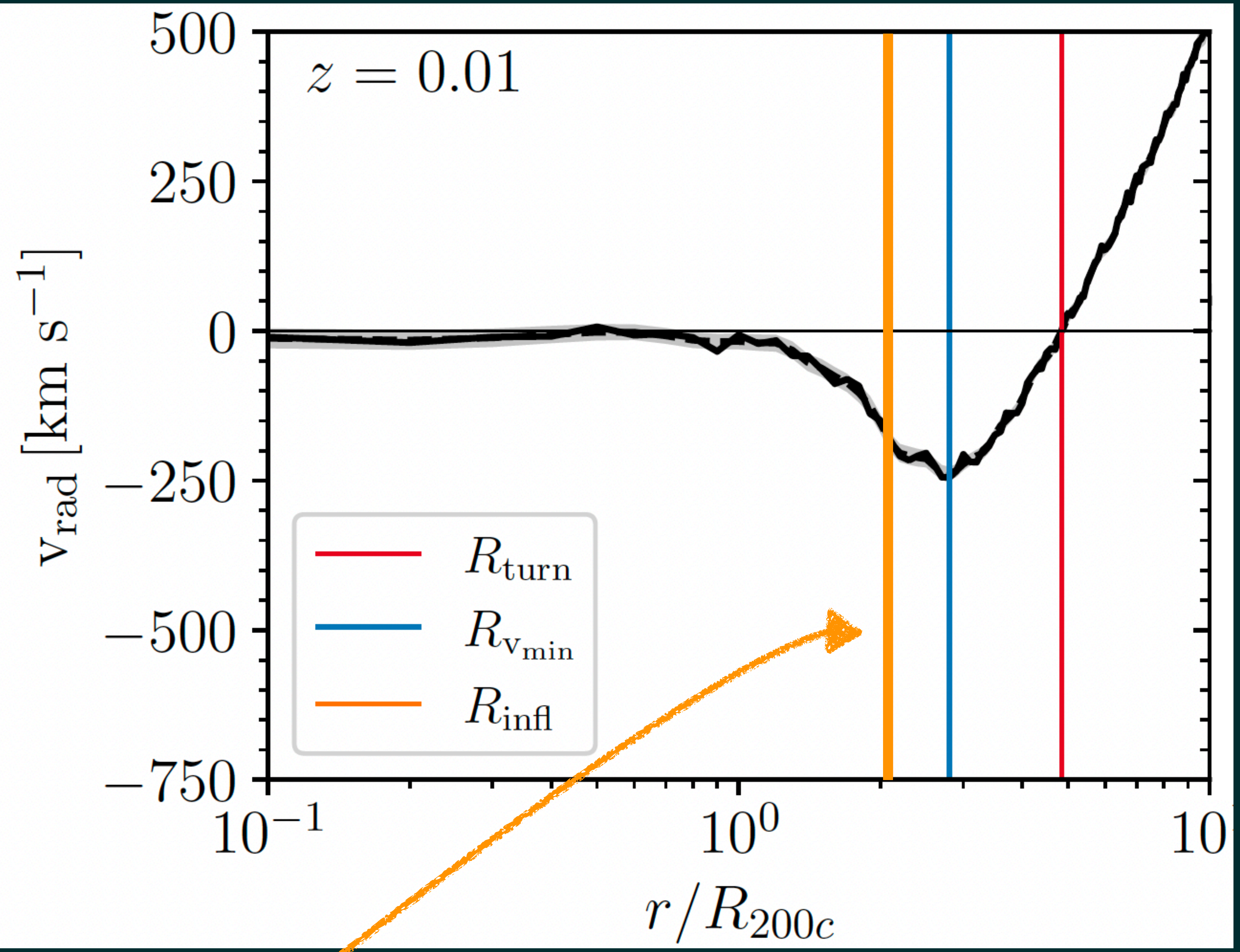

$$R_{infl} : \frac{dv_{rad}}{dr}$$

is minimum

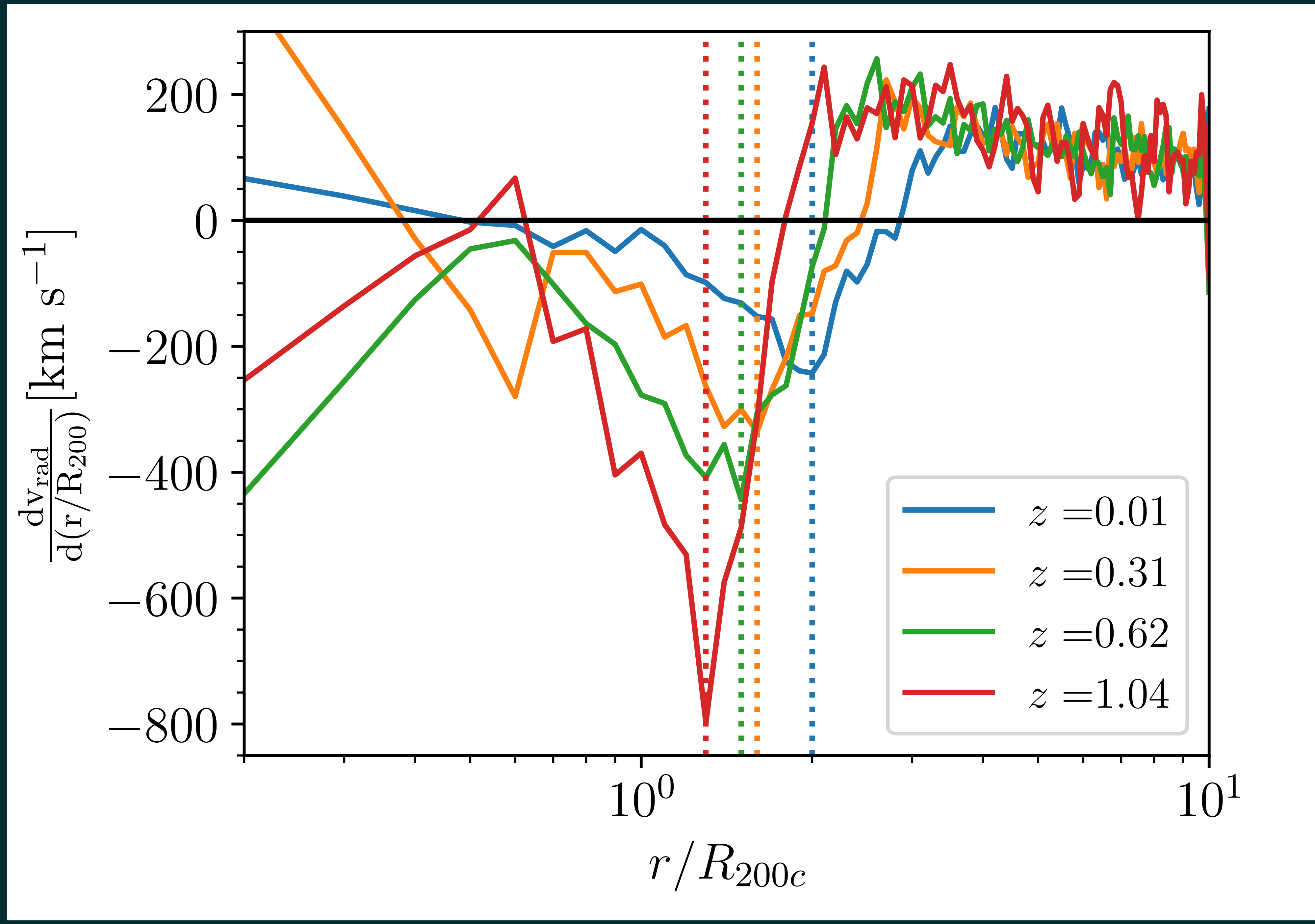

At $R_{infl} \longrightarrow$ ***maximum***

radial change of $v_{rad}(r)$

$\sim$

infall $\longrightarrow$ orbits

The inflection point of $v_{rad}(r)$

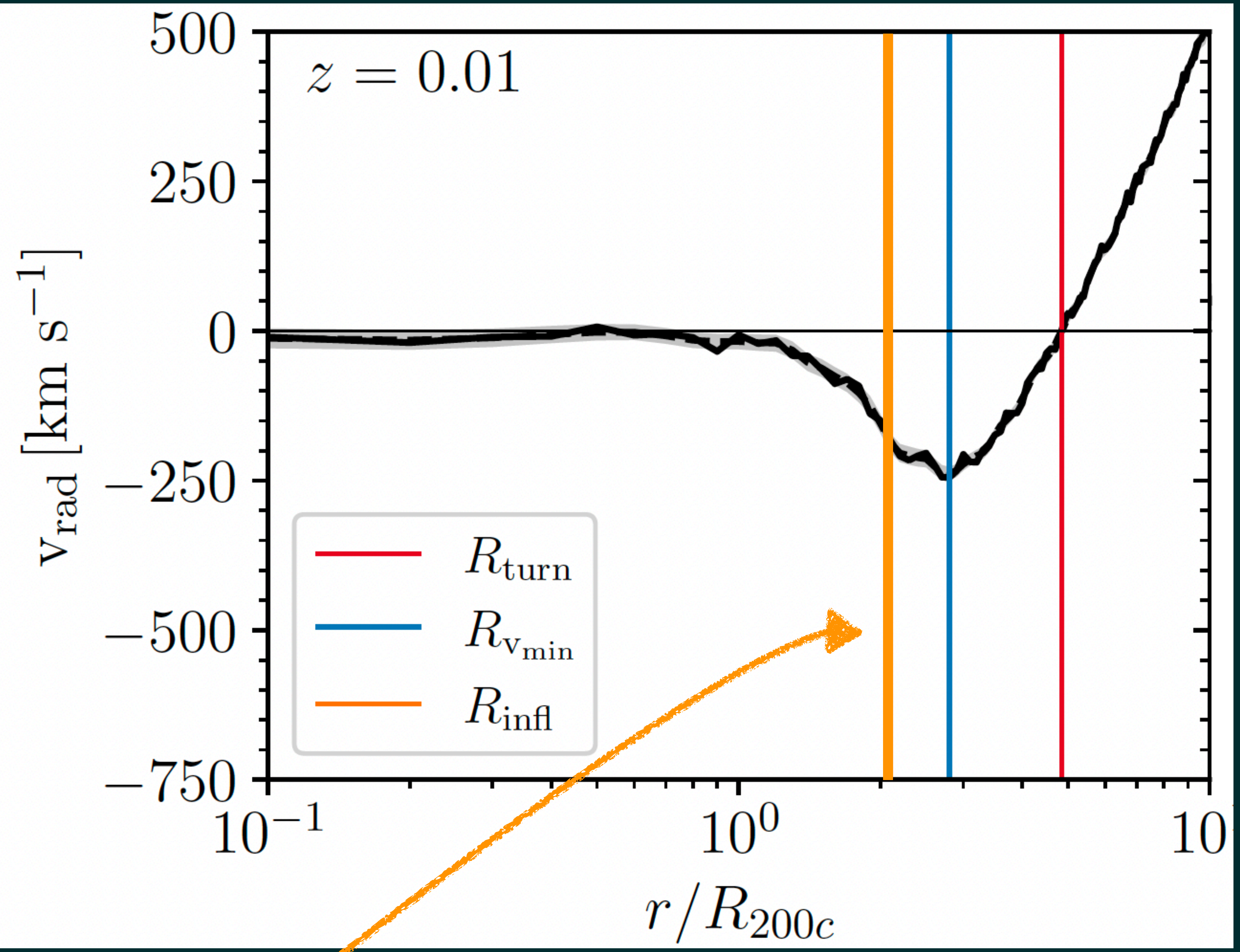

$$R_{infl} : \frac{dv_{rad}}{dr}$$

is minimum

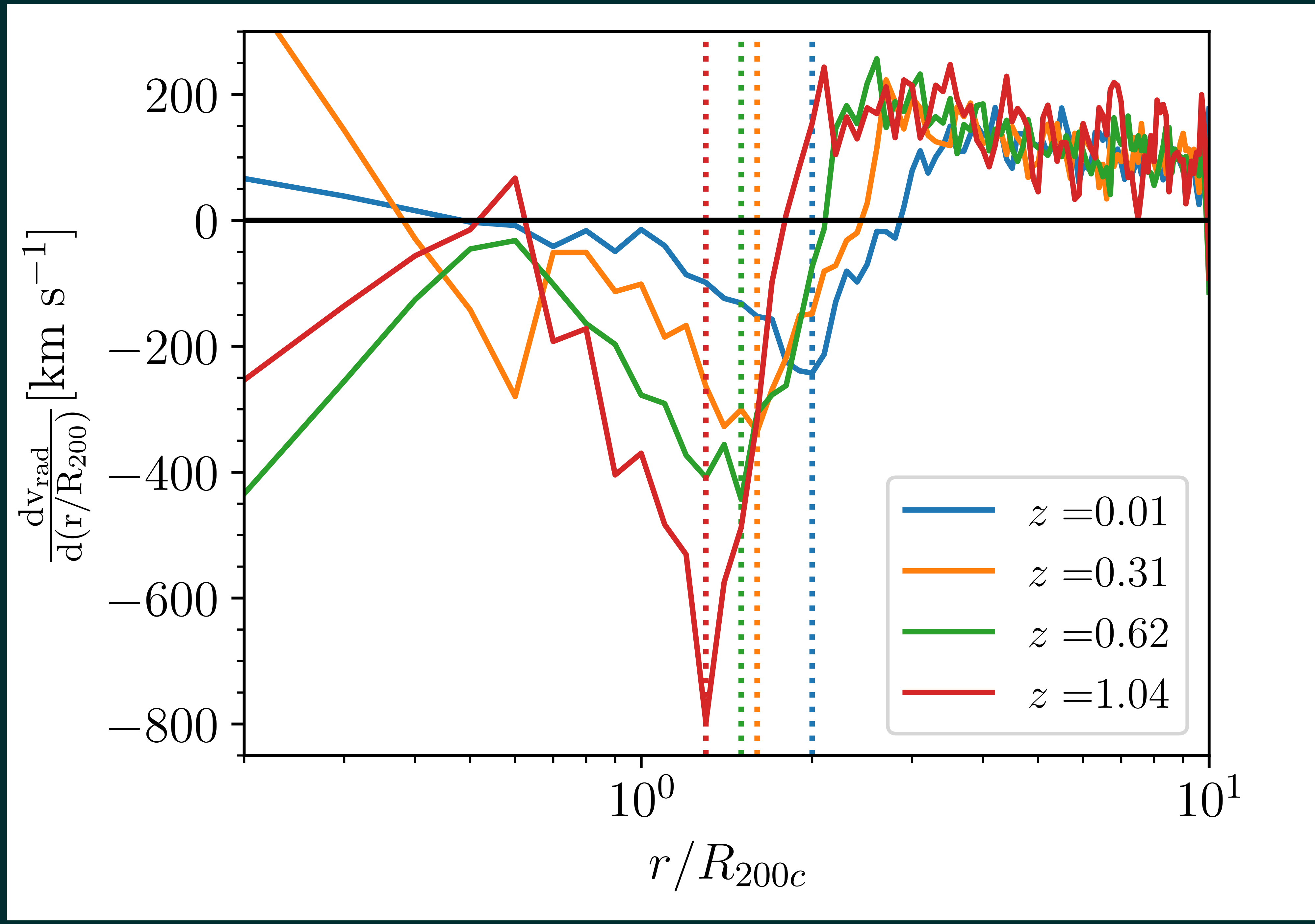

At $R_{infl} \longrightarrow$ ***maximum***

radial change of $v_{rad}(r)$

$\sim$

infall $\longrightarrow$ orbits

$$R_{200c} < R_{infl} < R_{v_{min}}$$

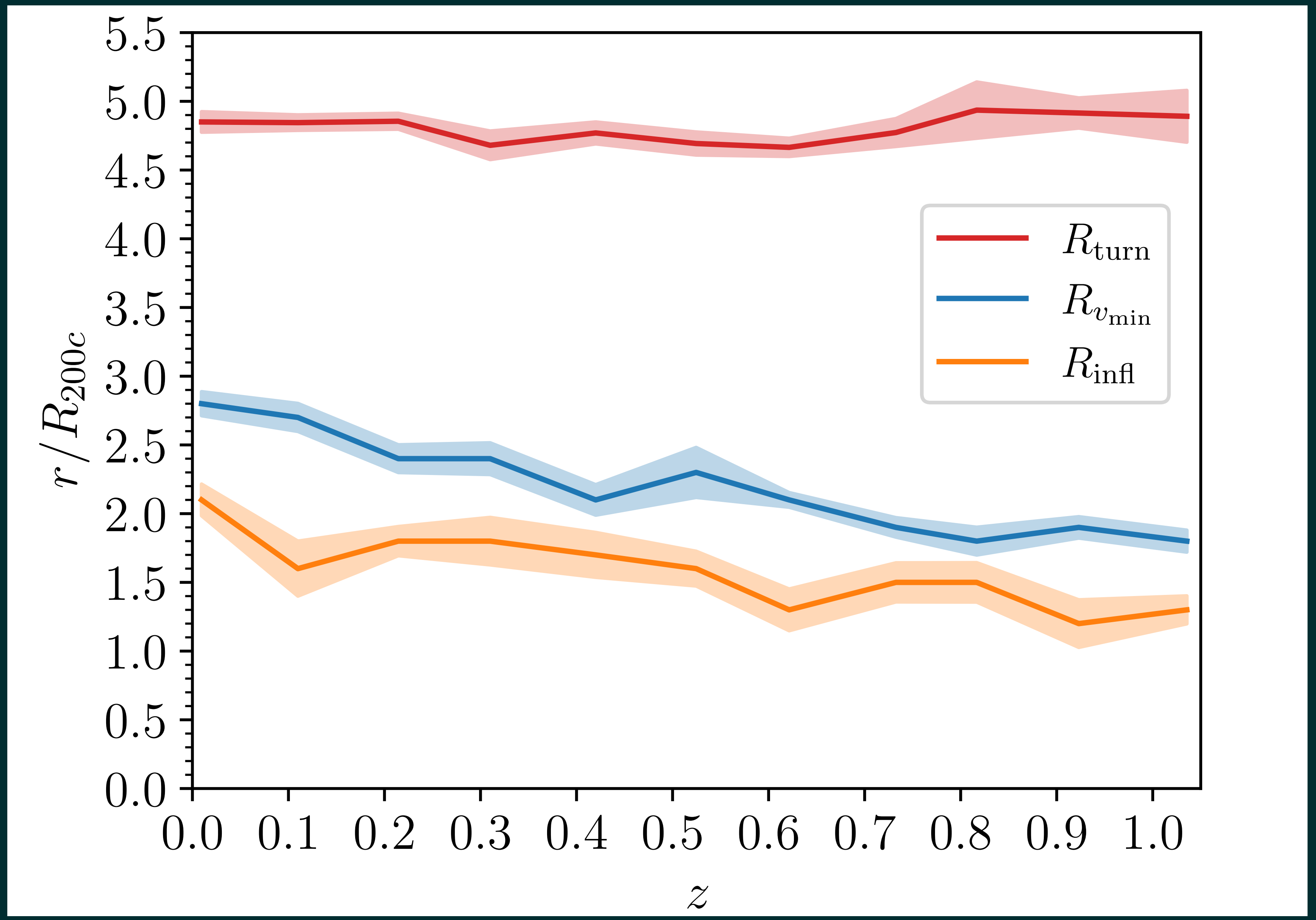

The inflection point of $\mathrm{v}_{\mathrm{rad}}(r)$

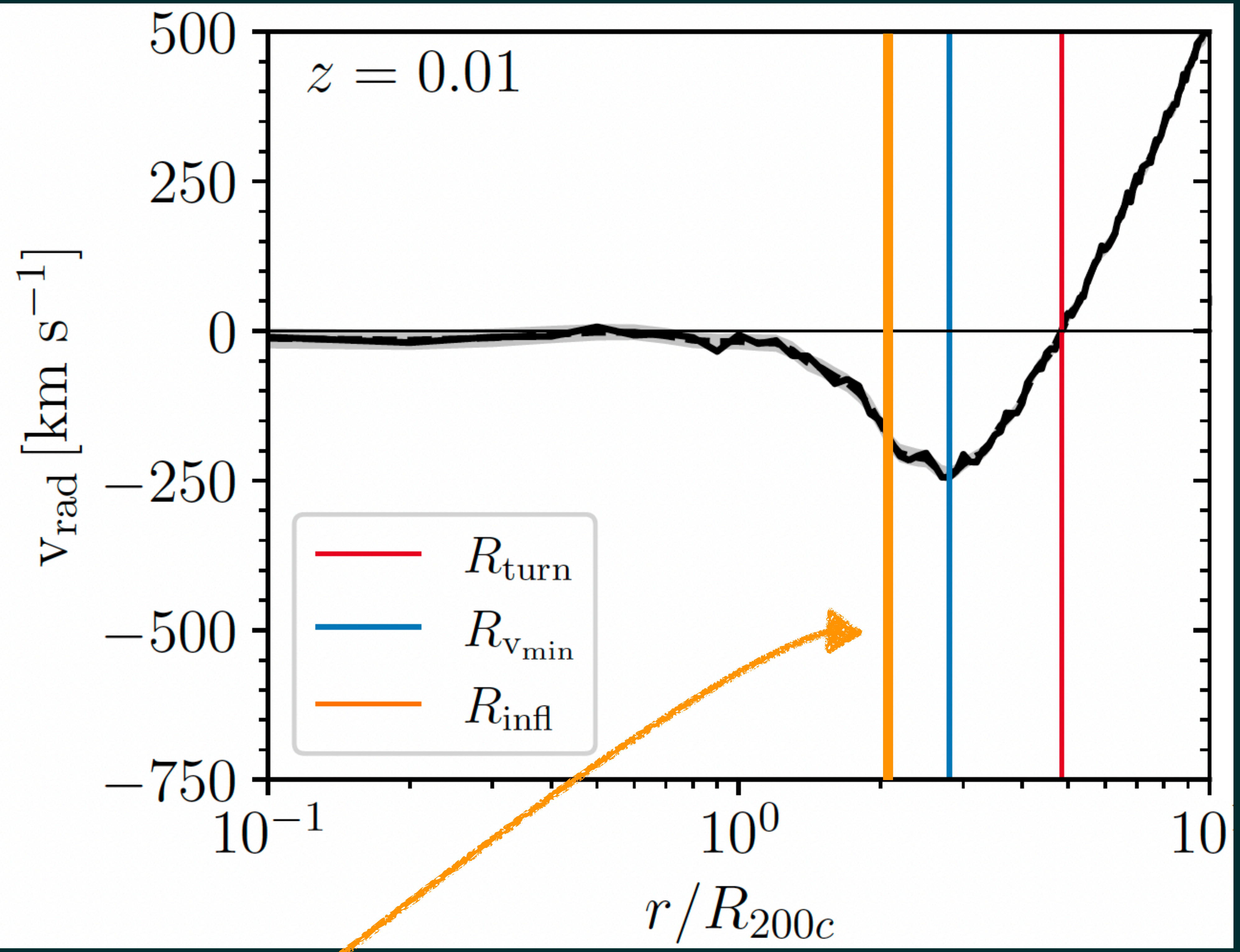

R_{infl} : $\dfrac{d\mathrm{v}_{\mathrm{rad}}}{dr}$ is minimum

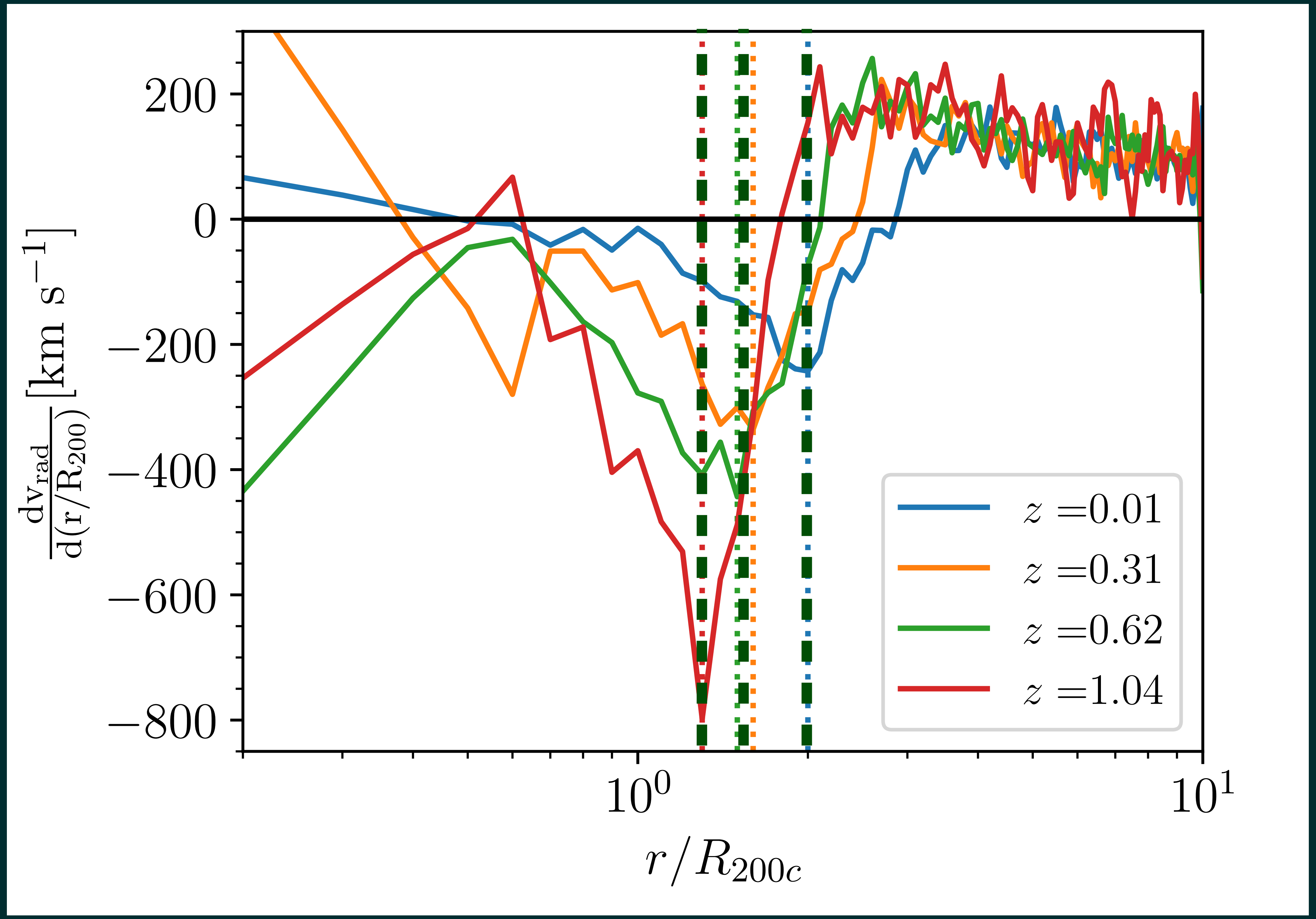

At $R_{\mathrm{infl}} \longrightarrow$ ***maximum***

radial change of $\mathrm{v}_{\mathrm{rad}}(r)$

$\sim$

infall $\longrightarrow$ orbits

$R_{200c} < R_{\mathrm{infl}} < R_{\mathrm{v_{min}}}$

as R_{spl}

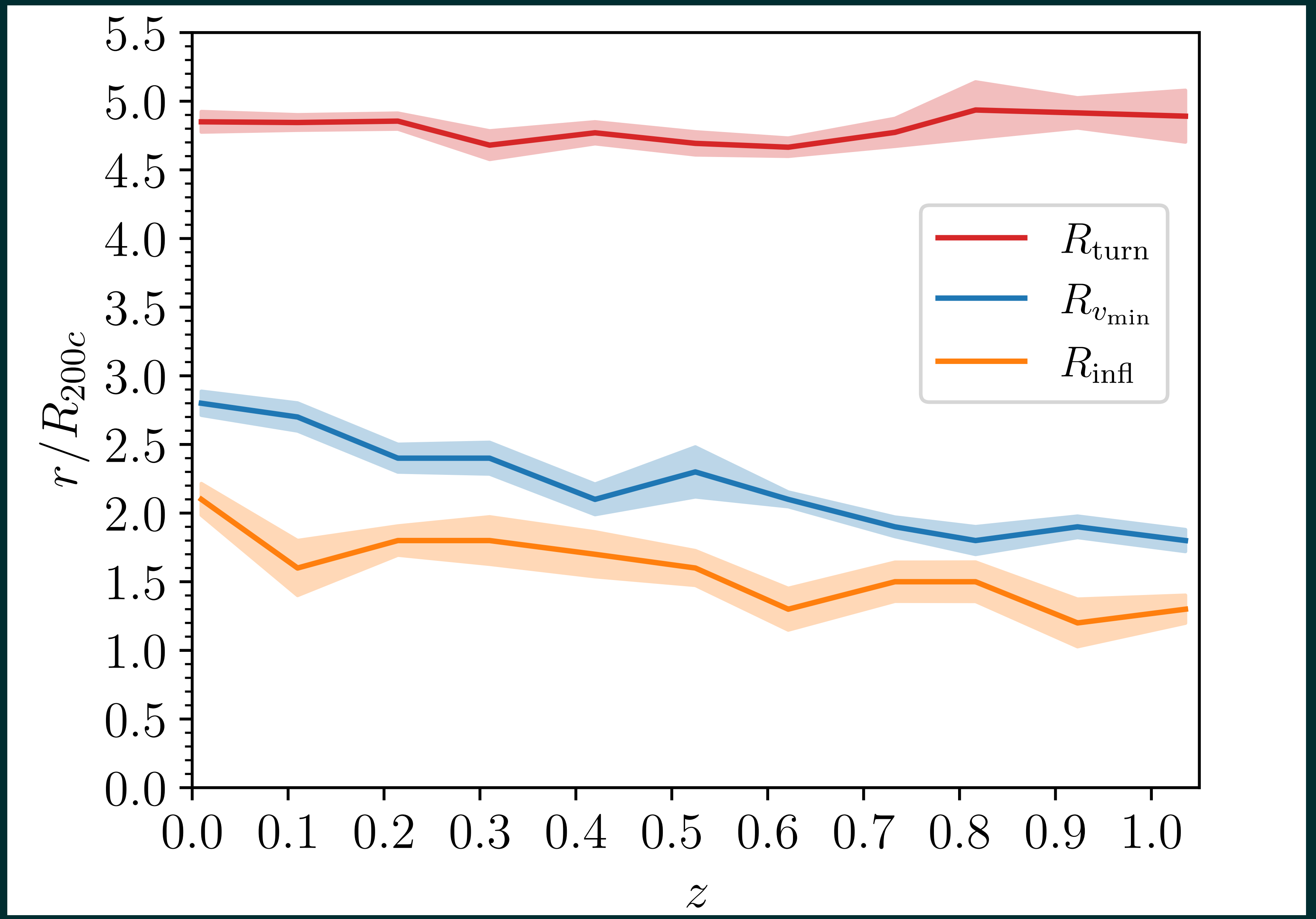

Velocity dispersion and radial velocity of galaxies

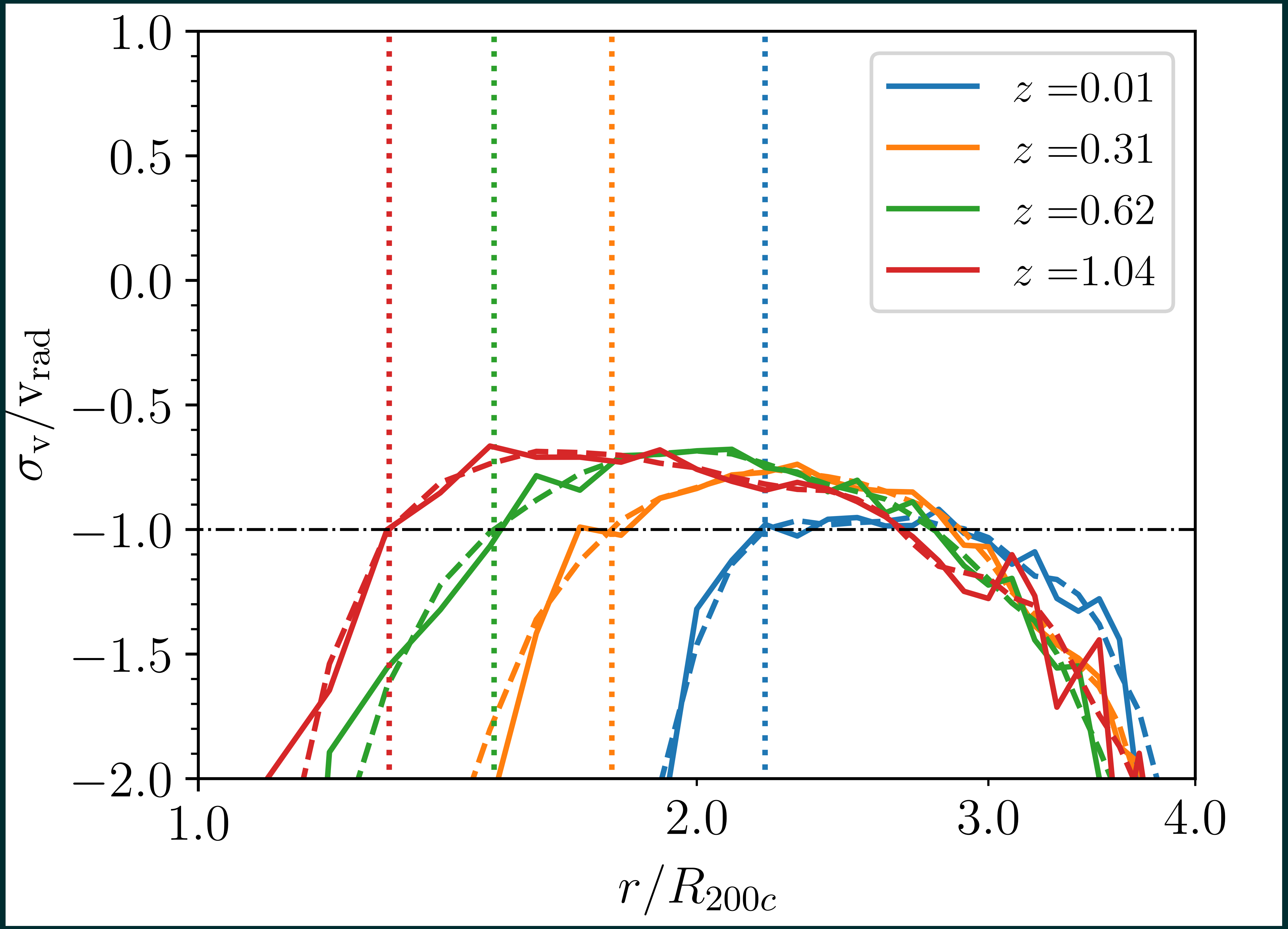

$\sigma_v(r)/v_{rad}(r)$ traces a ***dynamical transition*** in clusters

Dominant motions:

- < -1 $\longrightarrow$ nonradial
- > -1 $\longrightarrow$ radial
- = -1 $\longrightarrow$ ***transition***

Velocity dispersion and radial velocity of galaxies

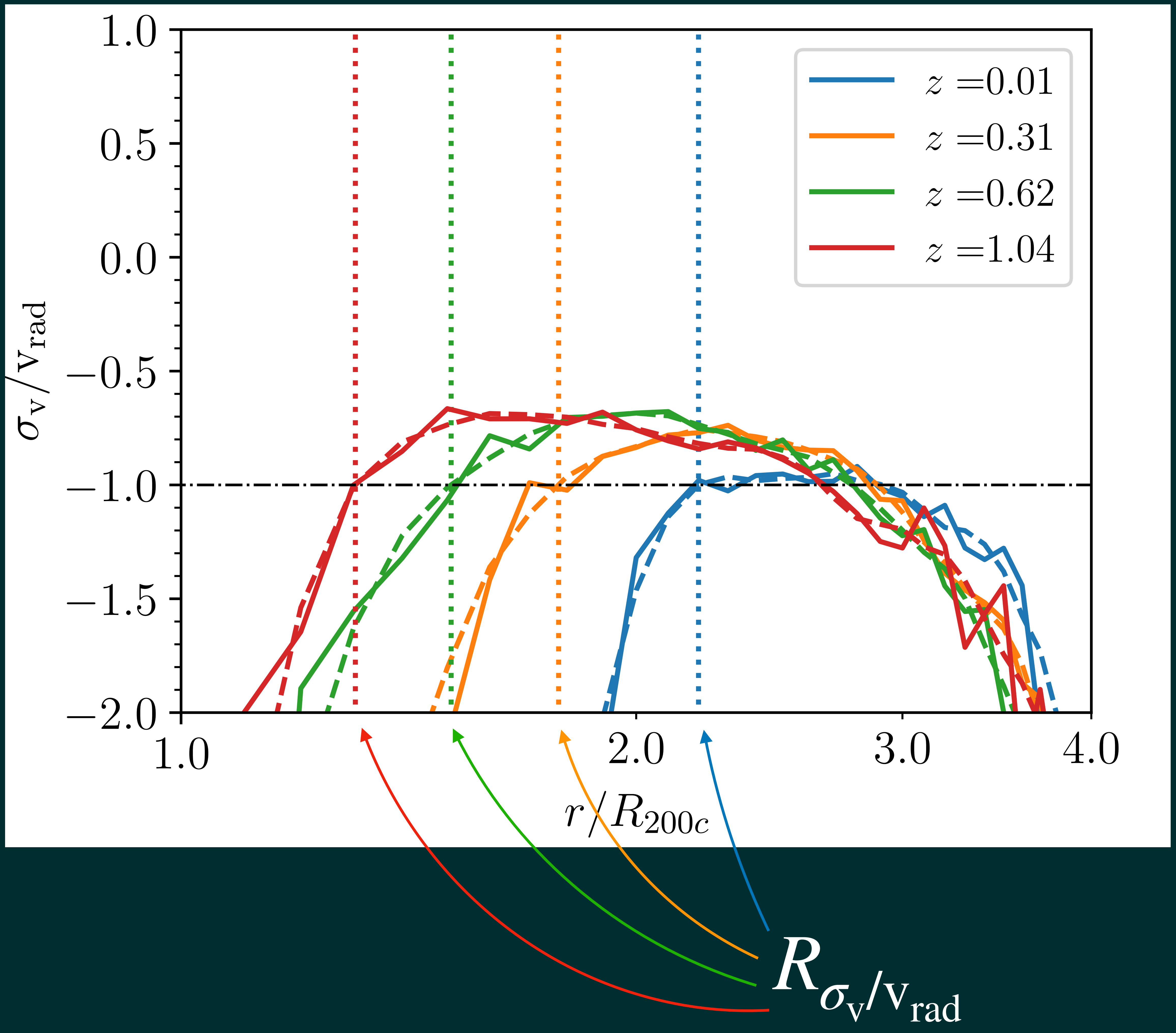

$\sigma_v(r)/v_{rad}(r)$ traces a ***dynamical transition*** in clusters

Dominant motions:

- < -1 $\longrightarrow$ nonradial
- > -1 $\longrightarrow$ radial
- = -1 $\longrightarrow$ ***transition***

Velocity dispersion and radial velocity of galaxies

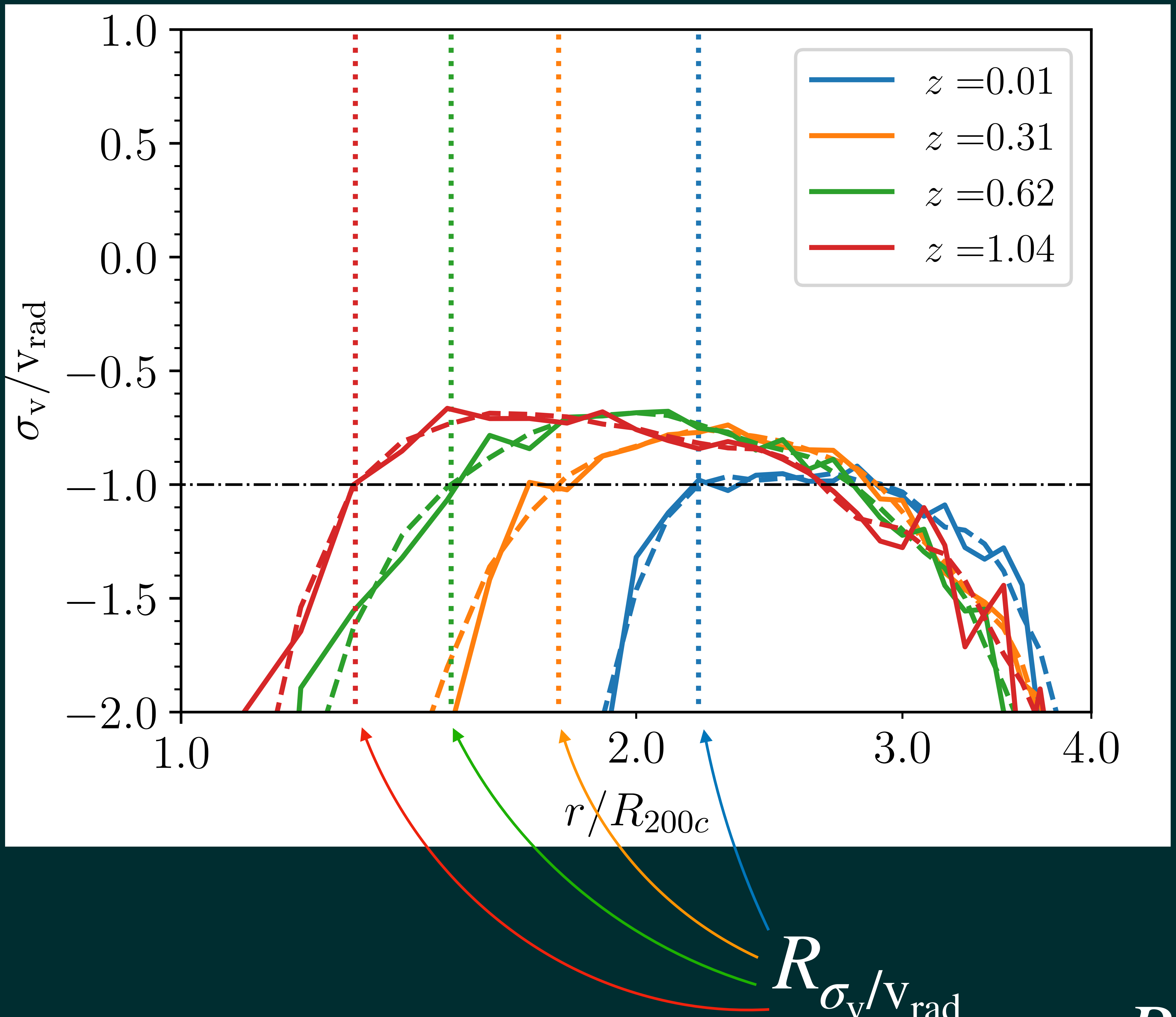

$\sigma_v(r)/v_{rad}(r)$ traces a ***dynamical transition*** in clusters

Dominant motions:

- < -1 $\longrightarrow$ nonradial
- > -1 $\longrightarrow$ radial
- = -1 $\longrightarrow$ ***transition***

$R_{200c} < R_{\sigma_v/v_{rad}} < R_{v_{min}}$ as R_{infl} and R_{spl}

Velocity dispersion and radial velocity of galaxies

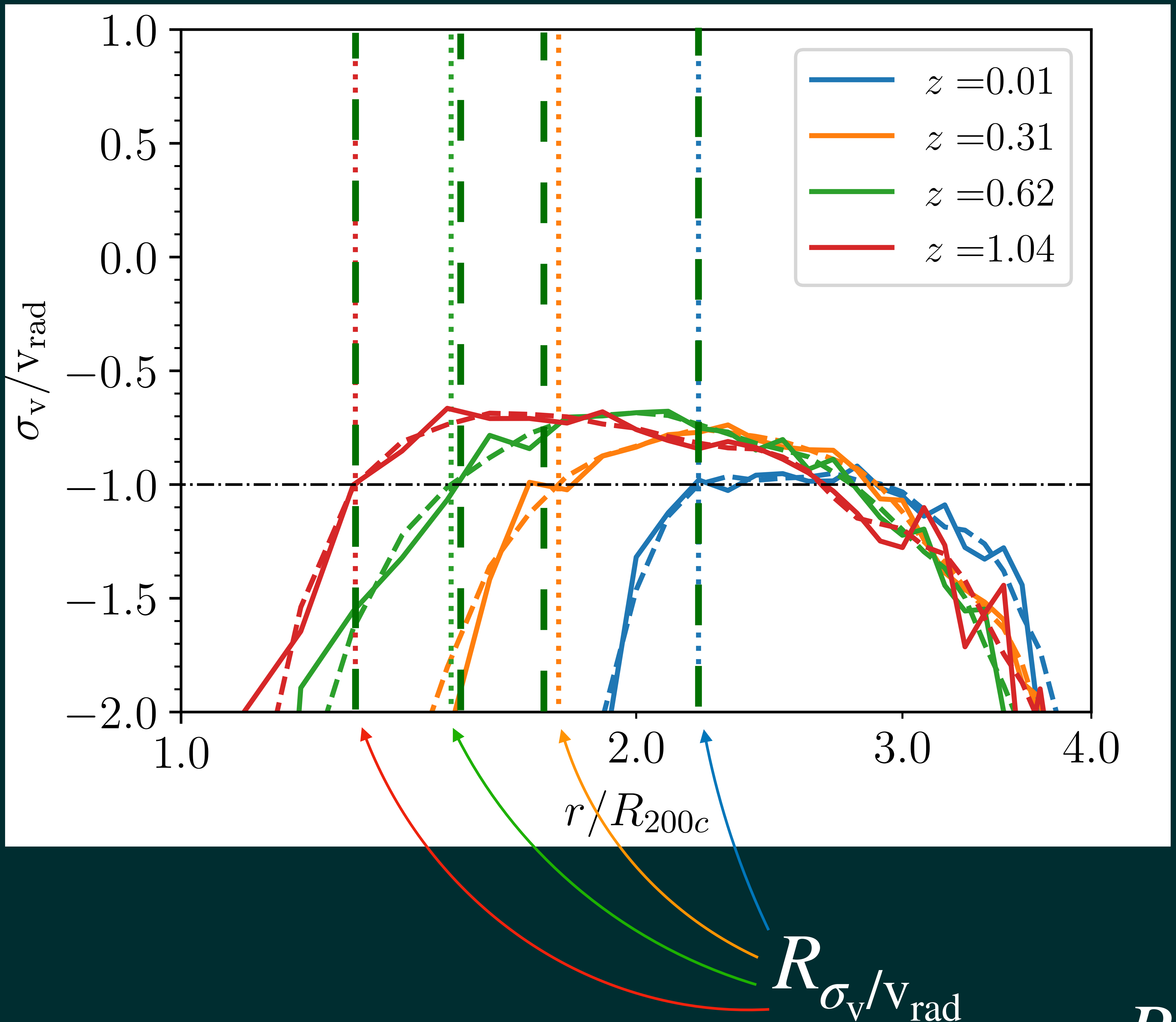

$\sigma_v(r)/v_{rad}(r)$ traces a ***dynamical transition*** in clusters

Dominant motions:

- < -1 $\longrightarrow$ nonradial
- > -1 $\longrightarrow$ radial
- = -1 $\longrightarrow$ ***transition***

$R_{200c} < R_{\sigma_v/v_{rad}} < R_{v_{min}}$ as R_{infl} and R_{spl}

Comparison between $R_{\rm spl}$, $R_{\rm infl}$, and $R_{\sigma_{\rm v}/{\rm v}_{\rm rad}}$

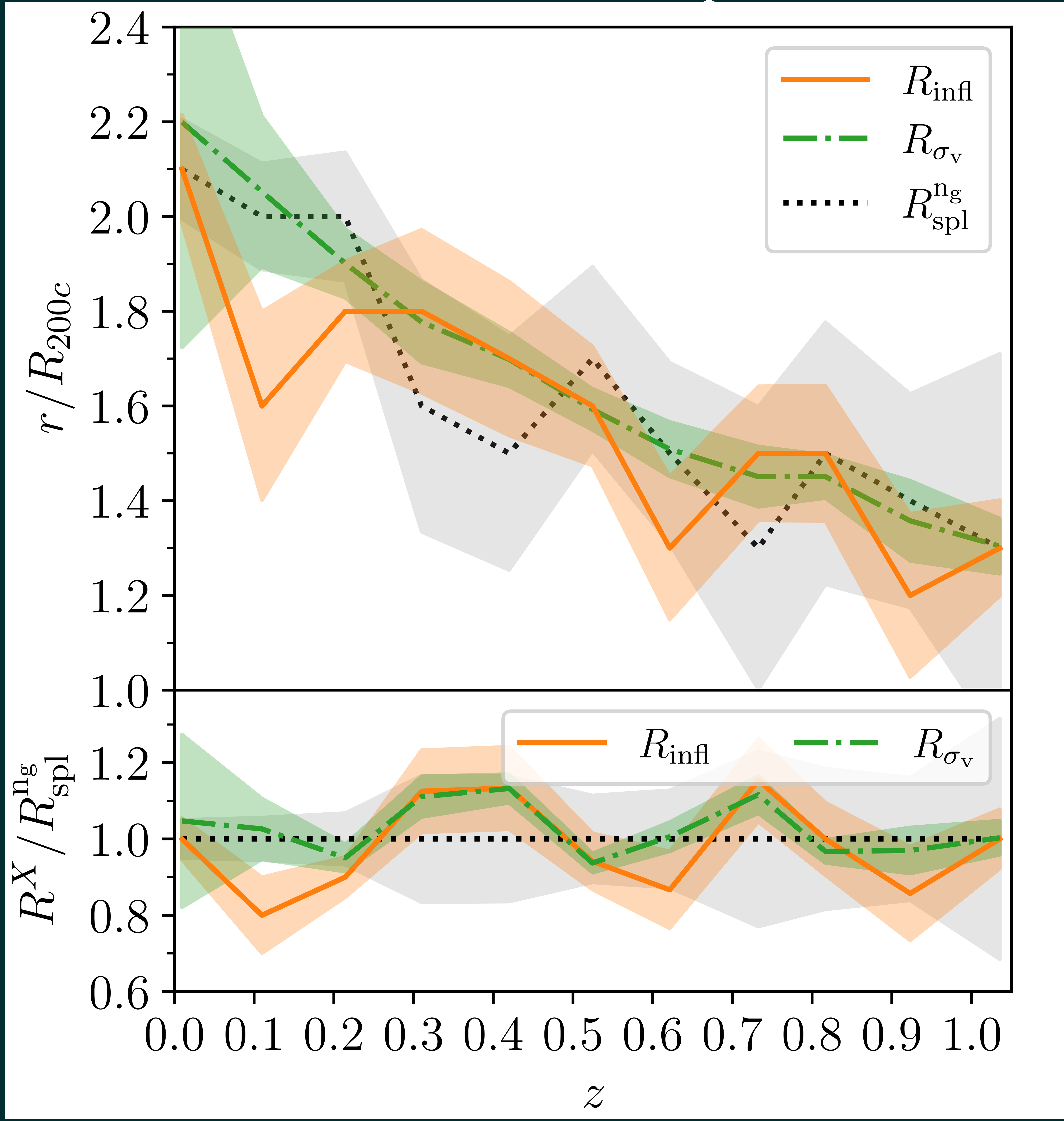

Similar redshift dependence

The three radii

coincide to within 1σ

Extended view of the splashback radius as inner boundary of clusters' infalling region

Comparison between $R_{\rm spl}$, $R_{\rm infl}$, and $R_{\sigma_{\rm v}/{\rm v}_{\rm rad}}$

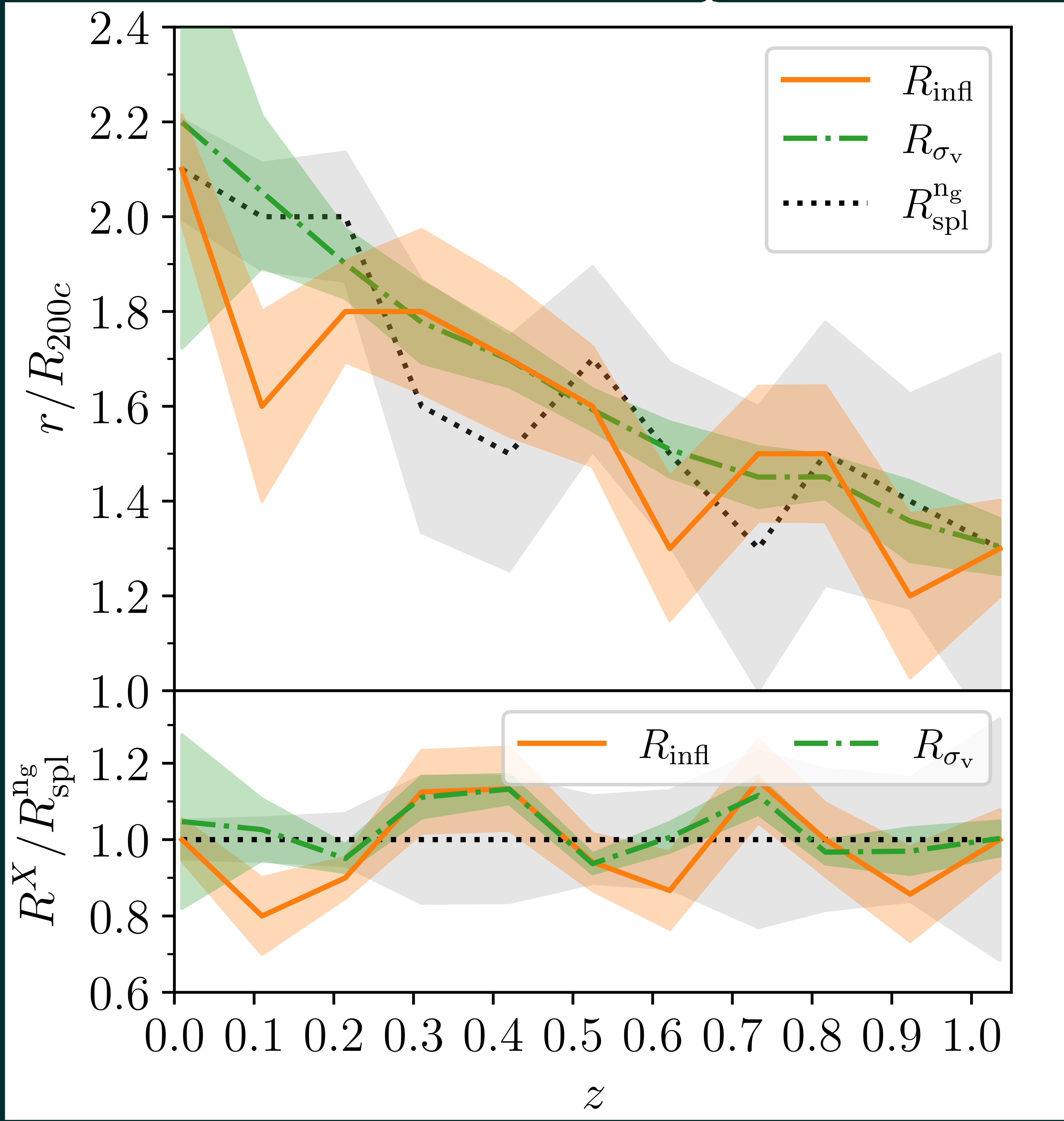

Similar redshift dependence

The three radii

coincide to within 1σ

Extended view of the splashback radius as inner boundary of clusters' infalling region

(More details in Pizzardo et al. 2024, A&A, 683, A82)

Dynamical radii and cluster growth

- Infall region: between $R_{\rm spl}$ ($\simeq R_{\rm infl}$) and $R_{\rm turn}$
- At $R_{\rm v_{min}}$ peak in radial velocity $\longrightarrow$ maximum accretion
- $R_{\rm spl} < R_{\rm v_{min}} < R_{\rm turn}$

These radii inform the study of cluster growth **(mass accretion)**

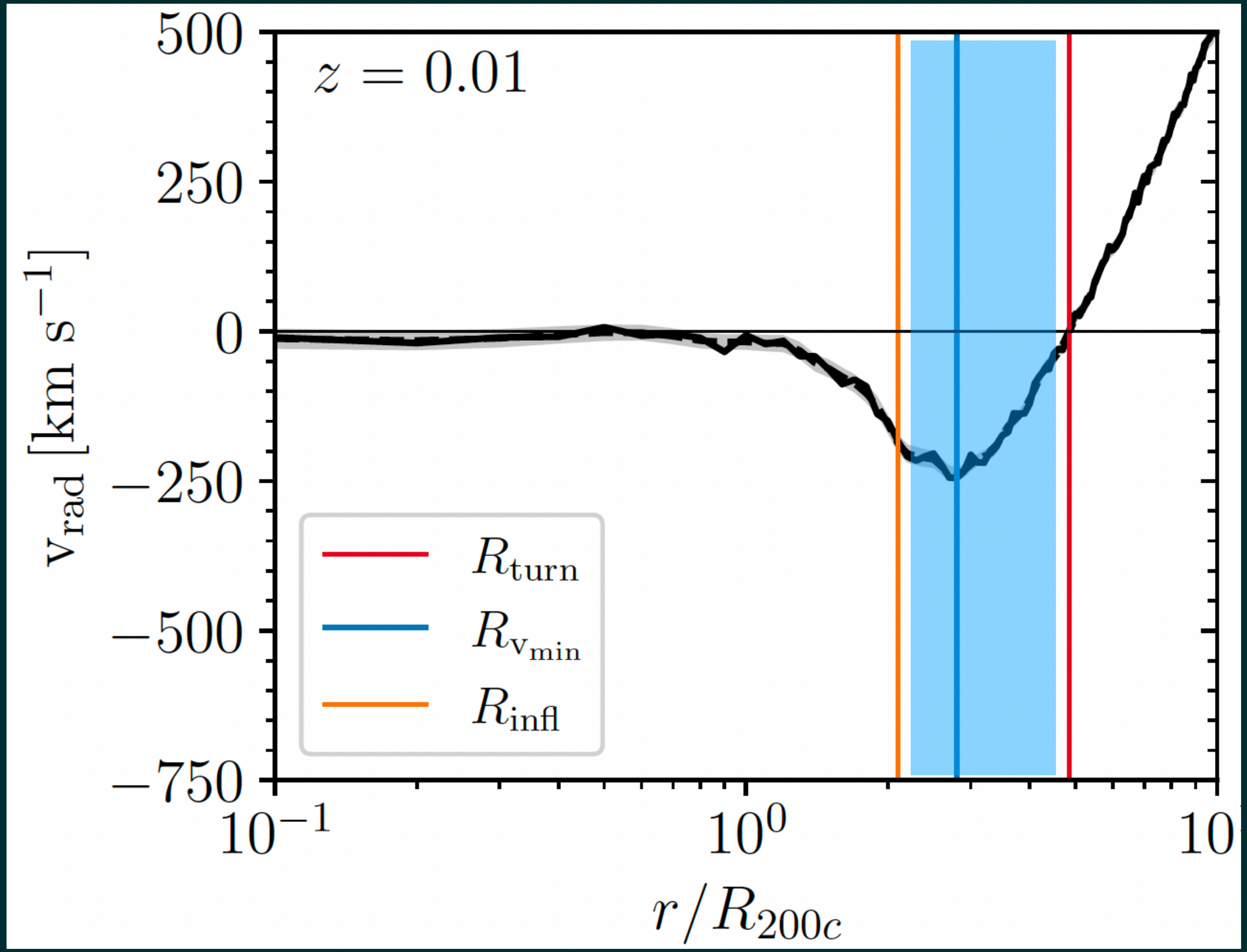

The growth of clusters

Mass accretion rate (MAR) sensitive to internal properties, growth model, dark energy

JKCS 041, $z = 1.9$

(Credits: NASA, ESO)

From merger trees: clusters accrete half of the mass later than $z = 0.5$

Abell 1689, $z = 0.18$

(Credits: NASA, ESA)

?

We develop a method to obtain MAR based on observations

Observable definition of MAR

Observable definition of MAR

$$\mathrm{MAR} = \mathscr{K}\frac{M_{\mathrm{shell}}}{t_{\mathrm{inf}}}$$

Observable definition of MAR

$$\mathrm{MAR} = \mathscr{K}\frac{M_{\mathrm{shell}}}{t_{\mathrm{inf}}}$$

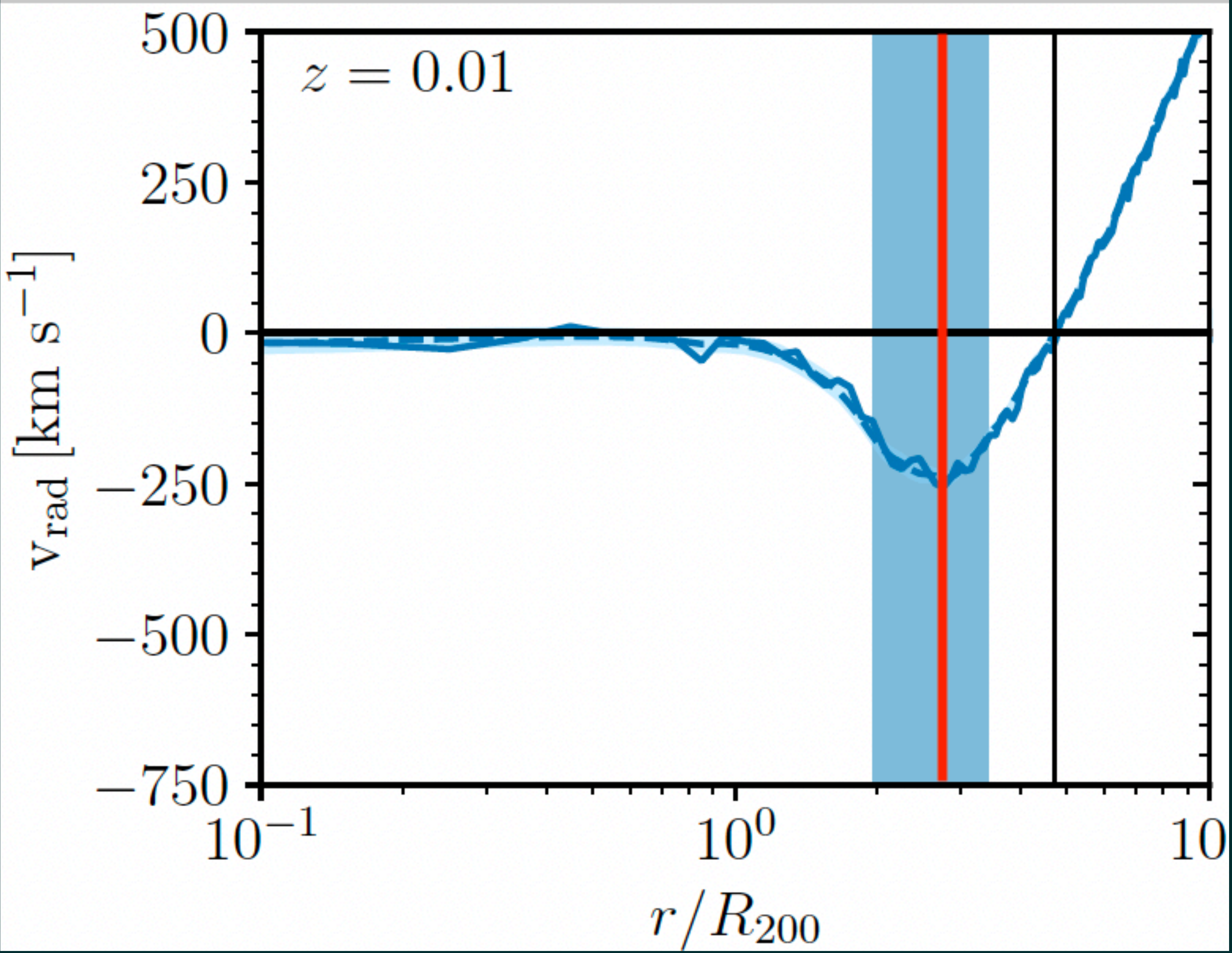

M_{shell} optimized for observations with caustic technique *(Diaferio 1999; Serra et al. 2011)*

t_{inf} from linear motion with non-constant acceleration

$\mathscr{K} \neq 1$ links MAR to $\mathrm{MAR_t}$

Observable definition of MAR

$$\mathrm{MAR} = \mathscr{K}\frac{M_{\mathrm{shell}}}{t_{\mathrm{inf}}}$$

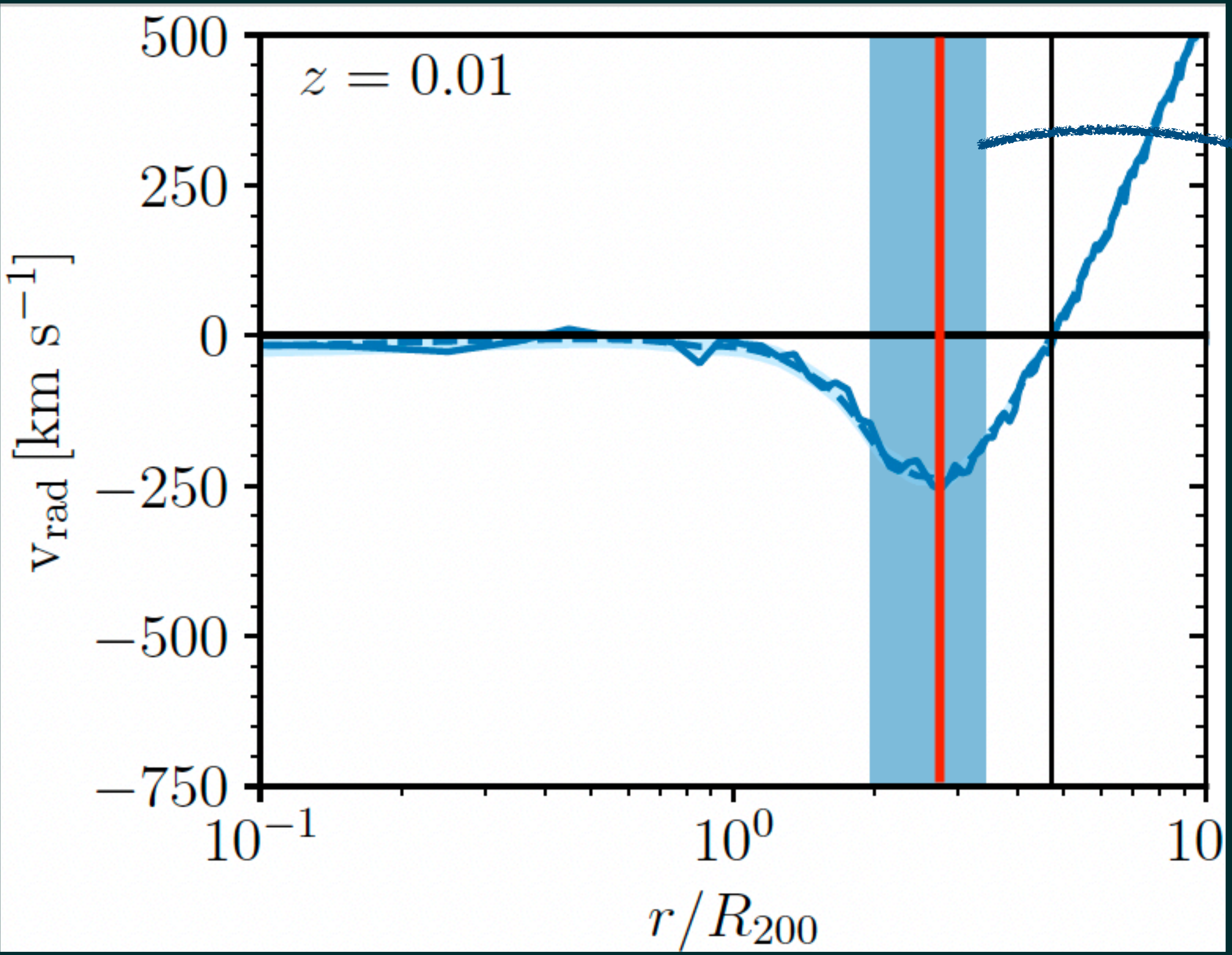

M_{shell} optimized for observations with caustic technique *(Diaferio 1999; Serra et al. 2011)*

t_{inf} from linear motion with non-constant acceleration

$\mathscr{K} \neq 1$ links MAR to $\mathrm{MAR_t}$

Observable definition of MAR

$$\mathrm{MAR} = \mathscr{K}\frac{M_{\mathrm{shell}}}{t_{\mathrm{inf}}}$$

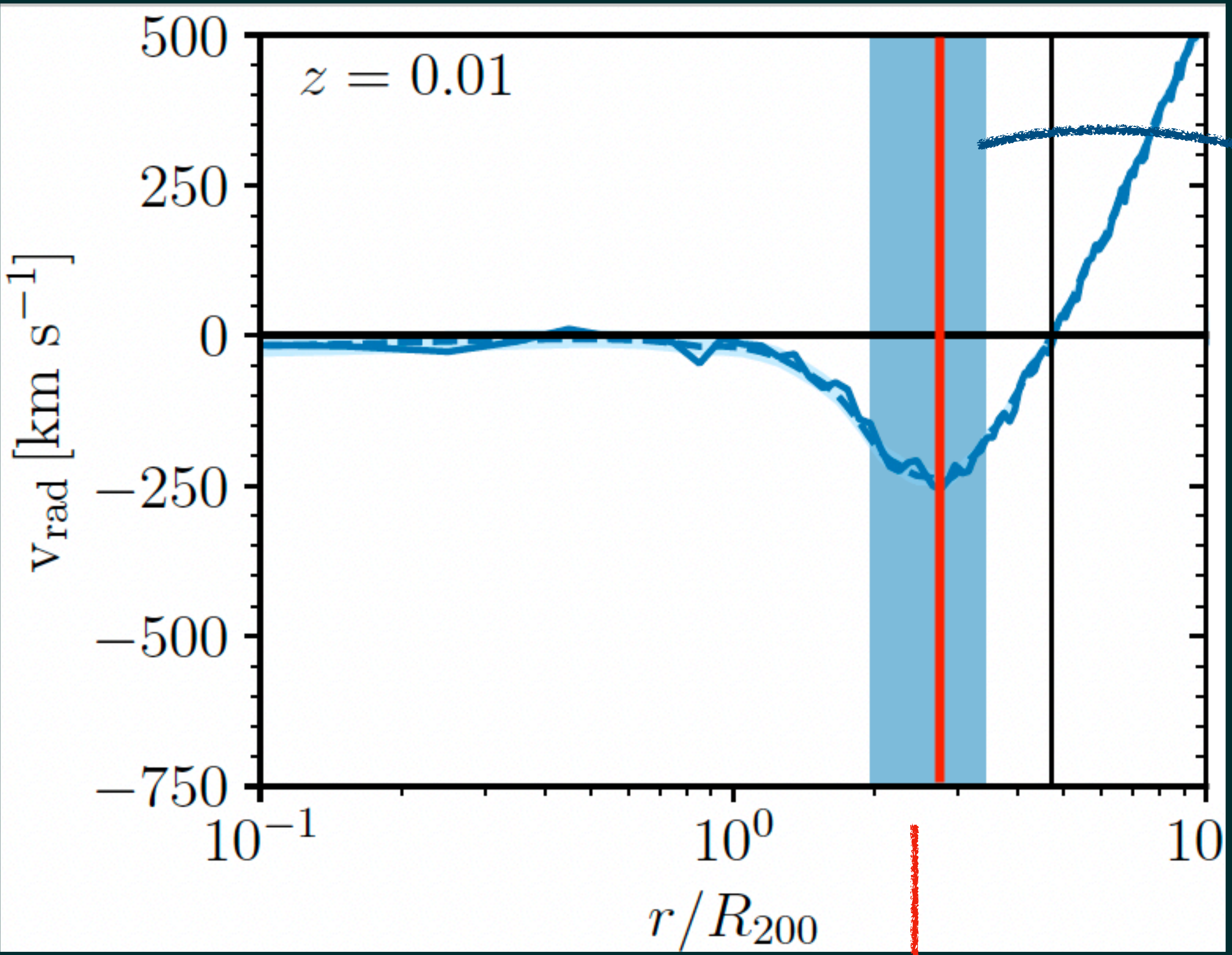

M_{shell} optimized for observations with caustic technique *(Diaferio 1999; Serra et al. 2011)*

t_{inf} from linear motion with non-constant acceleration

$\mathscr{K} \neq 1$ links MAR to $\mathrm{MAR_t}$

MAR: results

MAR: results

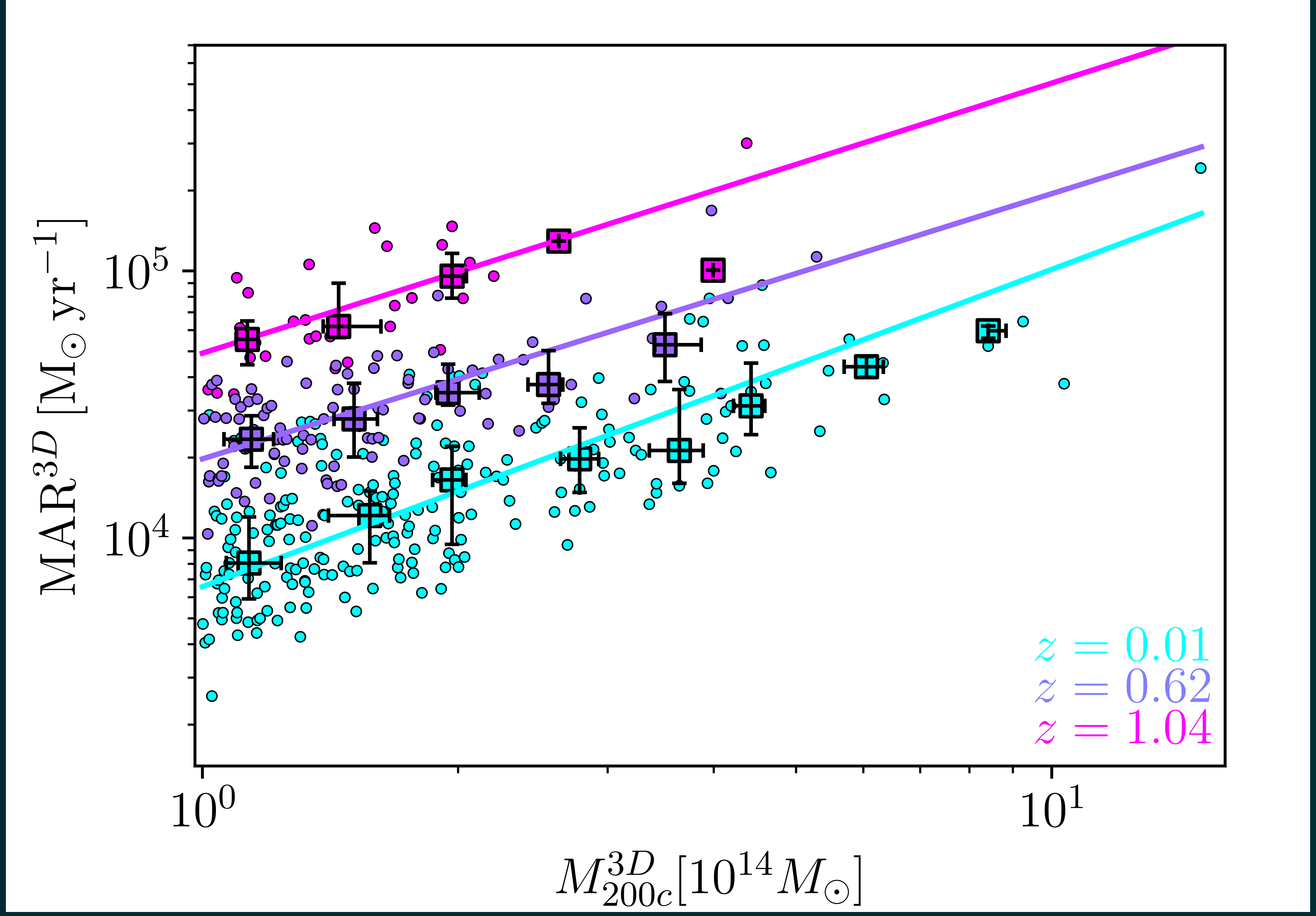

Strong correlation with cluster mass and redshift

- $M_{\mathrm{shell}} \propto M_{200}\,(\not\propto z)$
- $t_{\mathrm{inf}} \propto z\,(\not\propto M_{200})$

- MAR $\sim 10^4 - 10^5 \mathrm{M}_\odot$/yr for clusters with mass $10^{14} - 10^{15} \mathrm{M}_\odot$ and $0 \lesssim z \lesssim 1$
- Caustic (observable) MARs agree with true MARs within $\sim 10\,\%$
- Our MARs in agreement with merger-tree based MARs *(McBride+ 2009, Fakhouri+ 2010, Diemer+ 2017)*

MAR: results

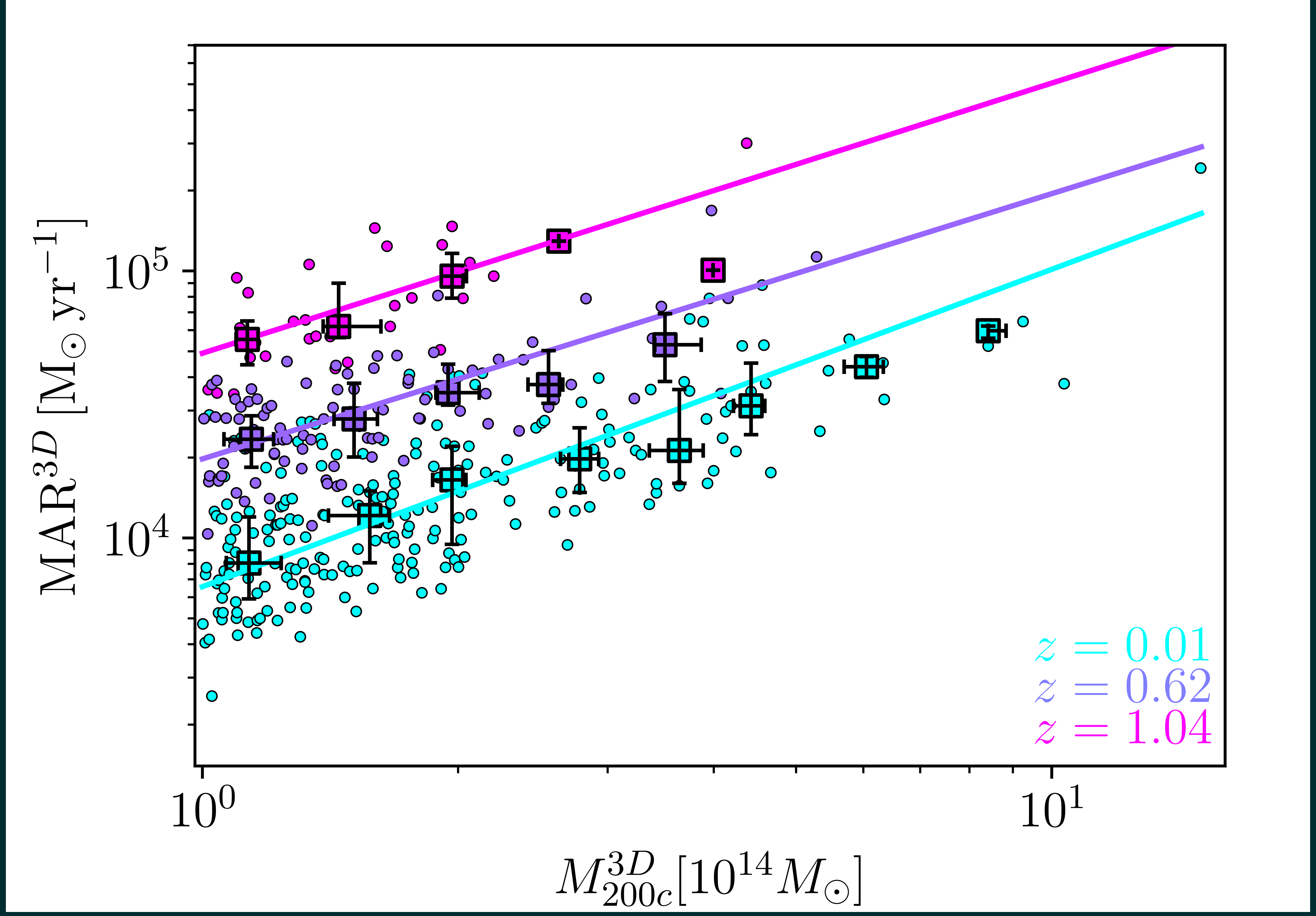

Strong correlation with cluster mass and redshift

- $M_{\rm shell} \propto M_{200}\,(\not\propto z)$
- $t_{\rm inf} \propto z\,(\not\propto M_{200})$

- MAR $\sim 10^4 - 10^5 \mathrm{M}_\odot/\mathrm{yr}$ for clusters with mass $10^{14} - 10^{15}\mathrm{M}_\odot$ and $0 \lesssim z \lesssim 1$
- Caustic (observable) MARs agree with true MARs within $\sim 10\,\%$
- Our MARs in agreement with merger-tree based MARs *(McBride+ 2009, Fakhouri+ 2010, Diemer+ 2017)*

(More details in Pizzardo et al. 2023, A&A, 680, A48)

Conclusions

- We use the ***galaxy radial velocity*** profiles $\mathrm{v}_{\mathrm{rad}}$ of 1697 ***IllustrisTNG clusters*** to explore their infalling region
- $\mathrm{v}_{\mathrm{rad}}$ allows to derive turnaround radius and minimum radial velocity radius
- We develop two ***new dynamical radii*** that mark the ***inner boundary of the infall*** region: R_{infl} and $R_{\sigma_{\mathrm{v}}/\mathrm{v}_{\mathrm{rad}}}$
- R_{infl} and $R_{\sigma_{\mathrm{v}}/\mathrm{v}_{\mathrm{rad}}}$ ***coincide*** with R_{spl} to within 1σ
- We show how galaxies as well as matter particles show clear signatures of the splashback physics
- We show how dynamical radii inform the observable study of ***cluster growth***.

Backup slides

The caustic technique

- Mass profile $M^C(r)$ beyond virialization
- It exploits the ***pattern*** of infall galaxies
- ***Independent*** from redshift and dynamical state

- $M^C(r)$ within $\sim 10\,\%$ of true $M^{3D}(r)$ up to $4R_{200c}$; uncertainty $\sim 20\% - 40\,\%$

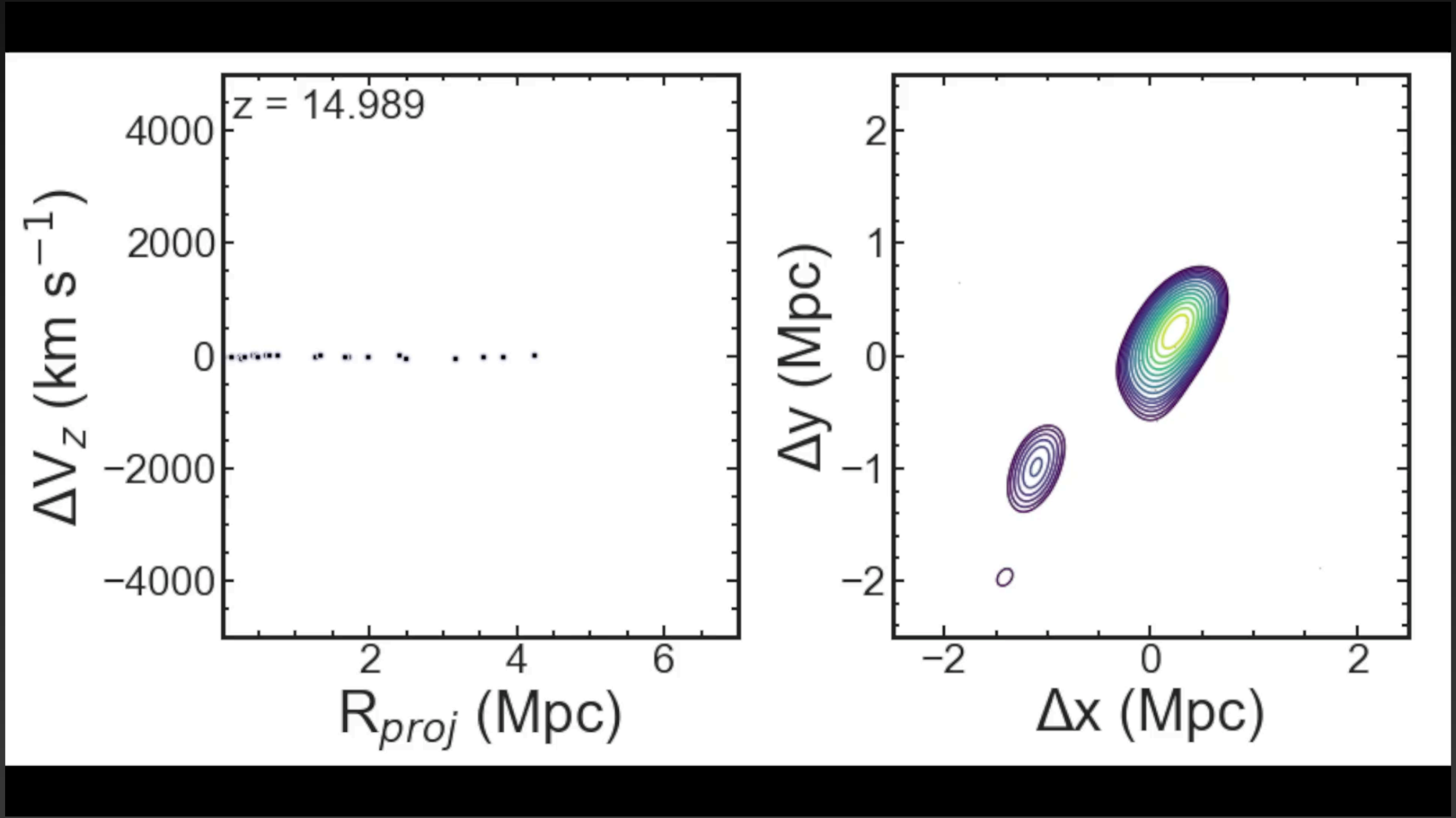

Credits: J. Sohn

The caustic technique

- Mass profile $M^C(r)$ beyond virialization
- It exploits the ***pattern*** of infall galaxies
- ***Independent*** from redshift and dynamical state

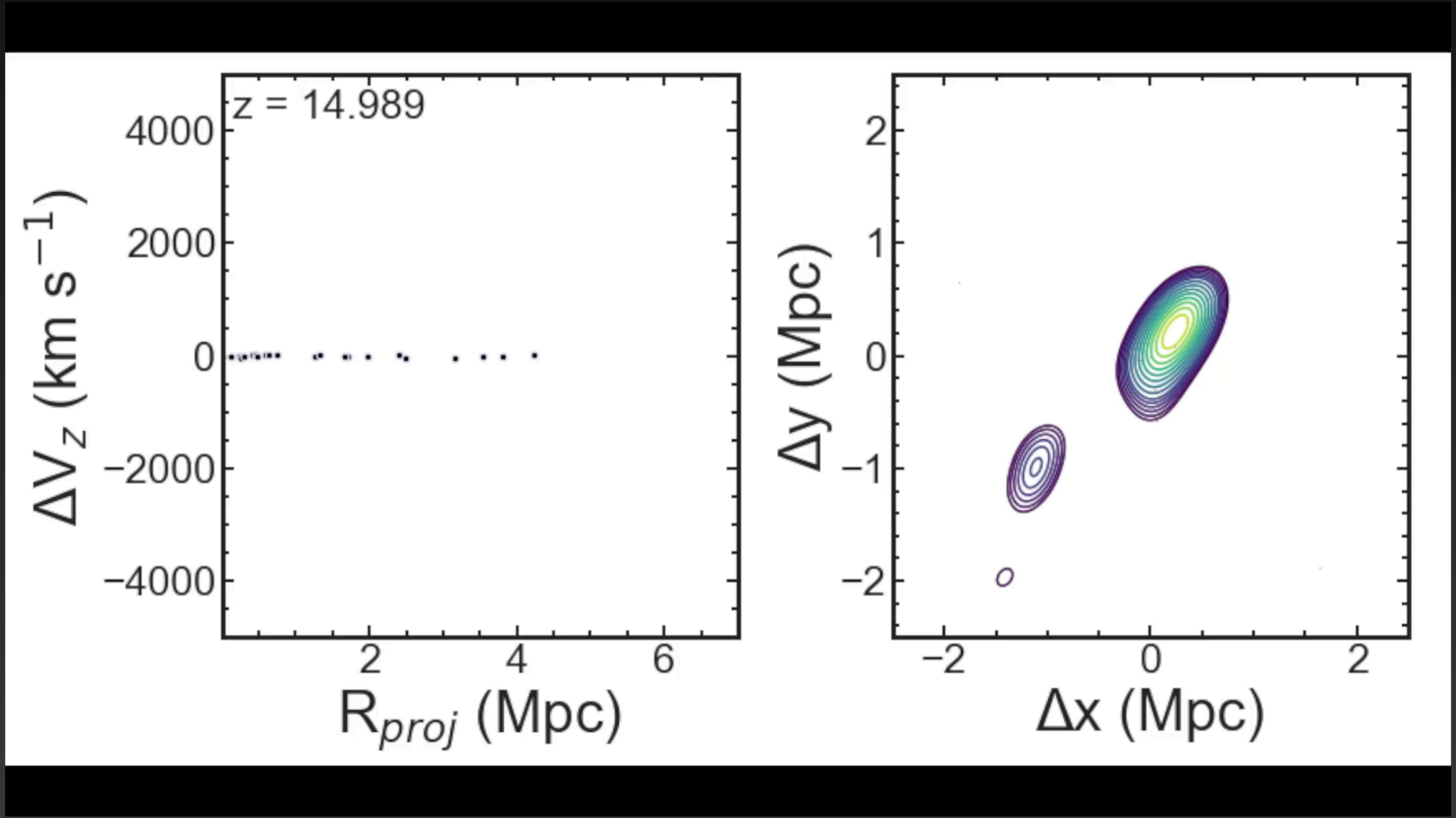

- $M^C(r)$ within $\sim 10\,\%$ of true $M^{3D}(r)$ up to $4R_{200c}$;

  uncertainty $\sim 20\% - 40\,\%$

Credits: J. Sohn

The caustic technique

The caustic technique

Data retrieval

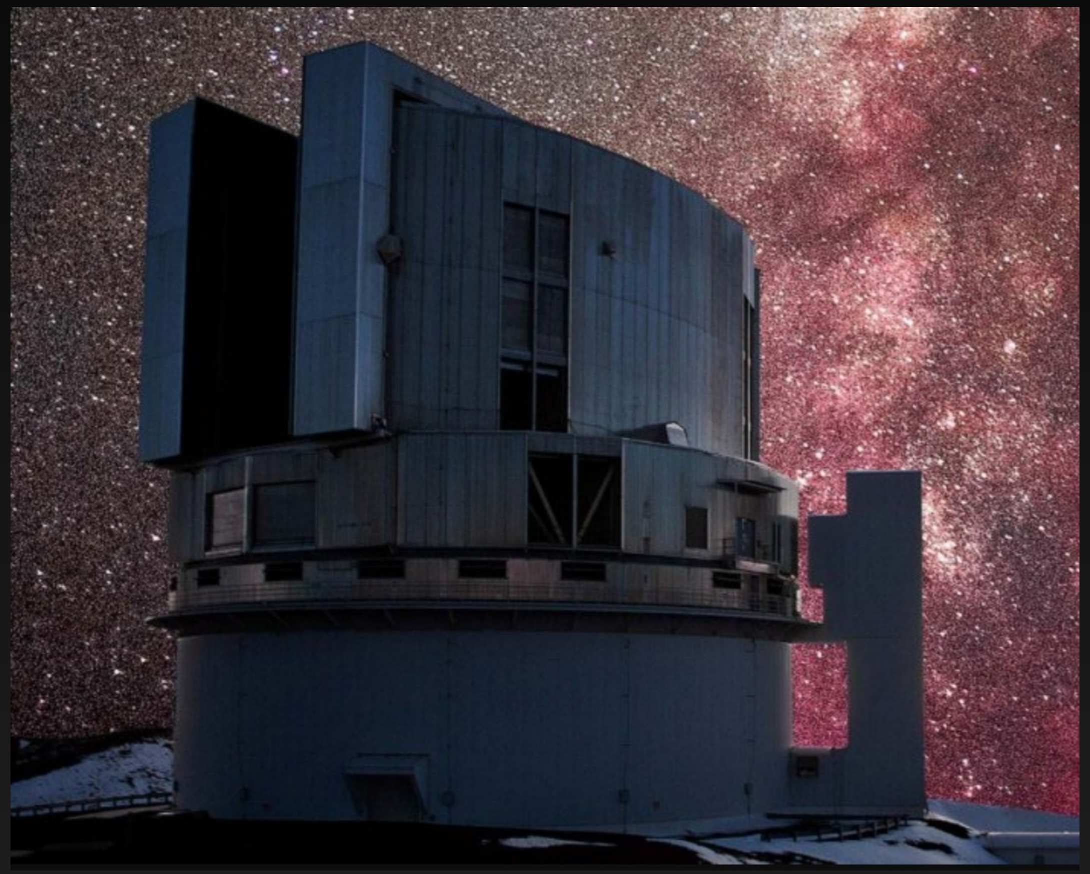

ABELL 1314

id	RA [deg]	δ [deg]	z	g	⋯
1	177.318260	49.589084	0.47415	19.3198	
2	177.379809	49.606580	0.05509	16.9693	
3	177.336652	49.615467	0.09051	17.4208	
4	177.352944	49.589621	0.05865	16.5336	
5	177.383568	49.542269	0.29258	18.8525	
⋯					

The caustic technique

Data retrieval

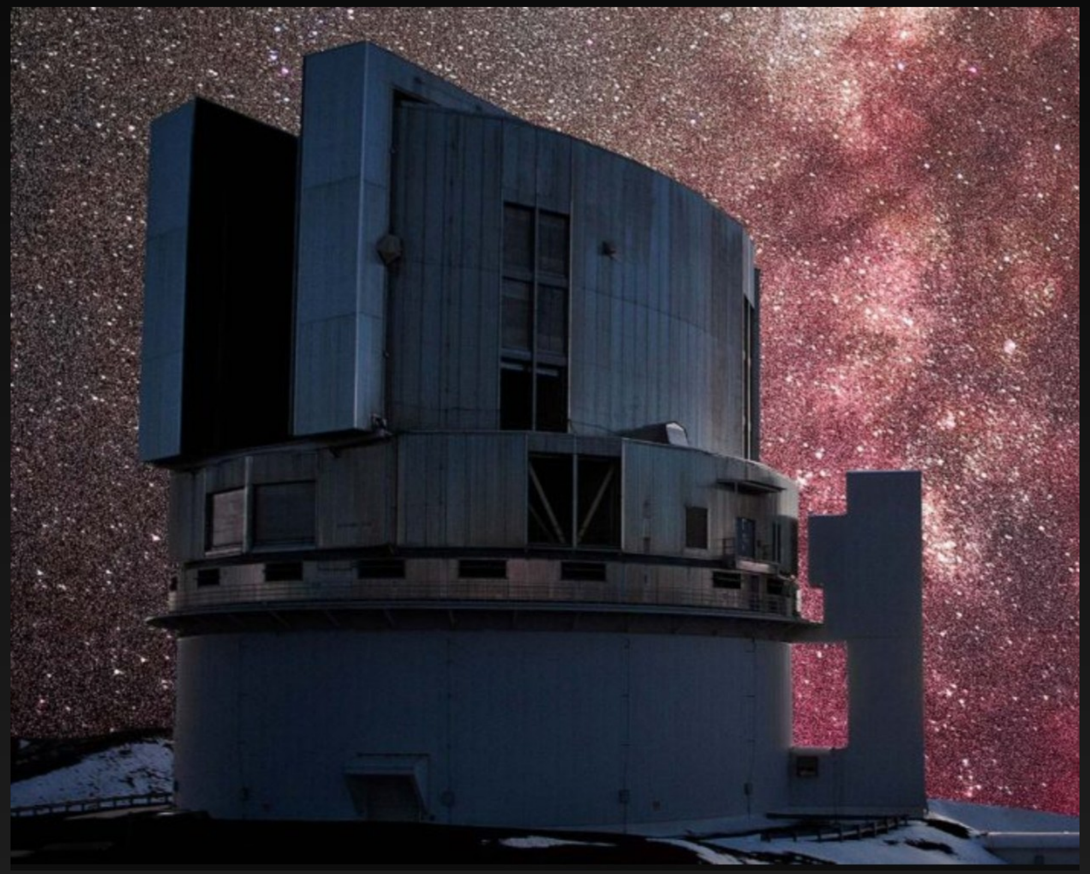

Caustic technique

ABELL 1314

id	RA [deg]	δ [deg]	z	g	⋯
1	177.318260	49.589084	0.47415	19.3198	
2	177.379809	49.606580	0.05509	16.9693	
3	177.336652	49.615467	0.09051	17.4208	
4	177.352944	49.589621	0.05865	16.5336	
5	177.383568	49.542269	0.29258	18.8525	
⋯					

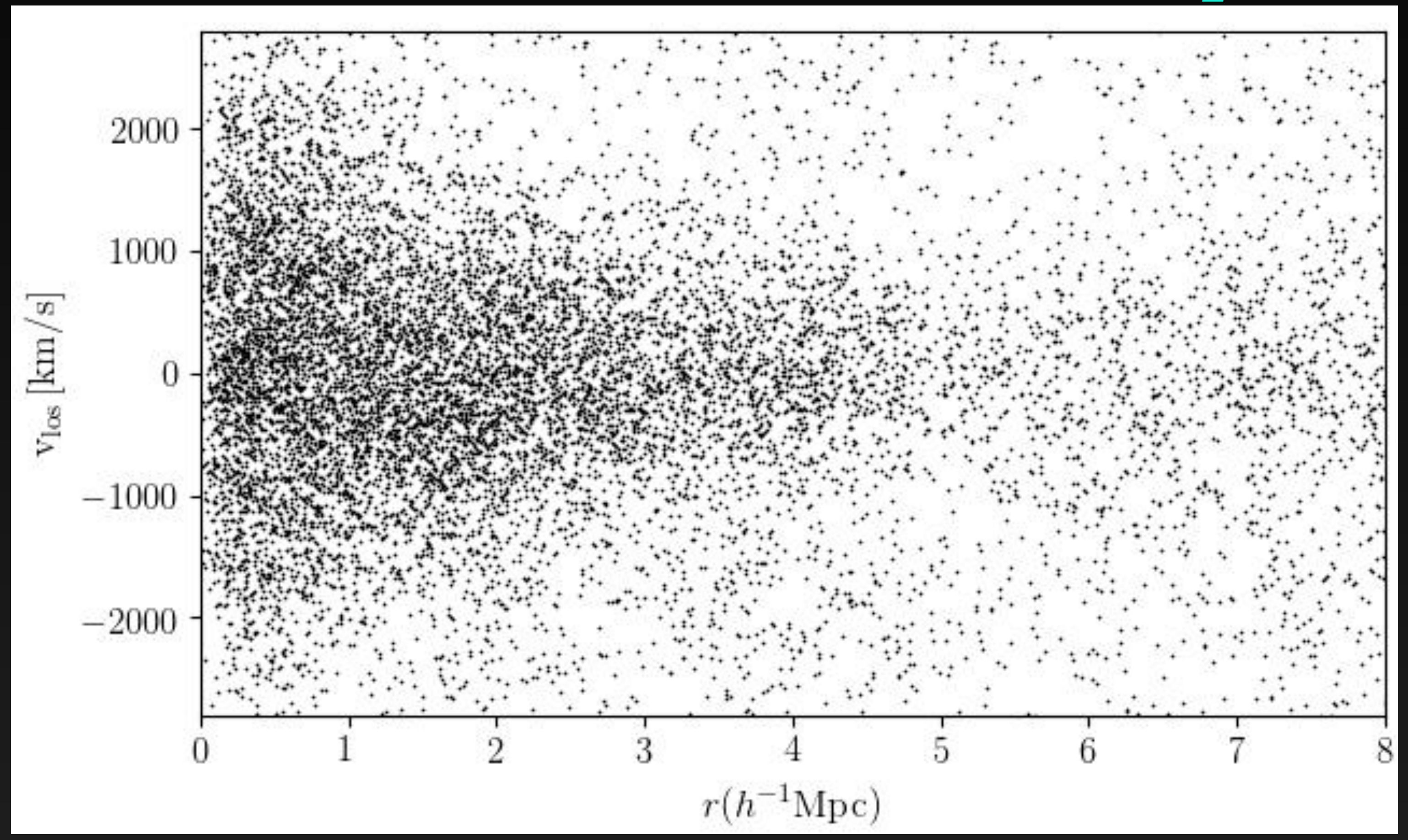

$$f_{2D}(r, v) = \kappa$$

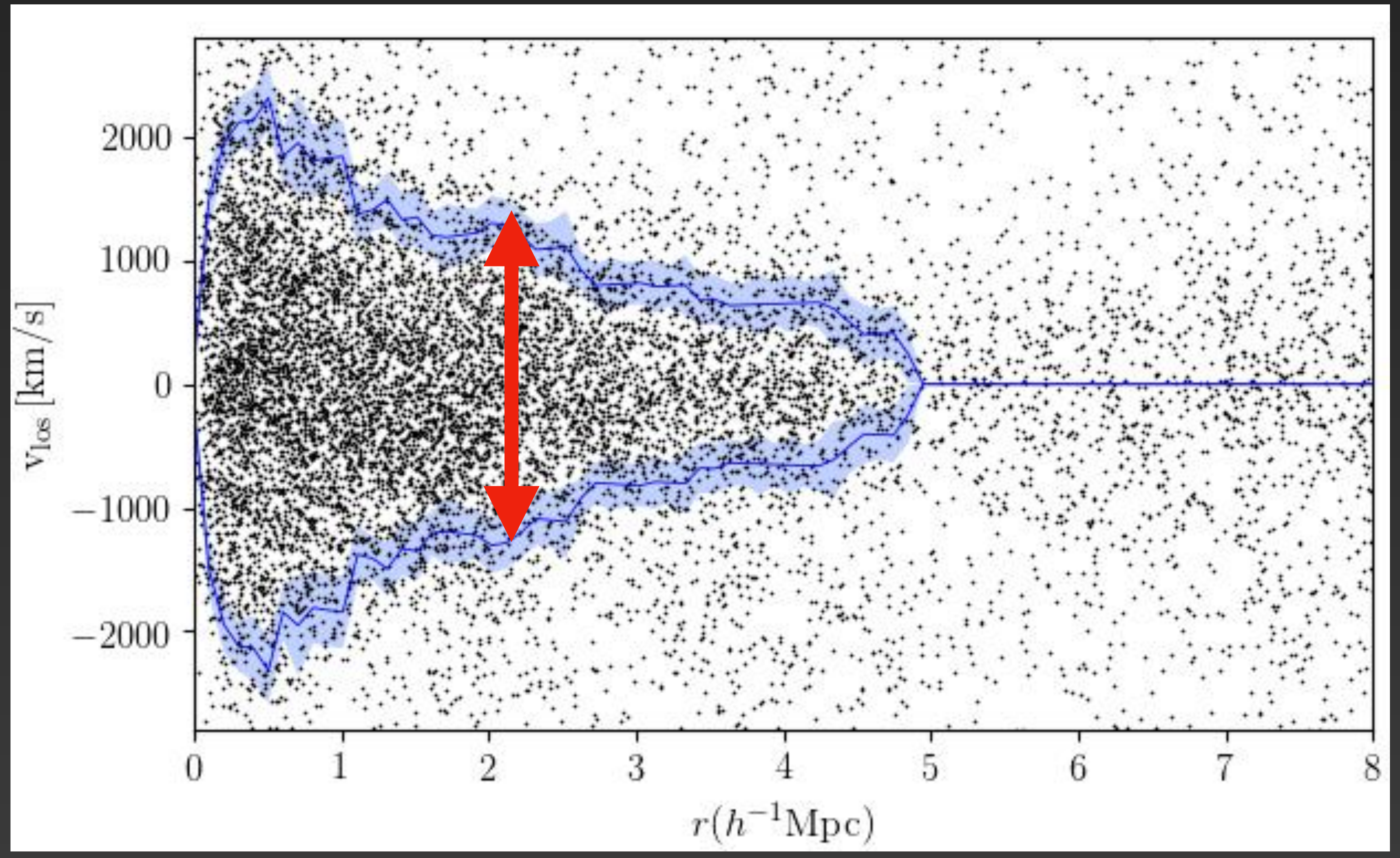

The caustic technique

Data retrieval

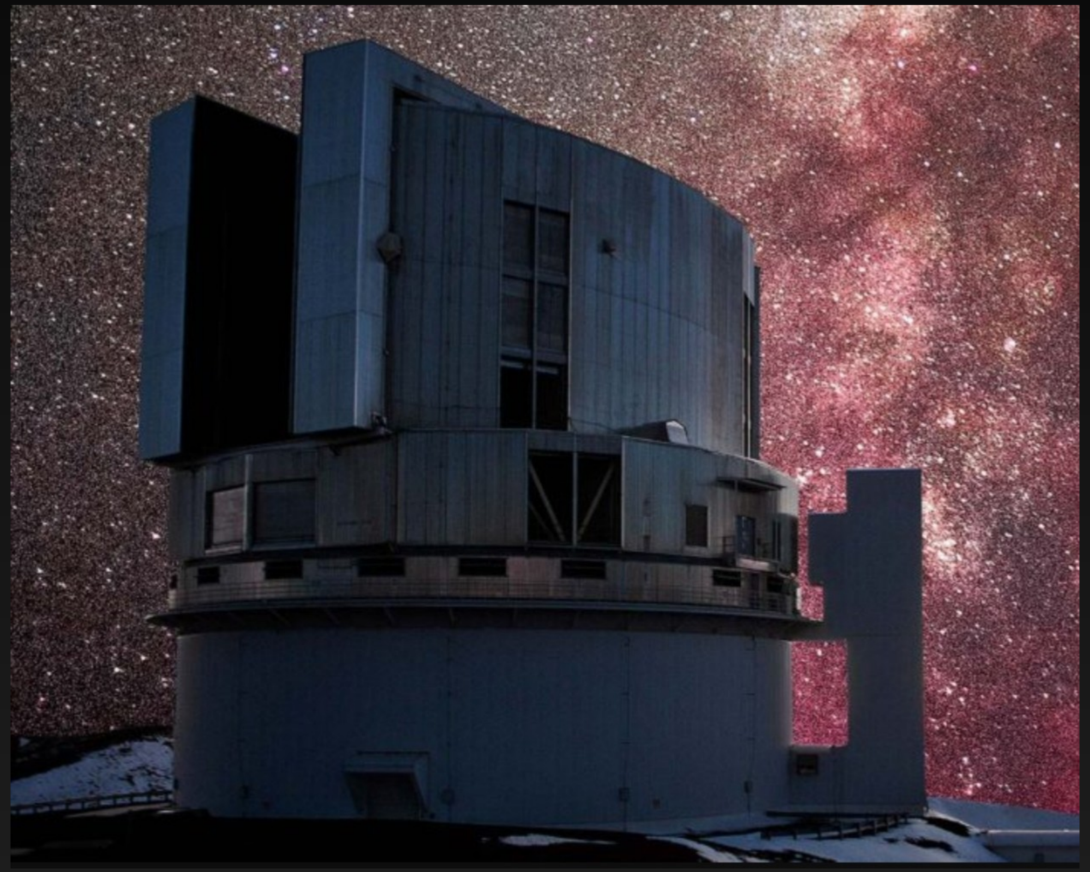

ABELL 1314

id	RA [deg]	δ [deg]	z	g	···
1	177.318260	49.589084	0.47415	19.3198	
2	177.379809	49.606580	0.05509	16.9693	
3	177.336652	49.615467	0.09051	17.4208	
4	177.352944	49.589621	0.05865	16.5336	
5	177.383568	49.542269	0.29258	18.8525	
···					

Caustic technique

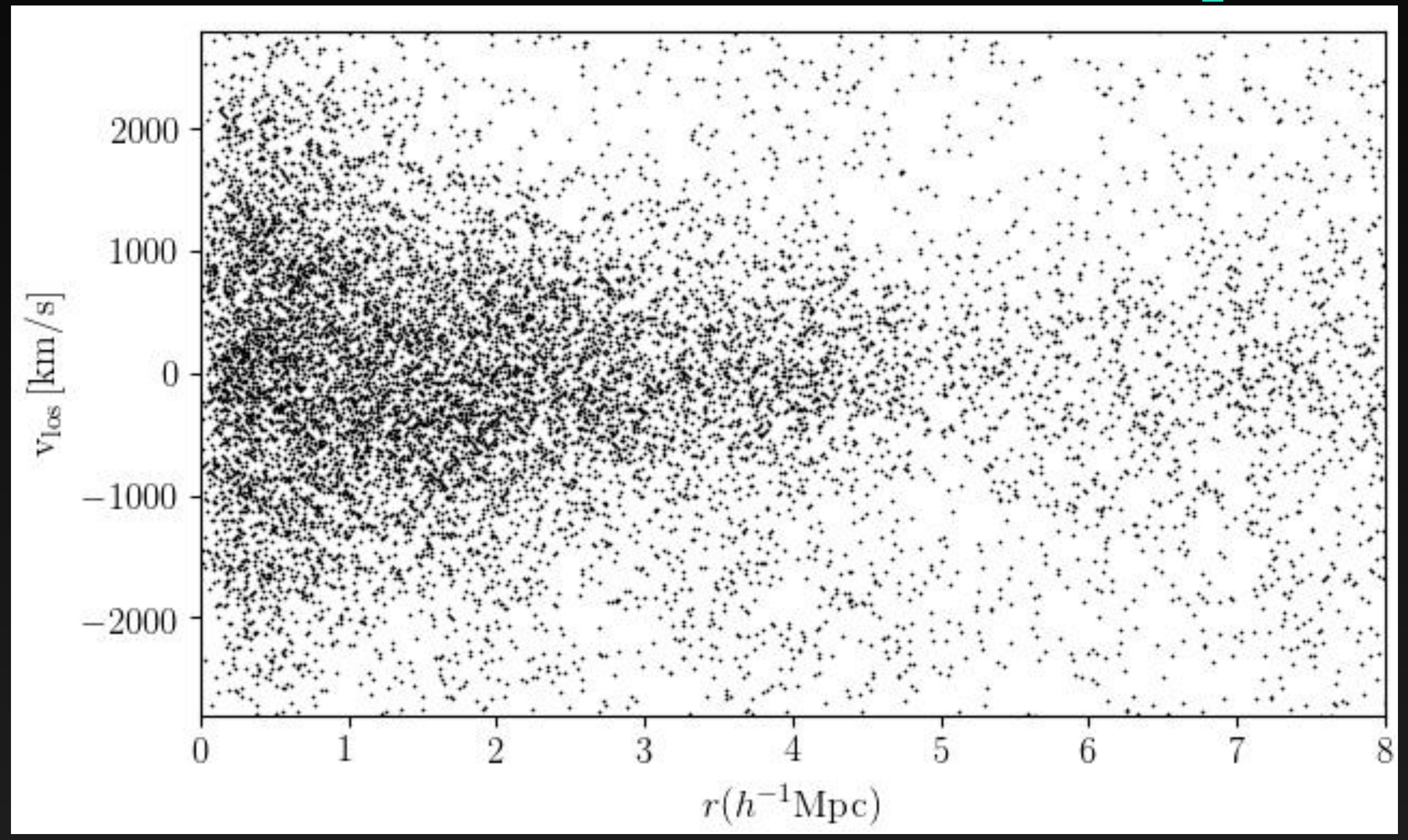

$$f_{2D}(r, v) = \kappa$$

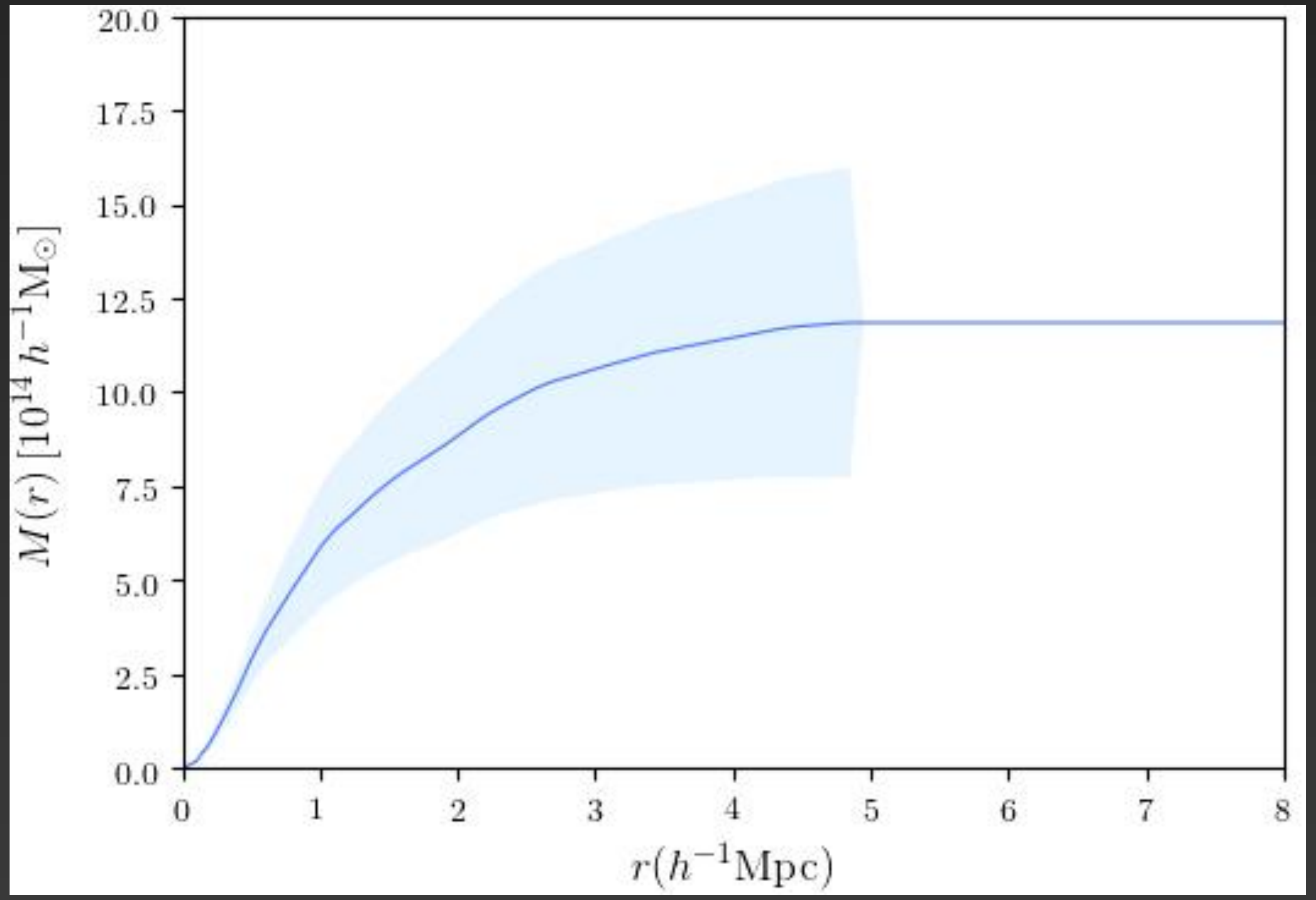

$$-2\phi = < v_{esc}^2 >$$

$$M(<r) \propto \int_0^r \mathscr{A}^2(r)\mathrm{d}\tilde{r}$$

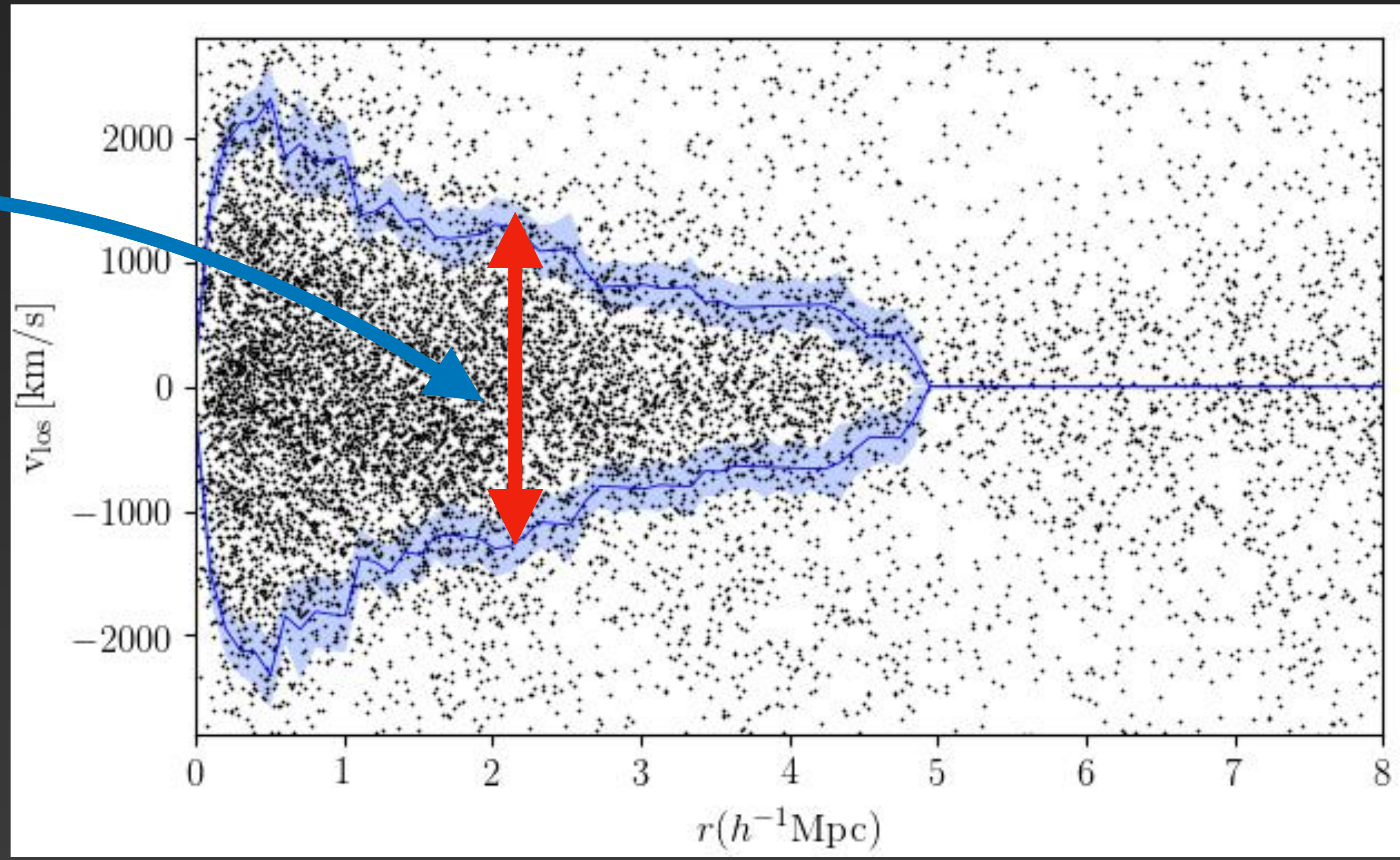

Observable definition of MAR

Observable definition of MAR

$$\mathrm{MAR} = \mathscr{K}\frac{M_{\mathrm{shell}}}{t_{\mathrm{inf}}}$$

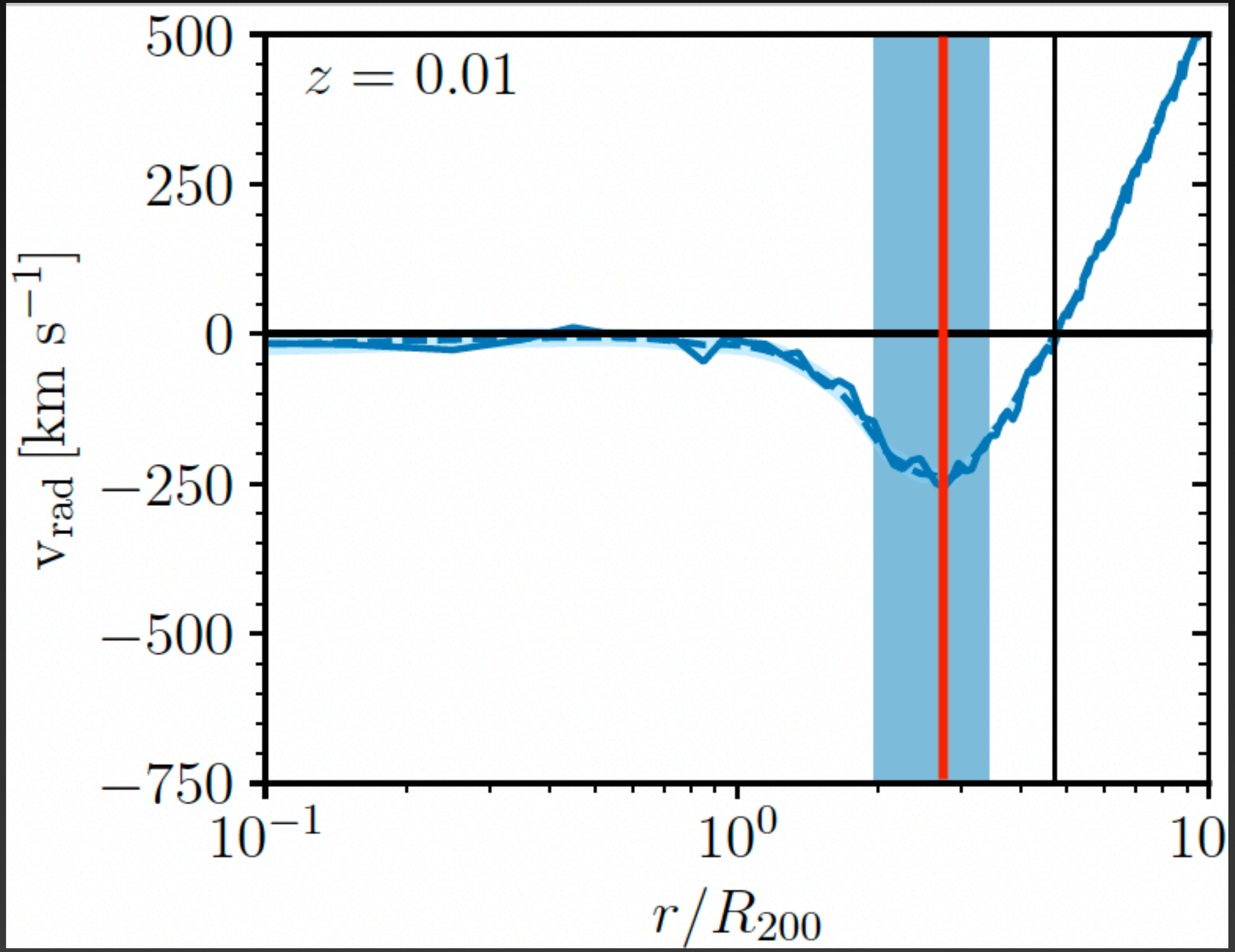

Observable definition of MAR

$$\mathrm{MAR} = \mathscr{K}\frac{M_{\rm shell}}{t_{\rm inf}}$$

$M_{\rm shell}$ optimized for observations with CT

$t_{\rm inf}$ from linear motion with non-constant acceleration

$\mathscr{K} \neq 1$ links MAR to $\mathrm{MAR_t}$

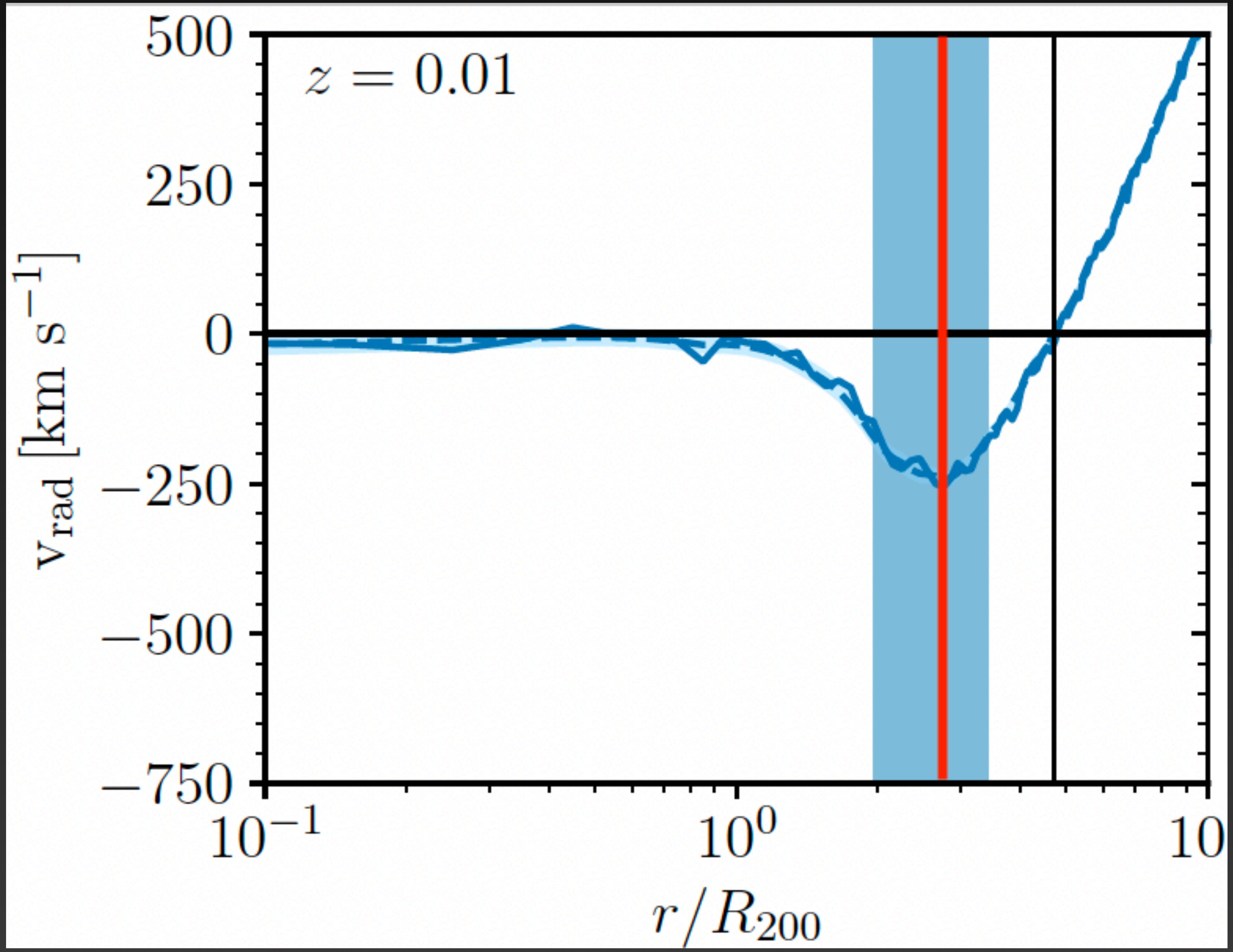

Calibration of the MAR

Calibration of the MAR

Mock catalogues of 1318 TNG clusters

Calibration of the MAR

Mock catalogues of 1318 TNG clusters

- Optimal shell thickness (Av_{min})

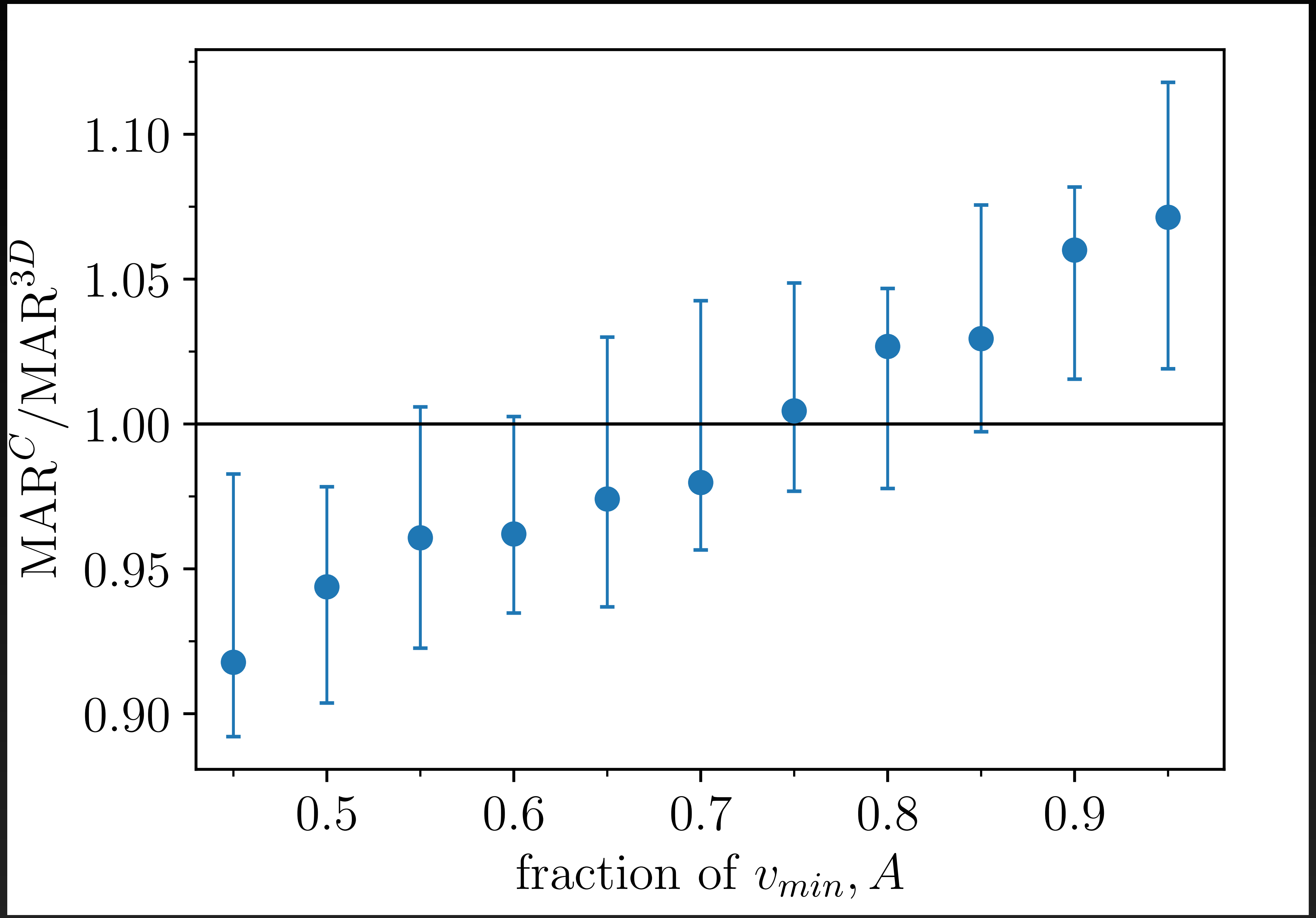

$A = 0.72$

Calibration of the MAR

Mock catalogues of 1318 TNG clusters

- Optimal shell thickness (Av_{min})
- $\mathscr{K}$ to link MAR to $\mathrm{MAR_t}$

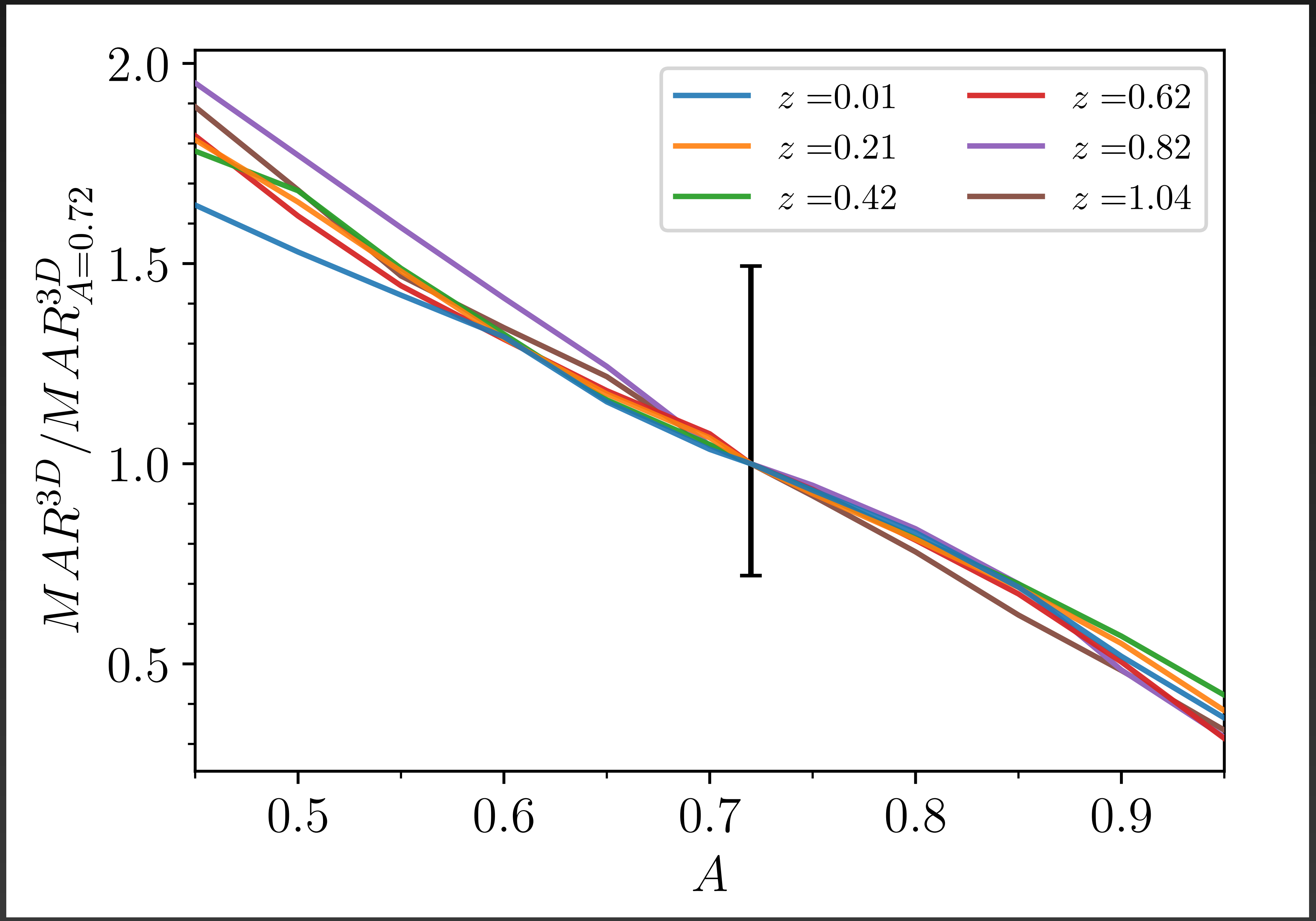

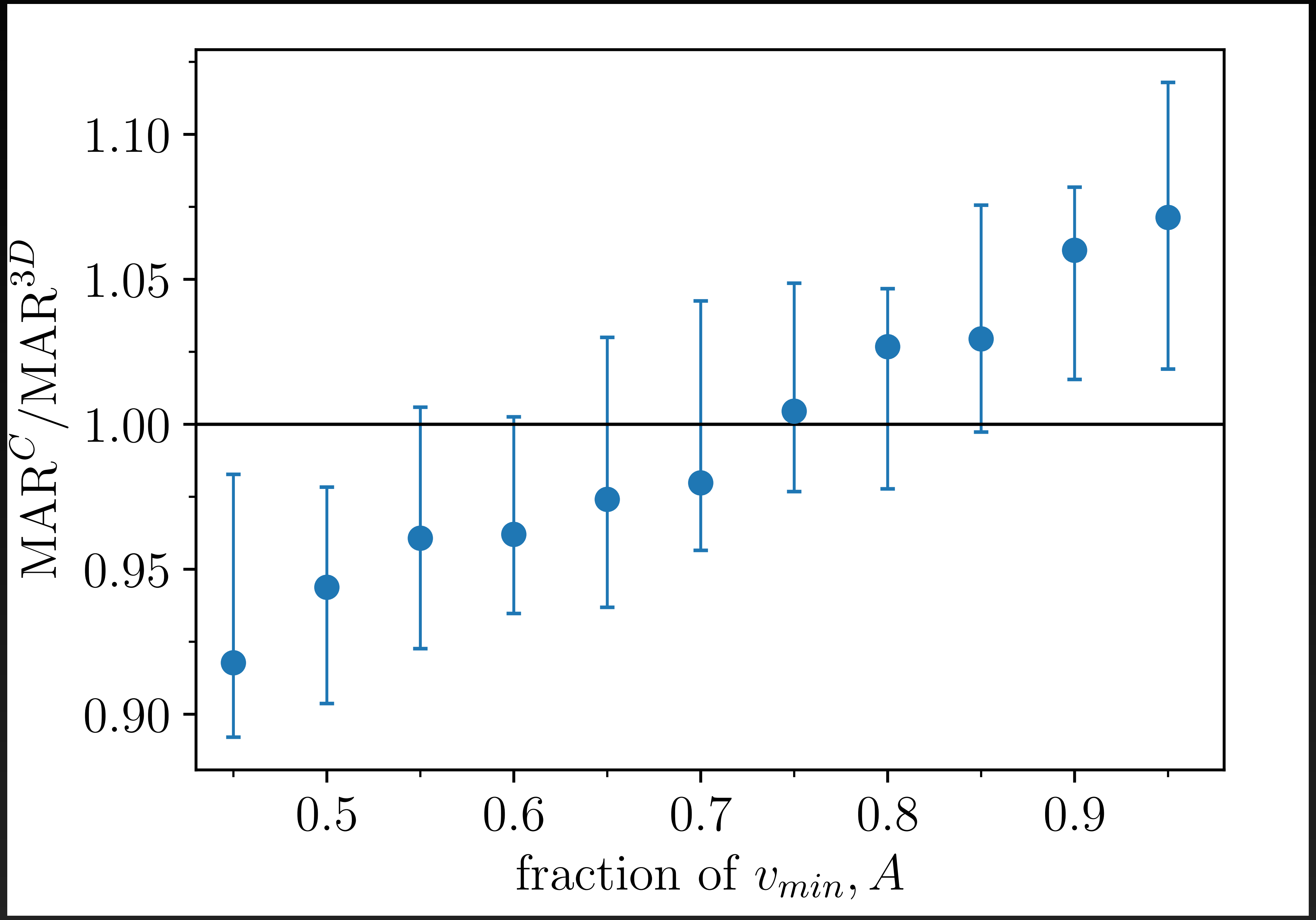

$$A = 0.72$$

$$\mathrm{MAR_t} \simeq 0.35\mathrm{MAR}$$

Caustic vs True mass profile

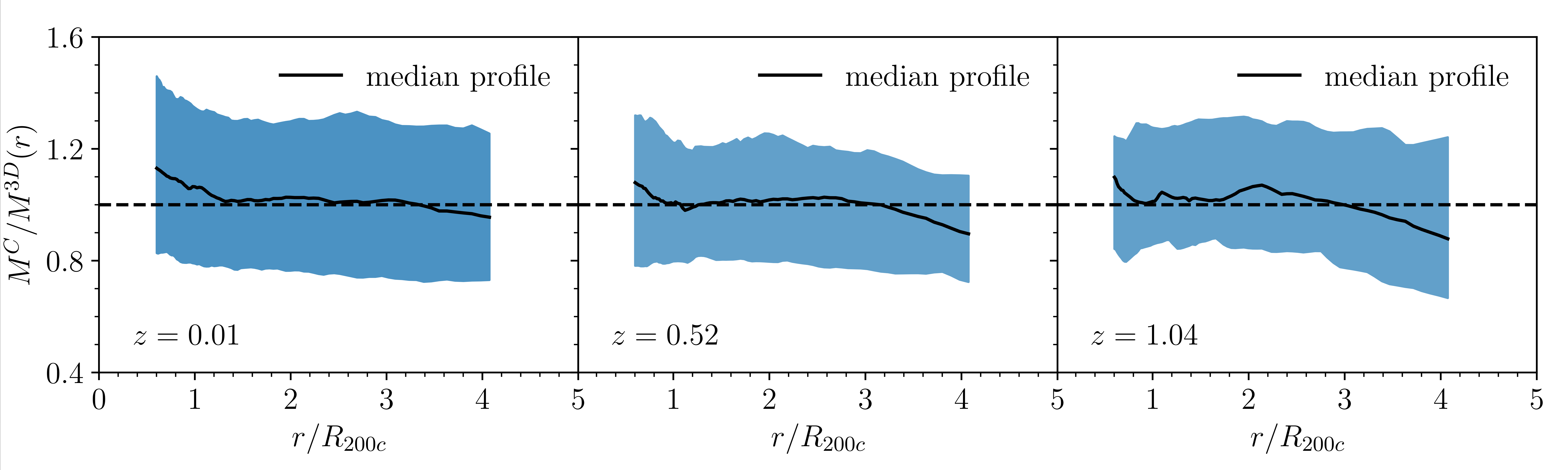

(More details in Pizzardo et al. 2023, A&A, 675, A56)

Expectations for M_{shell}

Strong correlation with cluster ***mass***

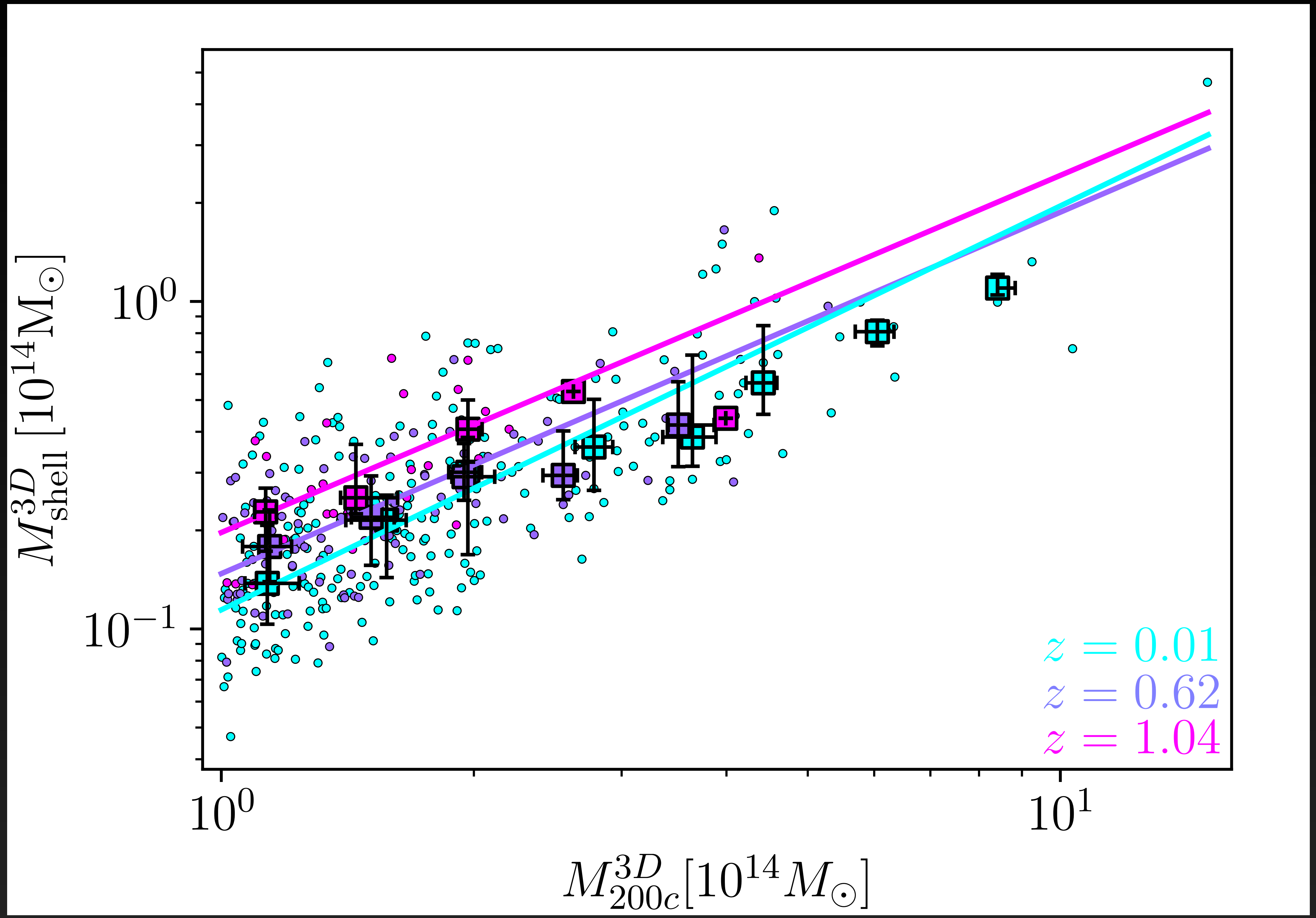

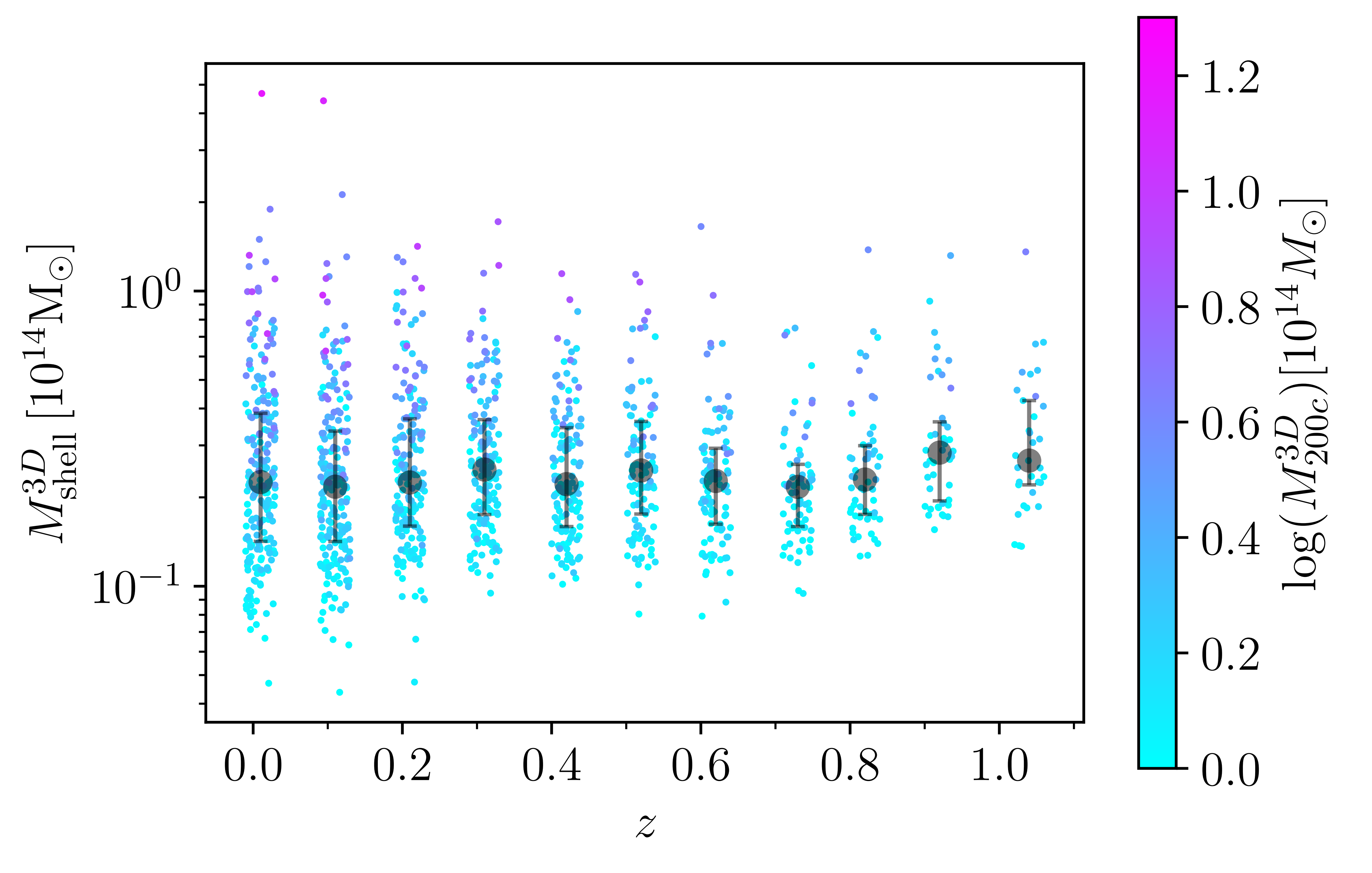

Weak correlation with redshift

The infall time, t_{inf}

Time for the center of the infalling shell to reach R_{200c}

Linear motion with non-constant Newtonian acceleration

The infall time, t_{inf}

Time for the center of the infalling shell to reach R_{200c}

Linear motion with non-constant Newtonian acceleration

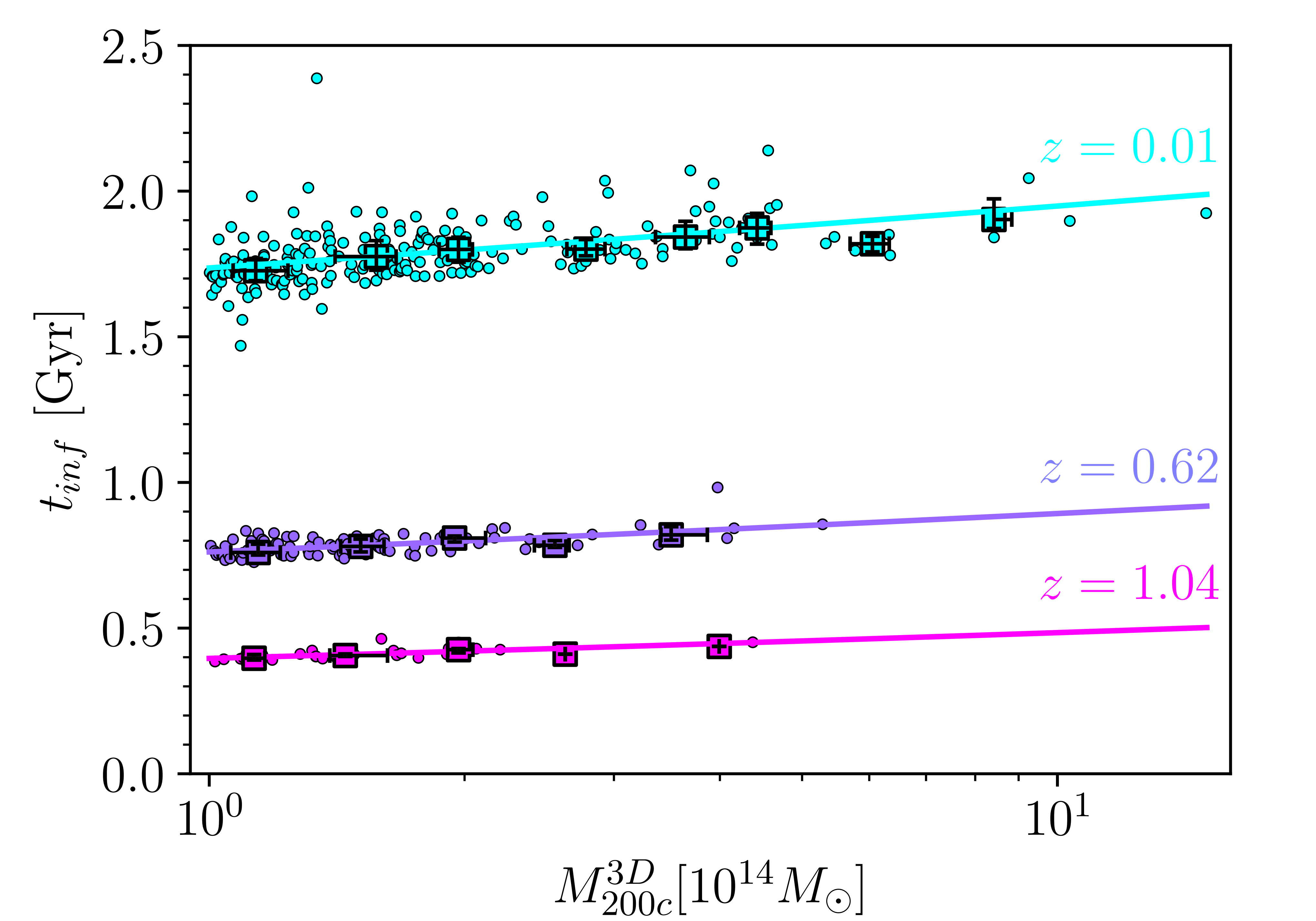

Strong correlation with redshift

The infall time, $t_{\rm inf}$

Time for the center of the infalling shell to reach R_{200c}

Linear motion with non-constant Newtonian acceleration

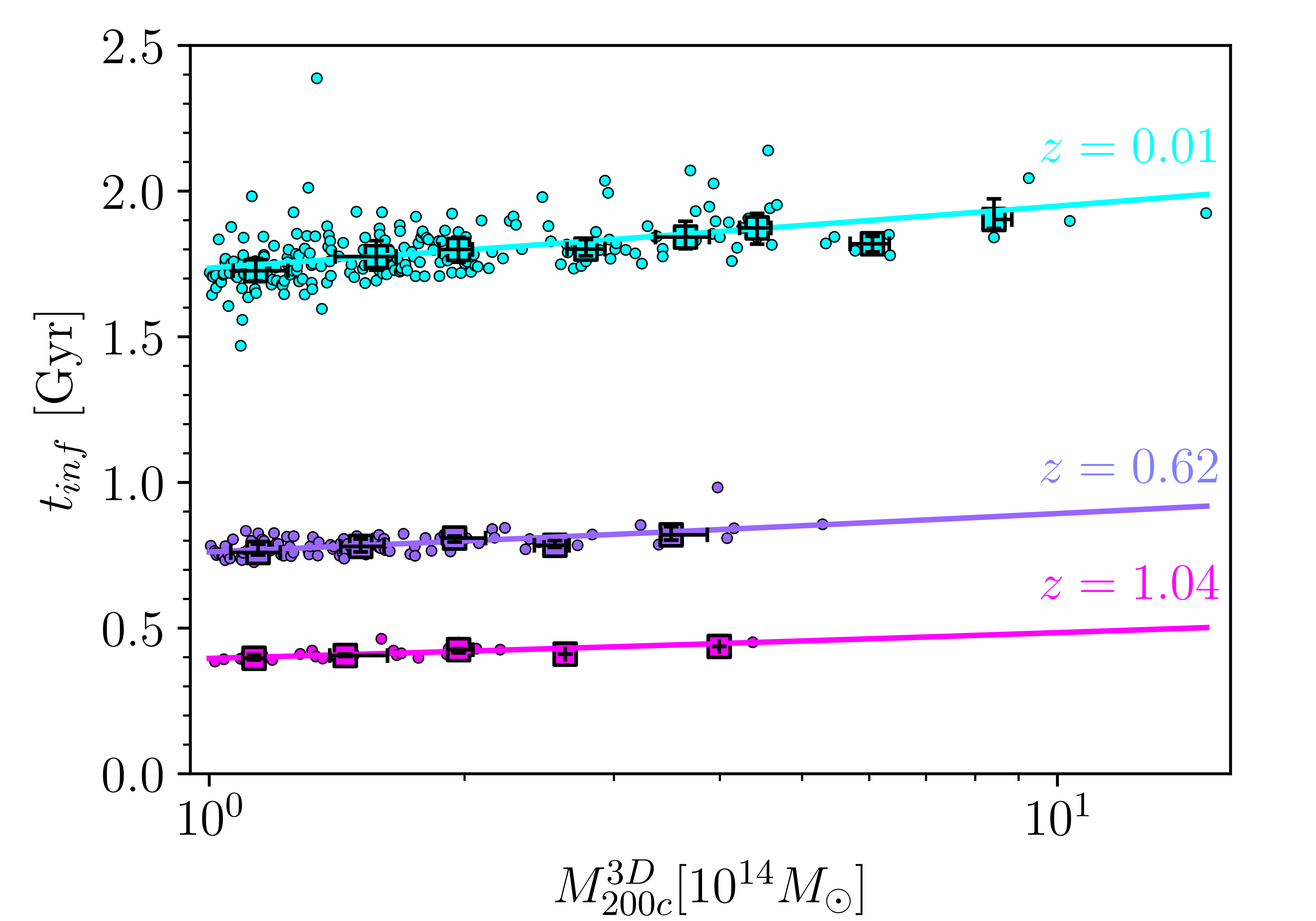

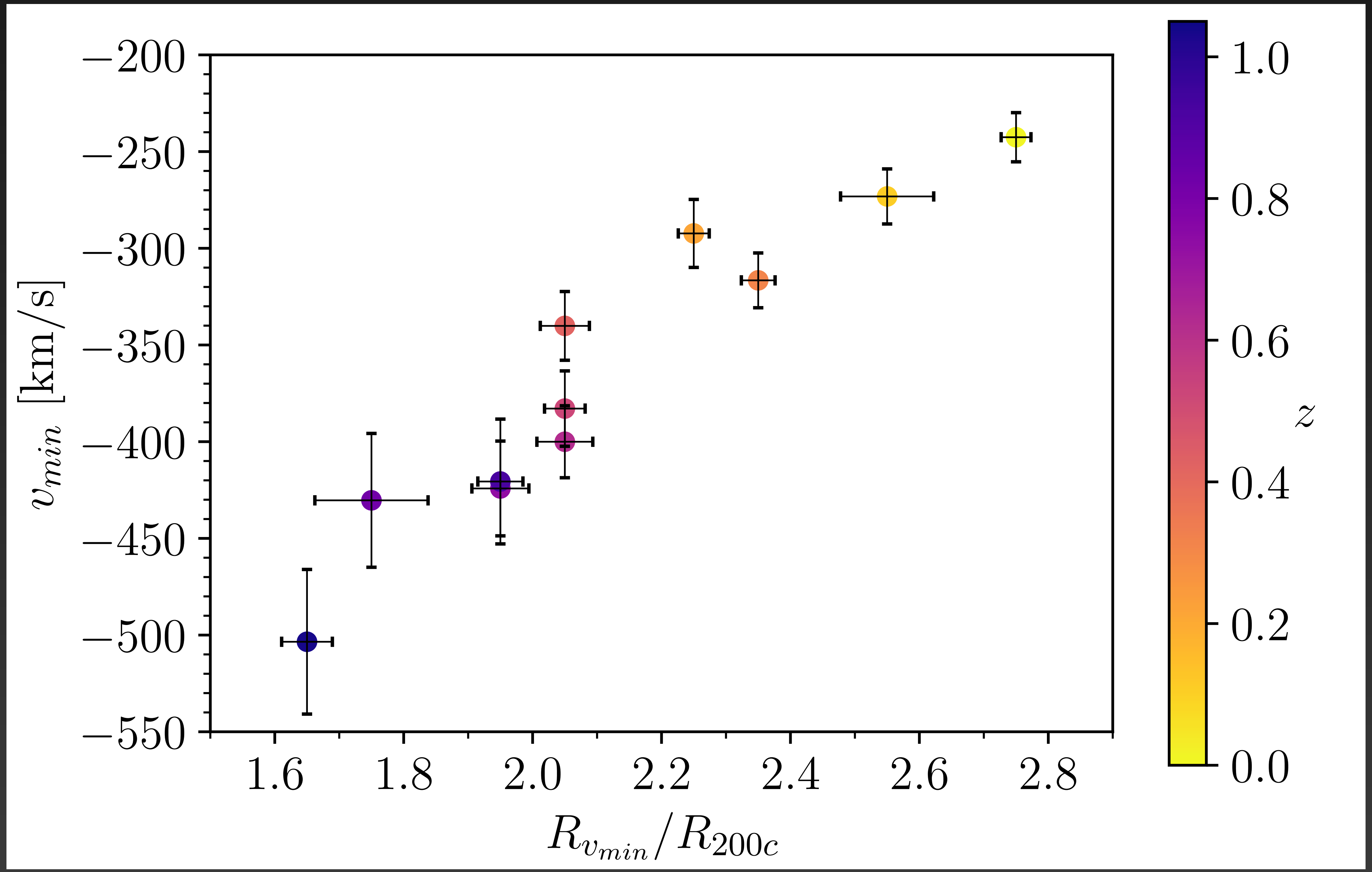

Strong correlation with redshift

The infall time, t_{inf}

Time for the center of the infalling shell to reach R_{200c}

Linear motion with non-constant Newtonian acceleration

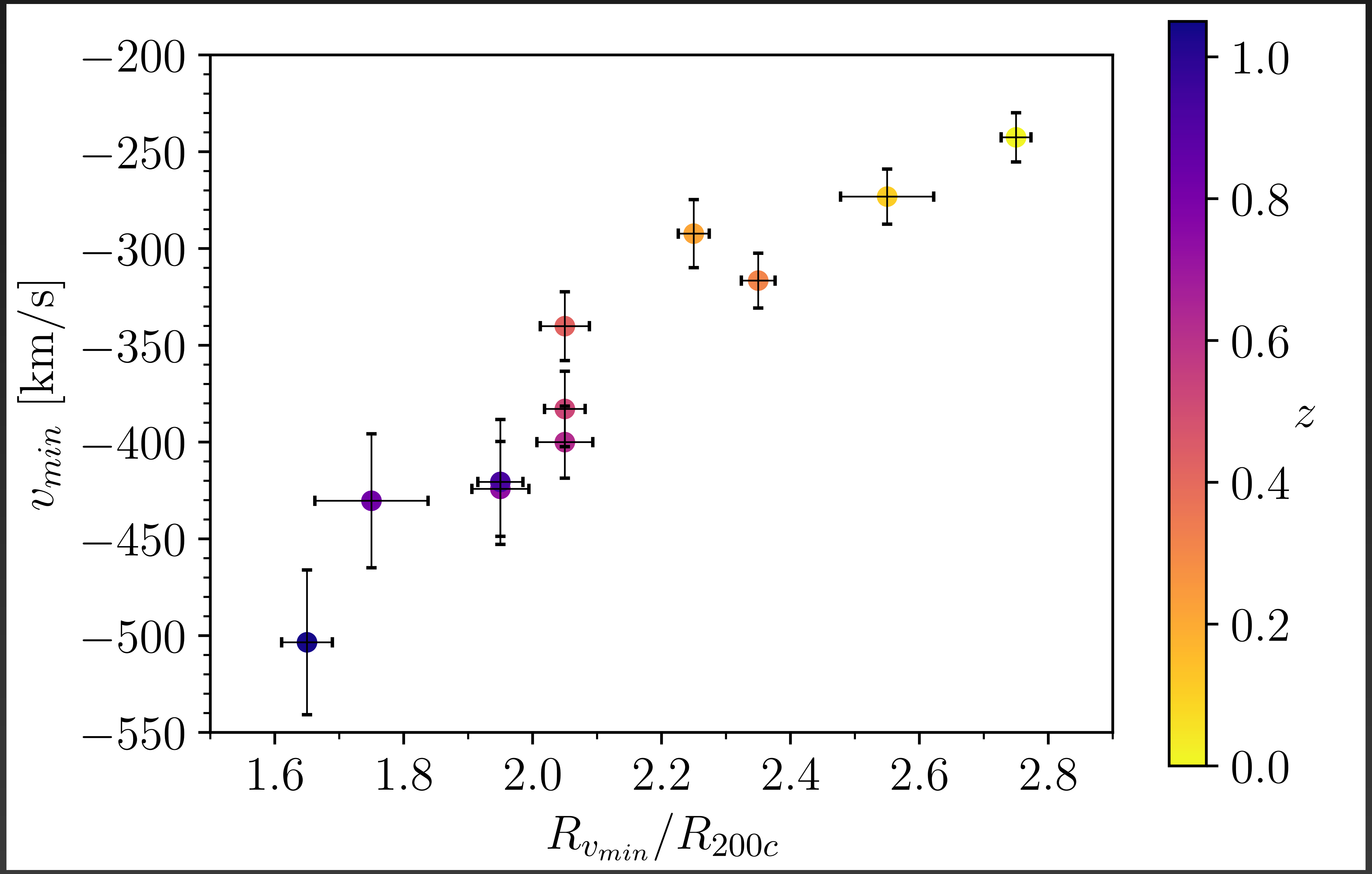

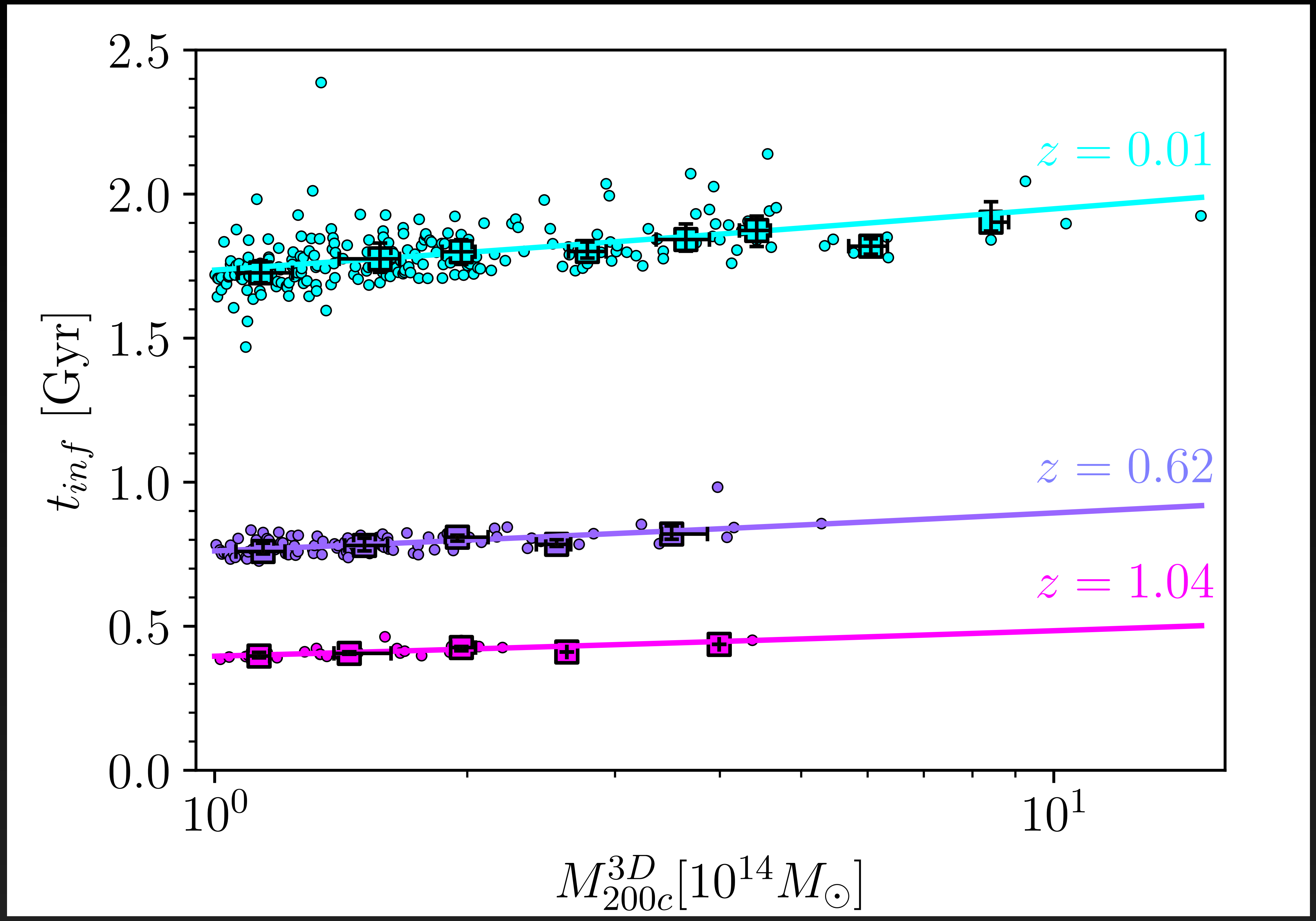

Strong correlation with redshift

Weak correlation with cluster mass

MAR: results

MAR: results

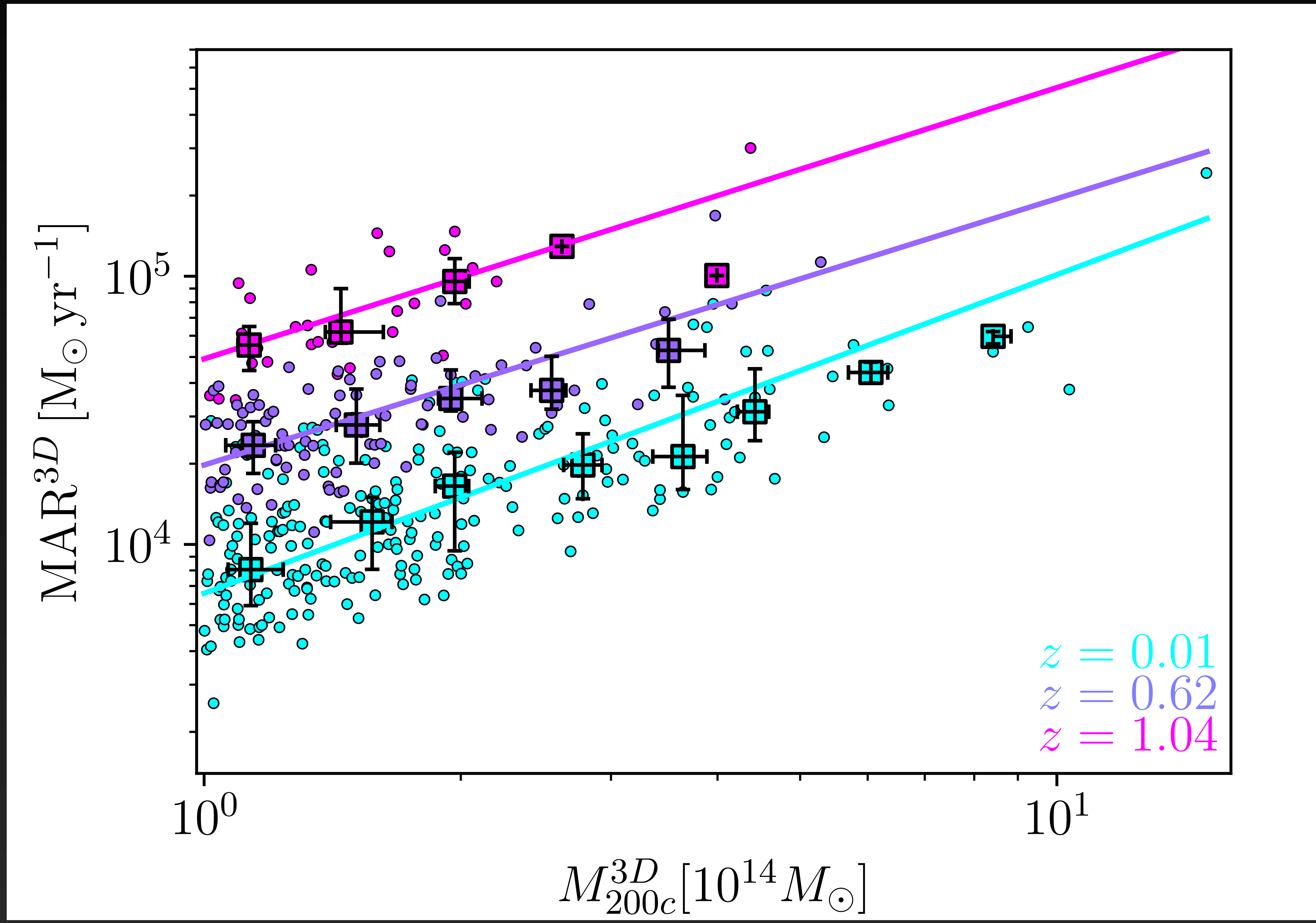

Strong correlation with clusters' mass and redshift

$$\mathrm{MAR} \sim 10^4 - 10^5 \mathrm{M}_\odot/\mathrm{yr}$$

MAR: results

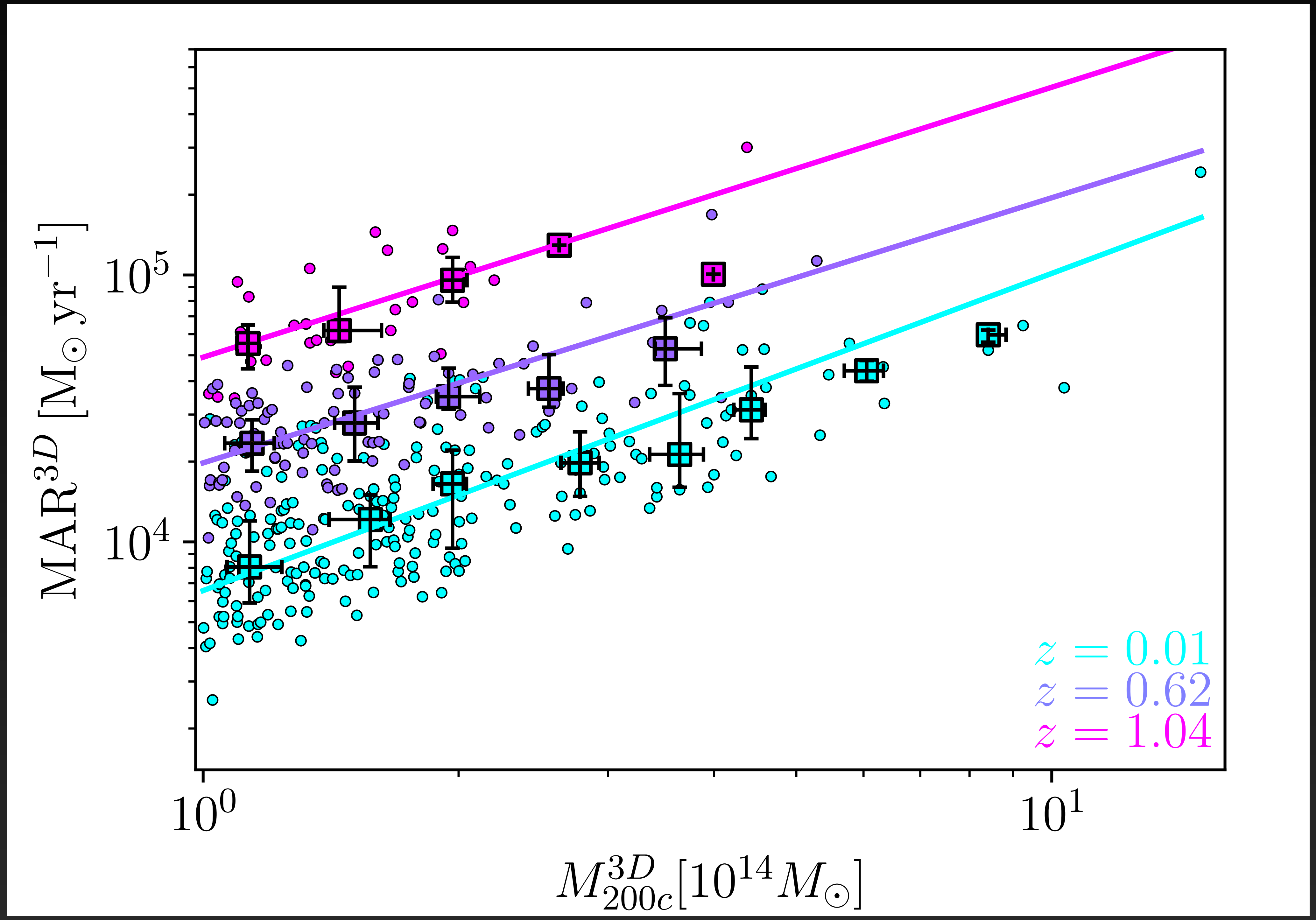

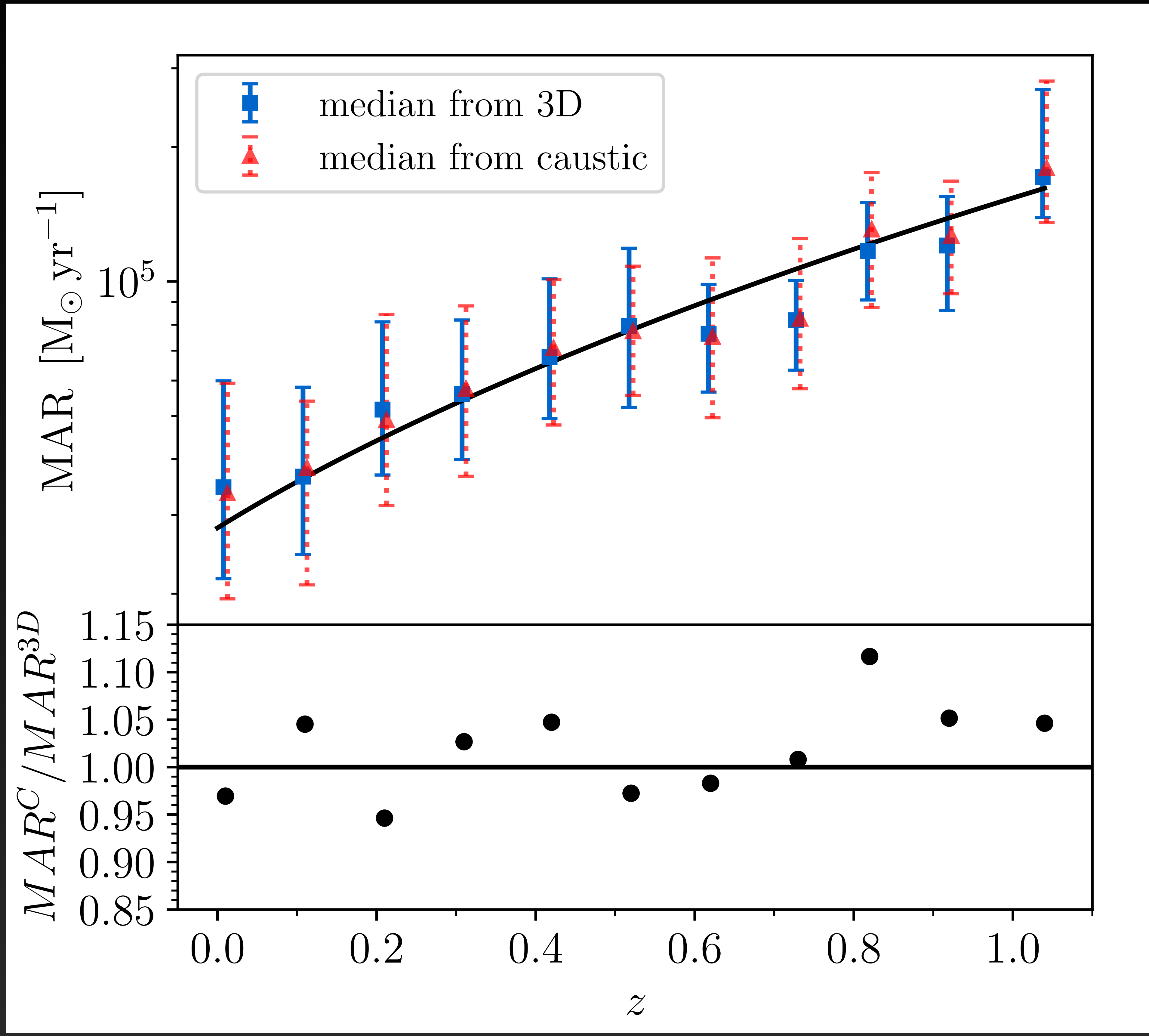

Strong correlation with clusters' mass and redshift

MAR $\sim 10^4 - 10^5 M_\odot$/yr

Caustic MARs agree with true MARs within $\sim 10\,\%$

Comparison with merger trees and observations

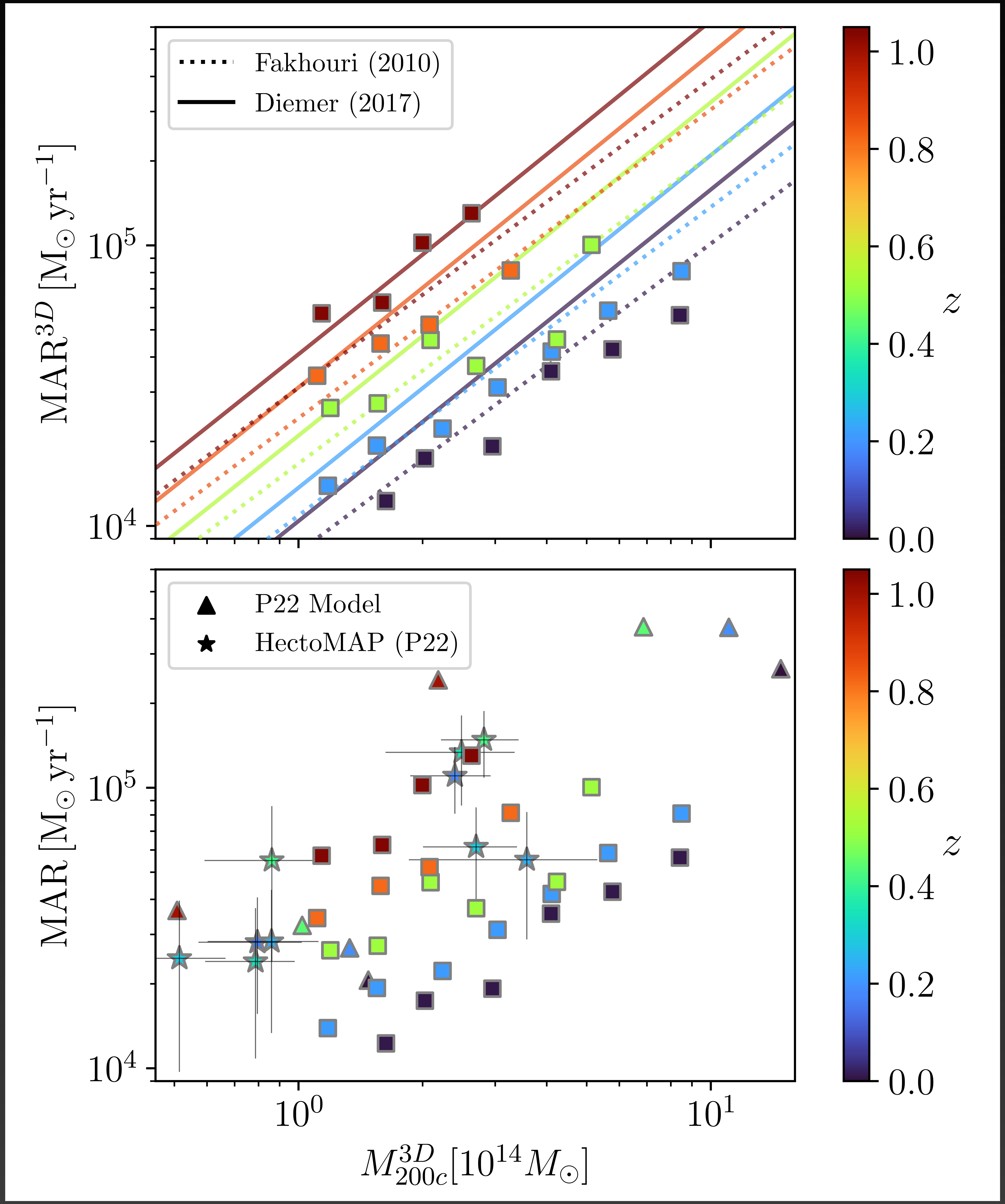

MARs within 1σ from ***merger trees***

MARs in ***agreement with real clusters*** MARs

MAR ***correlates*** with cluster's mass and redshift, MAR $\sim 10^4 - 10^5 \mathrm{M}_\odot/\mathrm{yr}$

(More details in Pizzardo et al. 2023, A&A, 680, A48)

Future prospects

Large samples of clusters with dense spectroscopy up to $\sim 4R_{200c}$ and $z \lesssim 1$ will ***enable measurement of MAR***

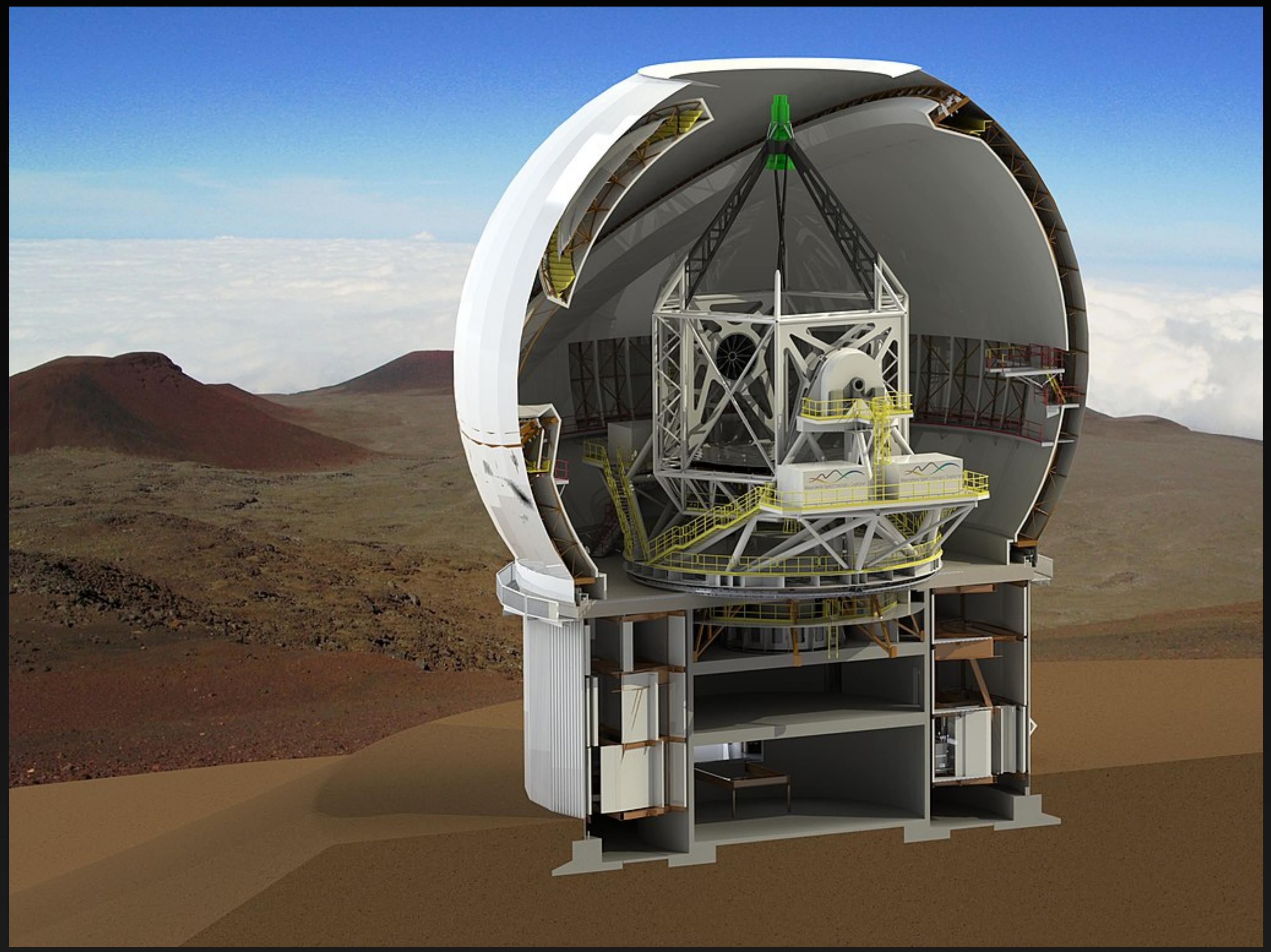

WEAVE on WHT,

MSE on CFHT, and

PFS on Subaru

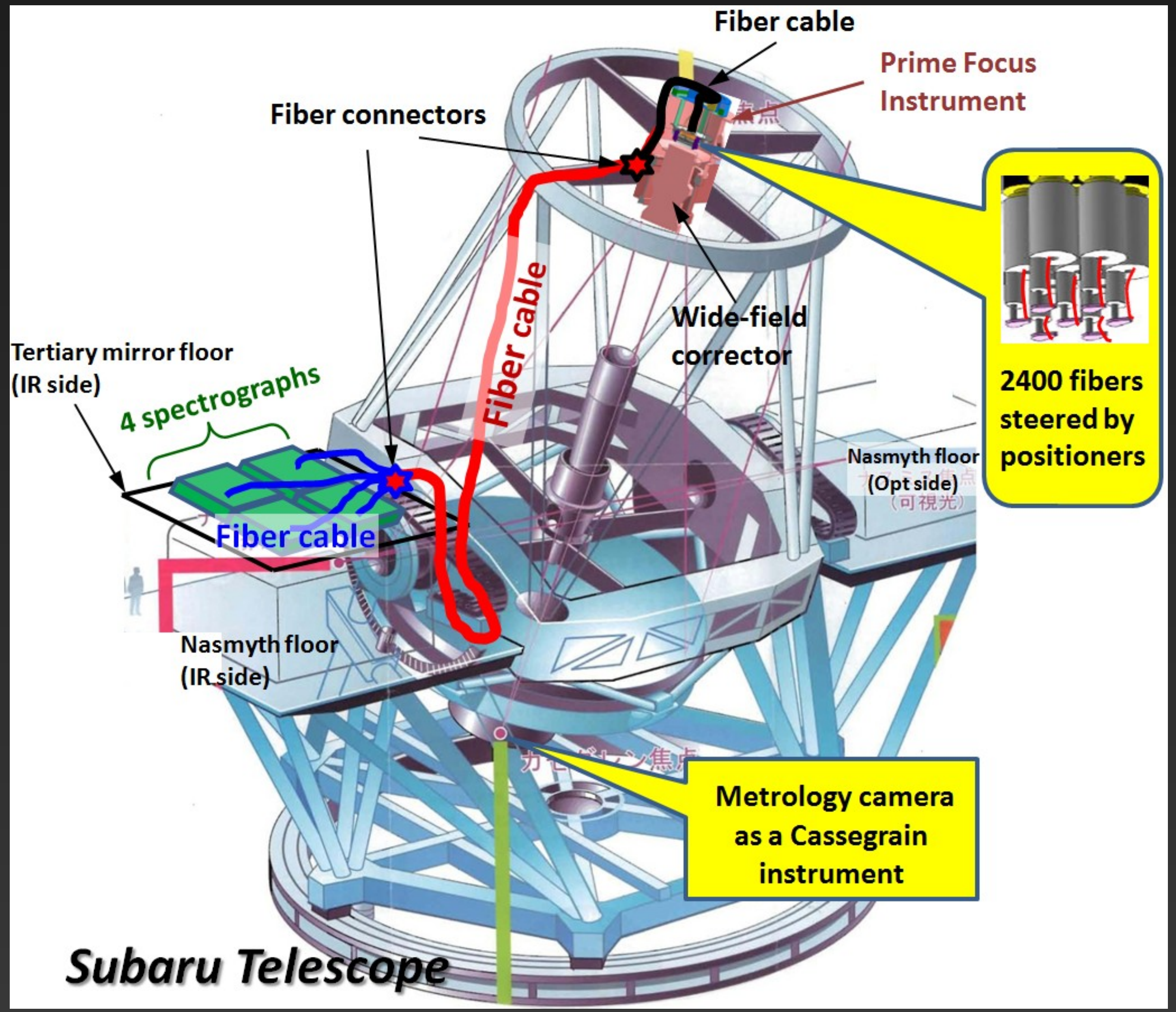

The accretion model

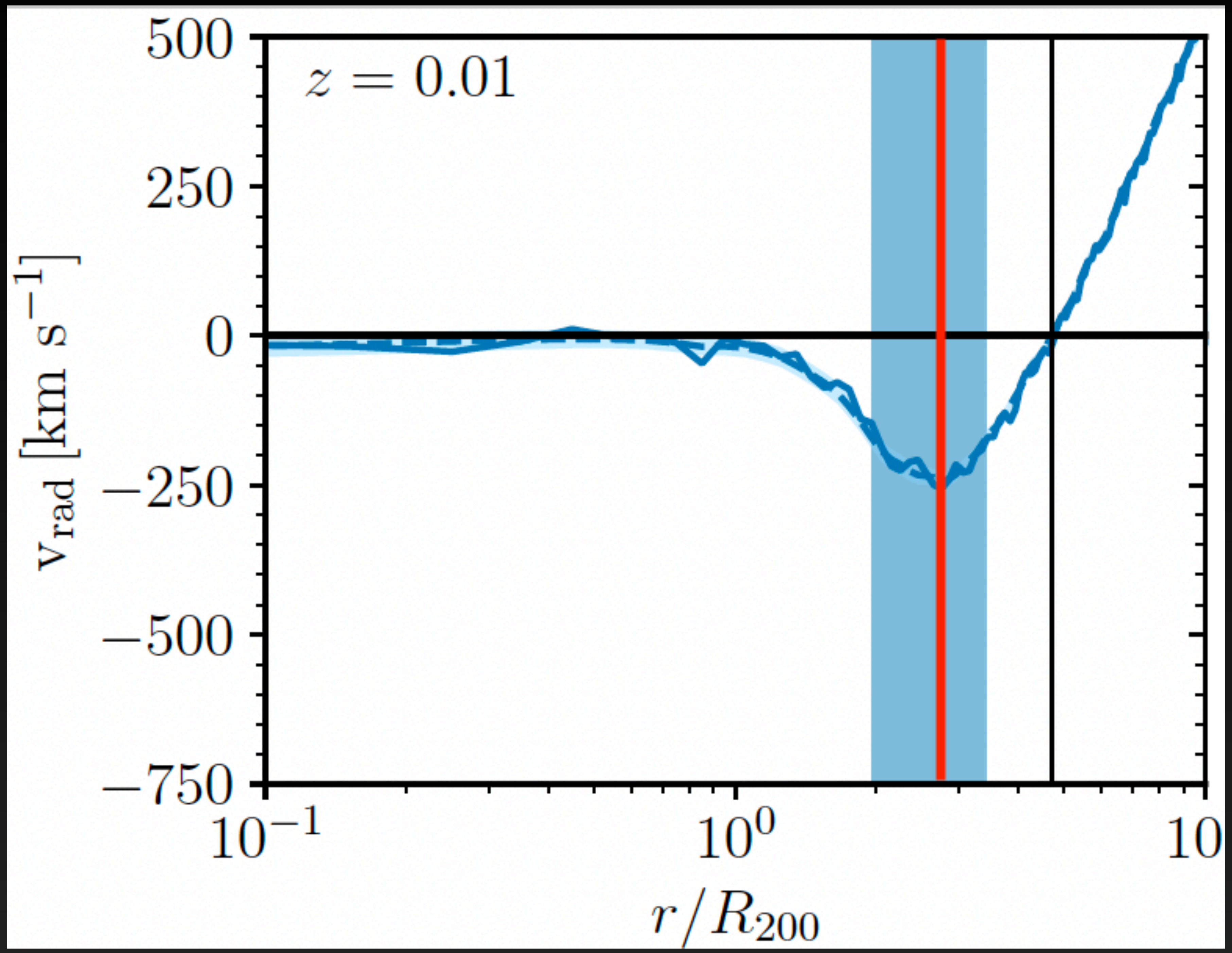

The accretion model

$$\mathrm{MAR_t} = 4\pi\rho(R_{v_{\mathrm{min}}})R^2_{v_{\mathrm{min}}}v_{\mathrm{min}}$$

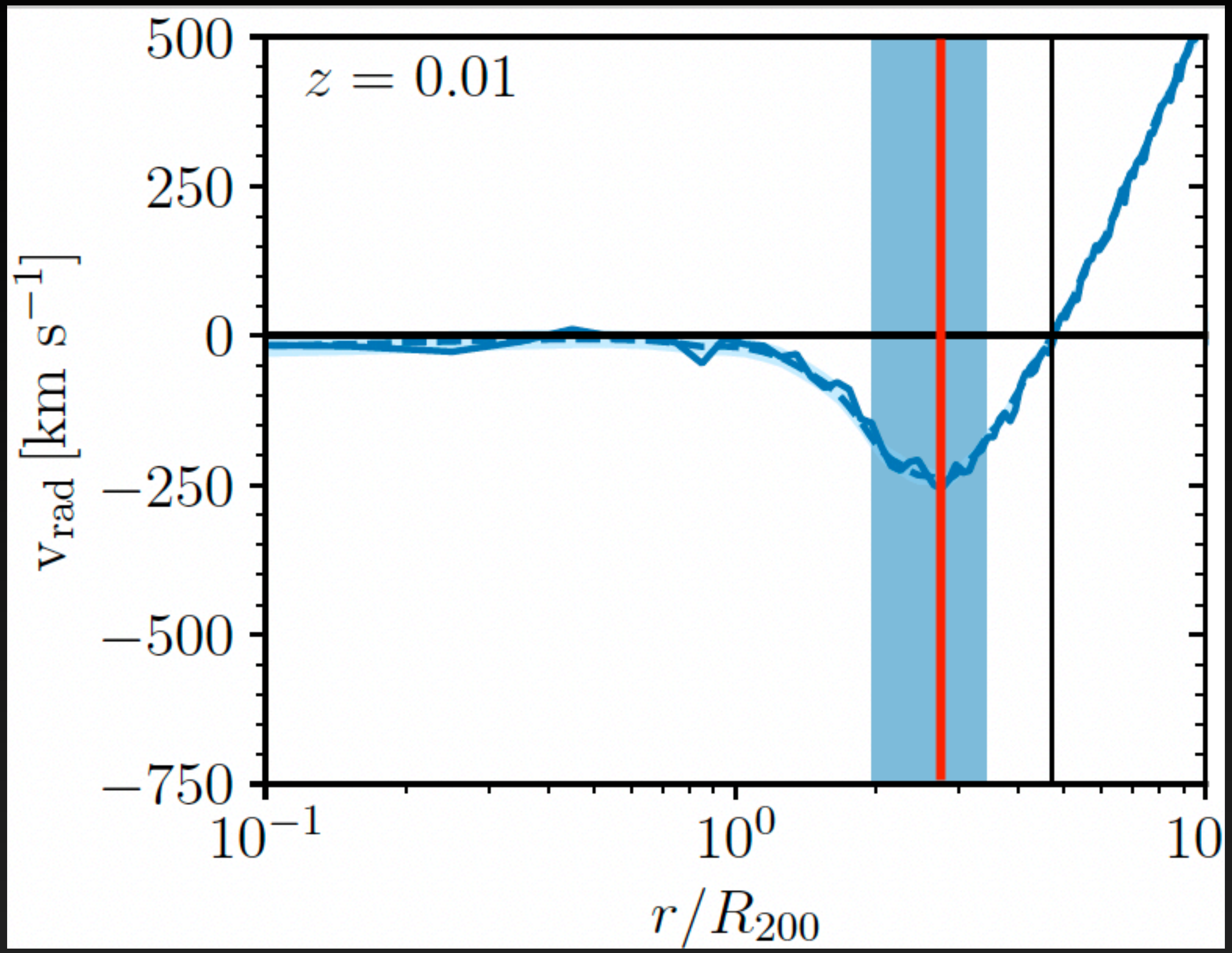

The accretion model

$$\mathrm{MAR}_t = 4\pi\rho(R_{v_{\min}})R^2_{v_{\min}}v_{\min}$$

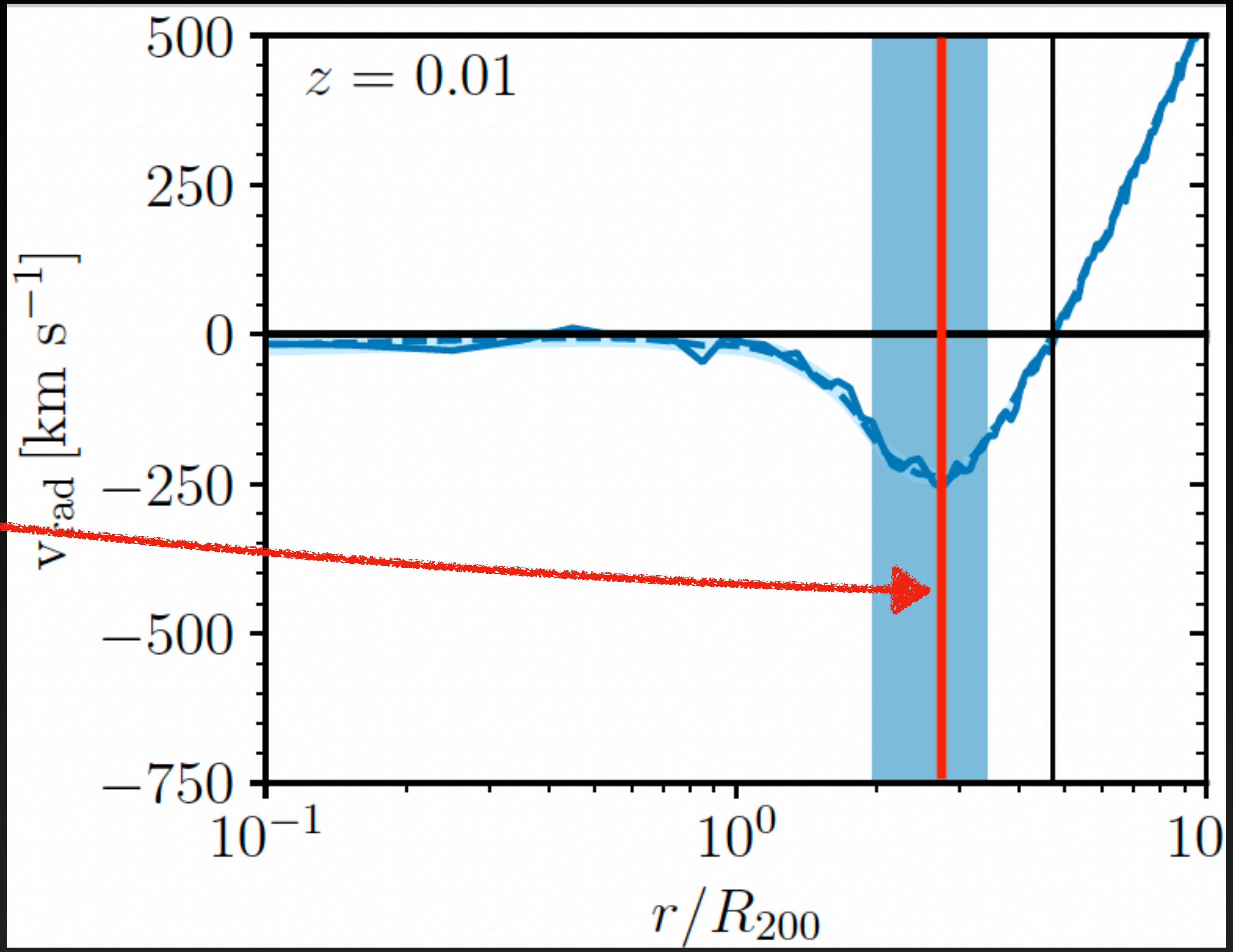

The accretion model

$$\mathrm{MAR}_t = 4\pi\rho(R_{v_{\min}})R^2_{v_{\min}}v_{\min}$$

Not observable!

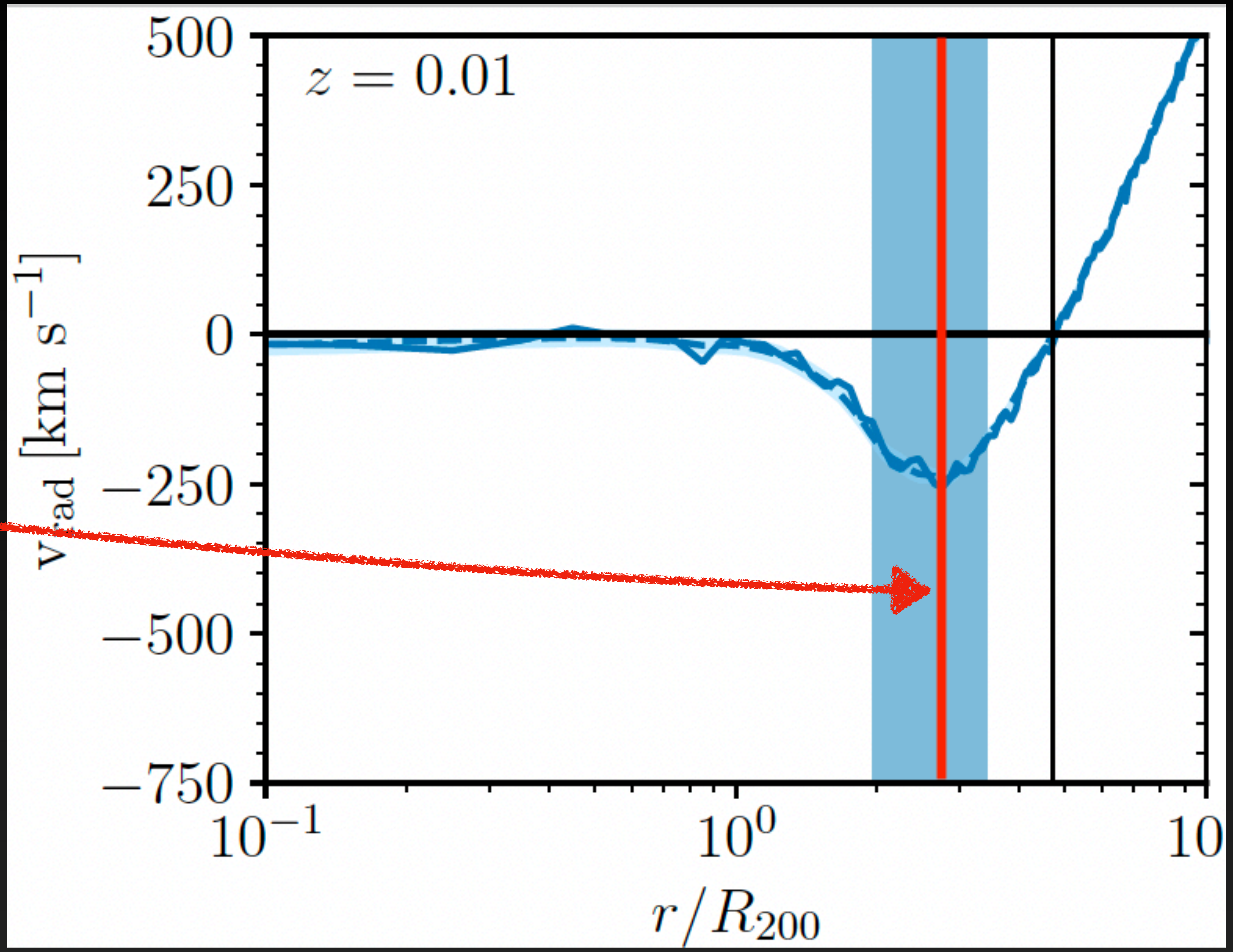

The accretion model

$$\mathrm{MAR_t} = 4\pi\rho(R_{v_{\min}})R^2_{v_{\min}}v_{\min}$$

Not observable!

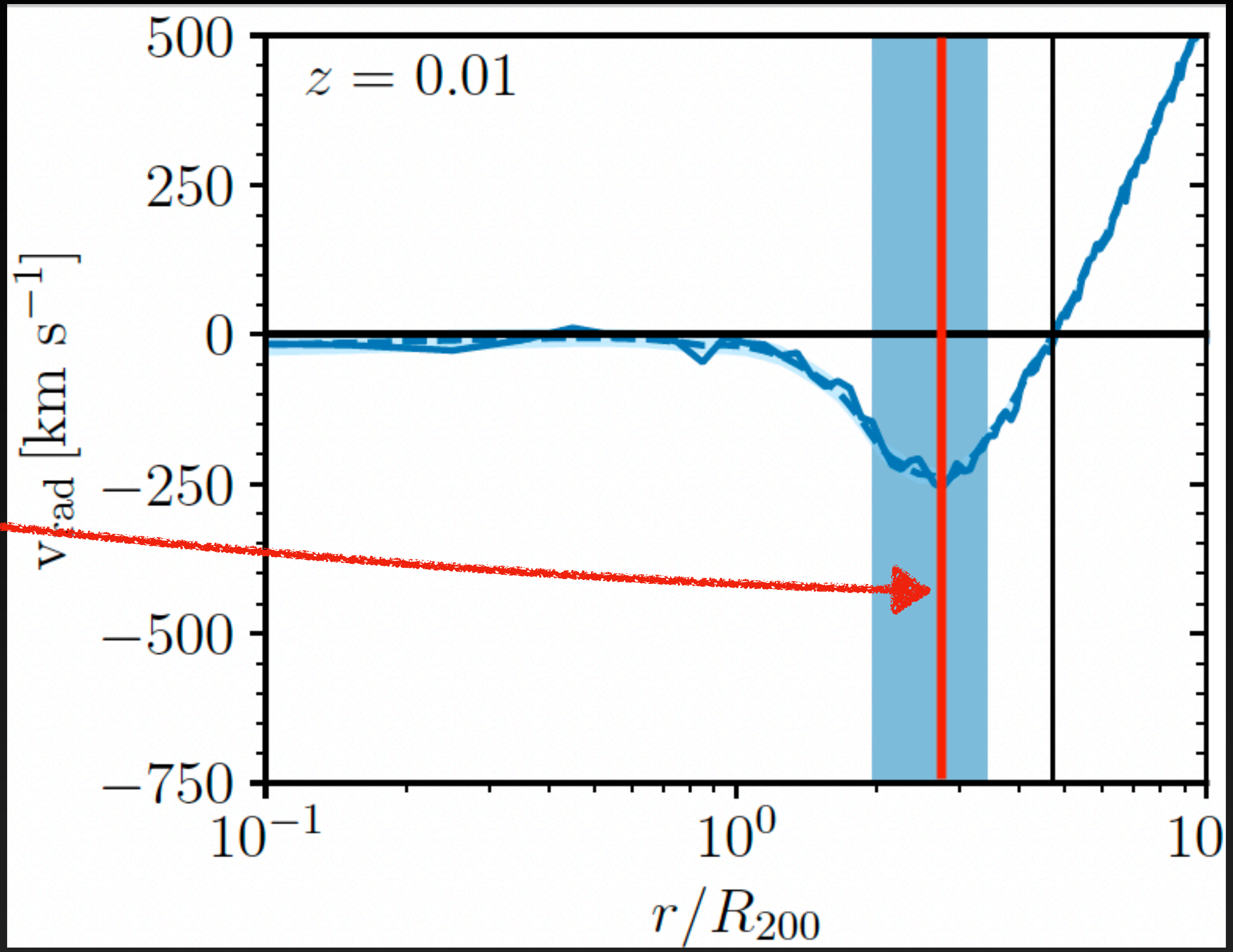

$$\mathrm{MAR} = \mathscr{K}\frac{M_{\rm shell}}{t_{\rm inf}}$$

The accretion model

$$\mathrm{MAR_t} = 4\pi\rho(R_{v_{\min}})R^2_{v_{\min}}\,v_{\min}$$

Not observable!

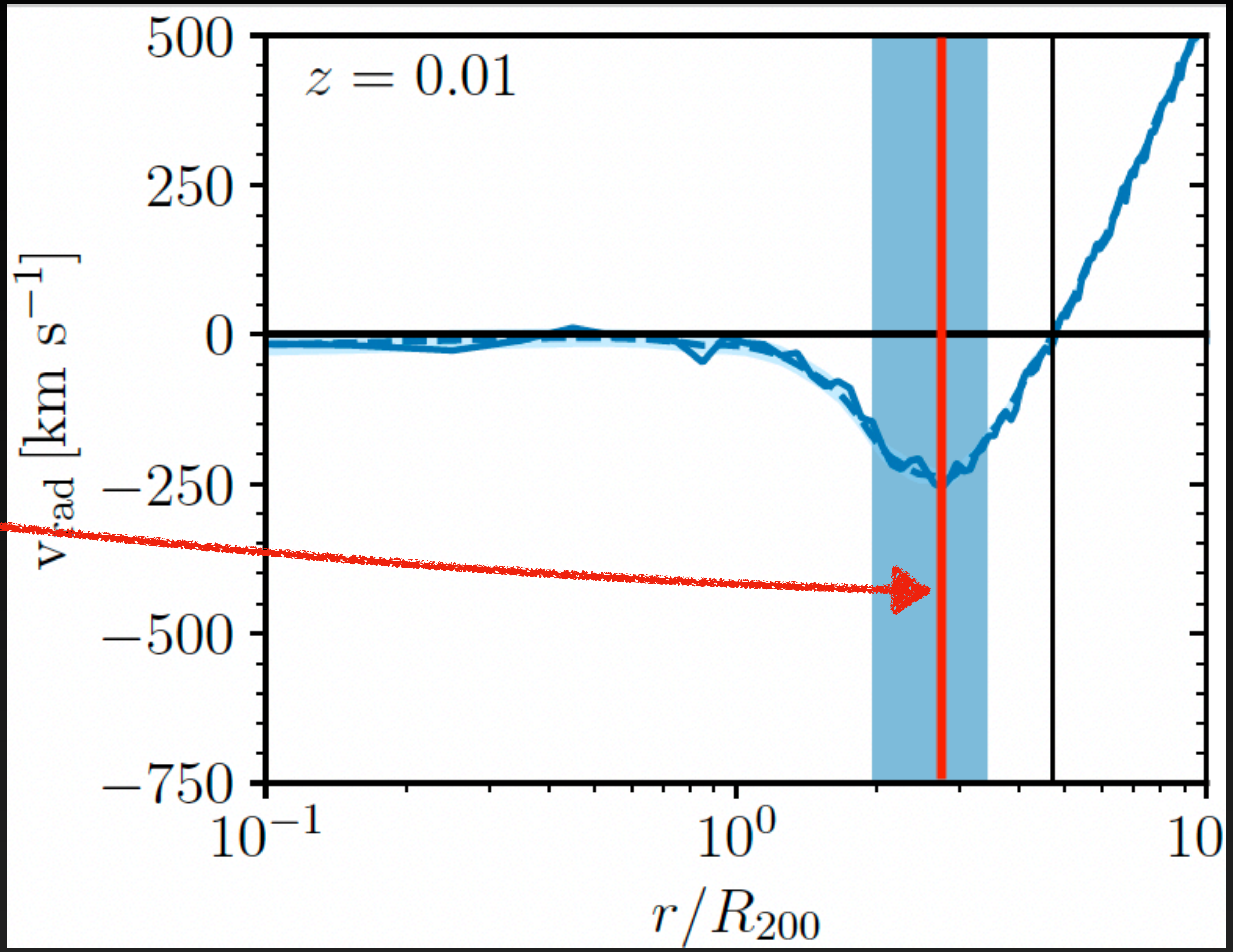

If $\Delta R = \mathrm{d}r$

$$\mathrm{MAR} = \mathscr{K}\frac{M_{\rm shell}}{t_{\rm inf}}$$

The accretion model

$$\mathrm{MAR_t} = 4\pi\rho(R_{v_{\min}})R_{v_{\min}}^2 v_{\min}$$

Not observable!

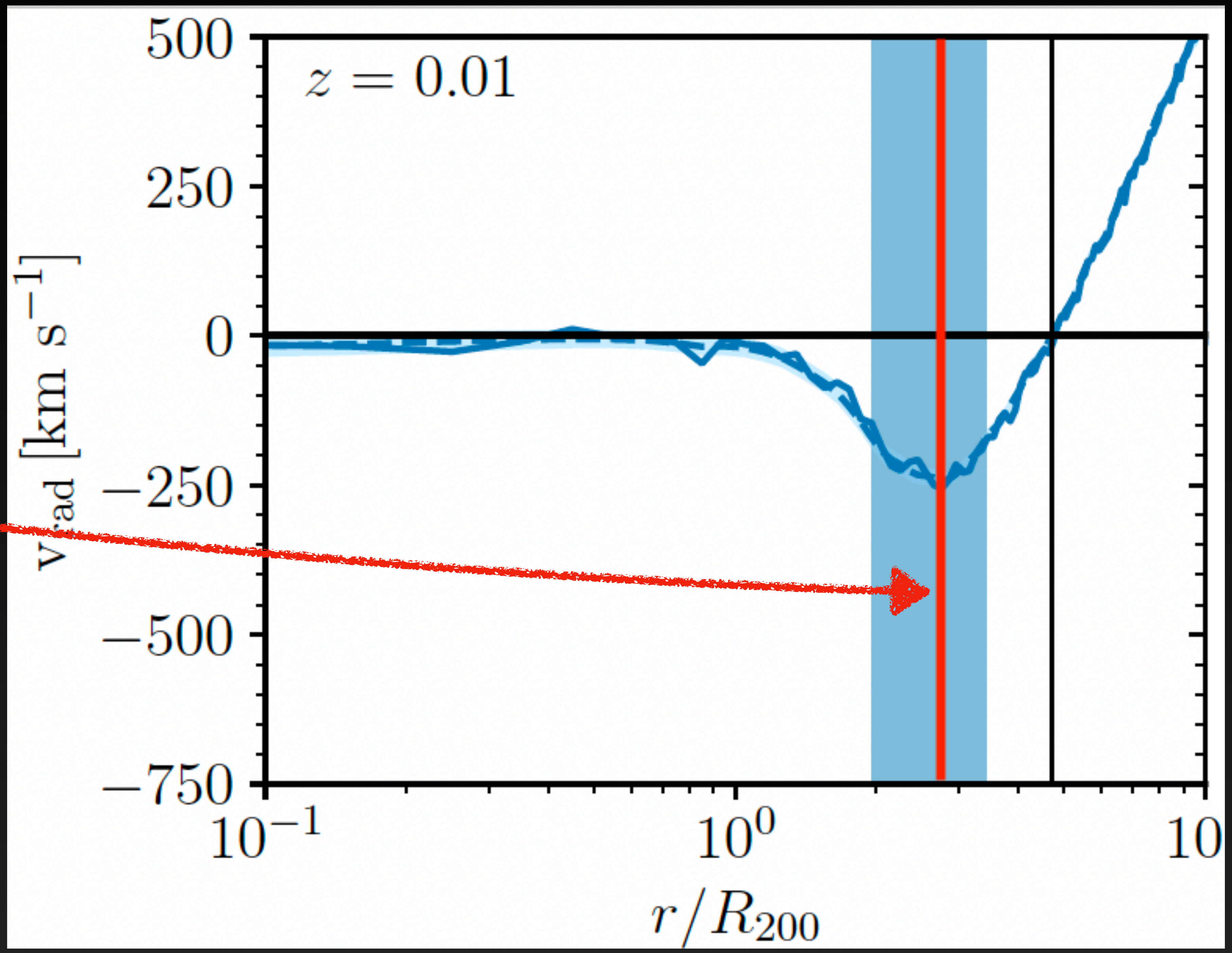

If $\Delta R = \mathrm{d}r$

$$\mathrm{MAR} = \underbrace{\mathcal{K}}_{=1}\frac{M_{\rm shell}}{t_{\rm inf}}$$

The accretion model

$\mathrm{MAR_t} = 4\pi\rho(R_{v_{\min}})R^2_{v_{\min}}\,v_{\min}$

Not observable!

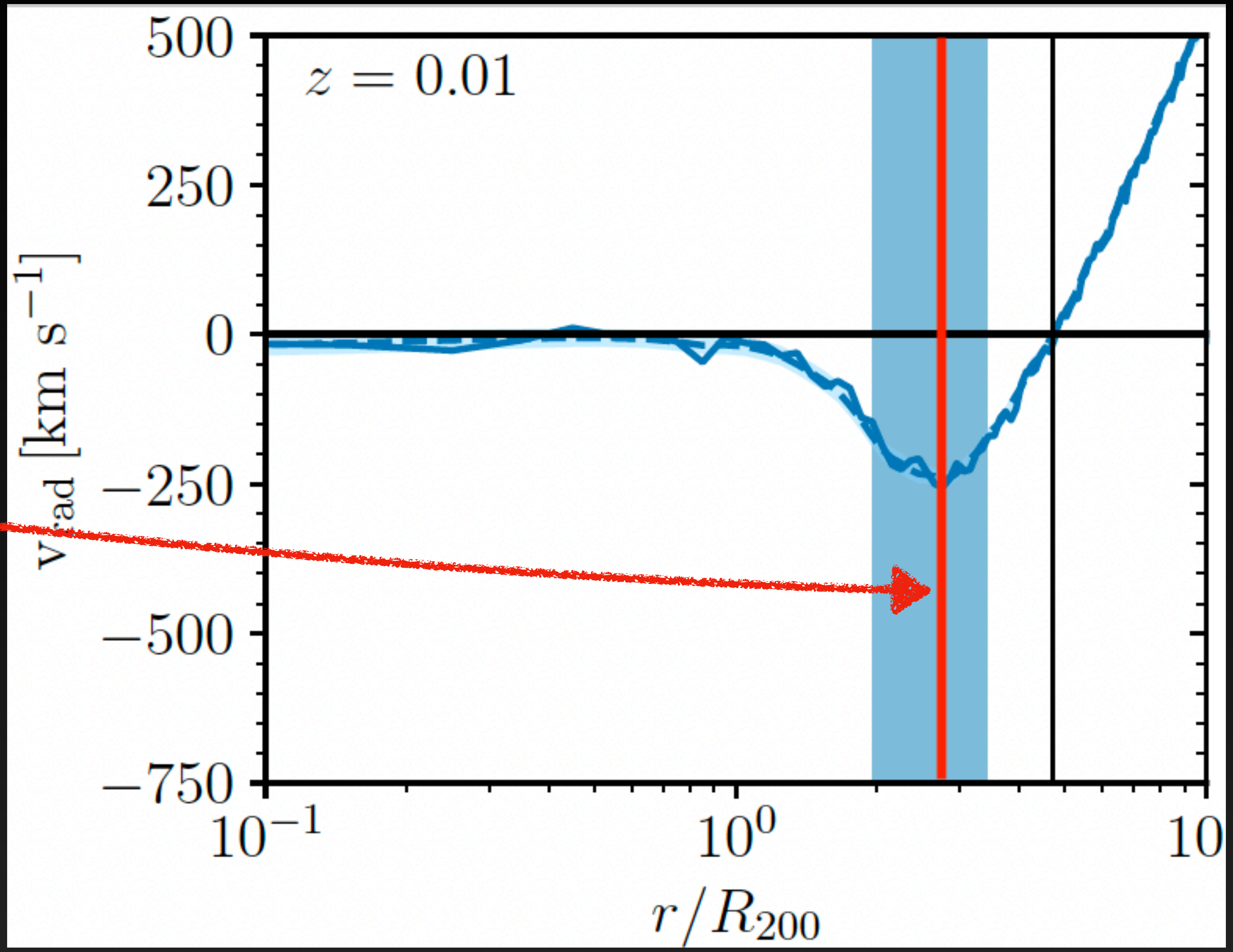

If $\Delta R = \mathrm{d}r$

$$\mathrm{MAR} = \underbrace{\mathscr{K}}_{=1}\,\frac{M_{\mathrm{shell}}}{t_{\mathrm{inf}}}, \quad M_{\mathrm{shell}} = 4\pi\rho(R_{v_{\min}})R^2_{v_{\min}}$$

The accretion model

$\mathrm{MAR_t} = 4\pi\rho(R_{v_{\min}})R^2_{v_{\min}}\, v_{\min}$

Not observable!

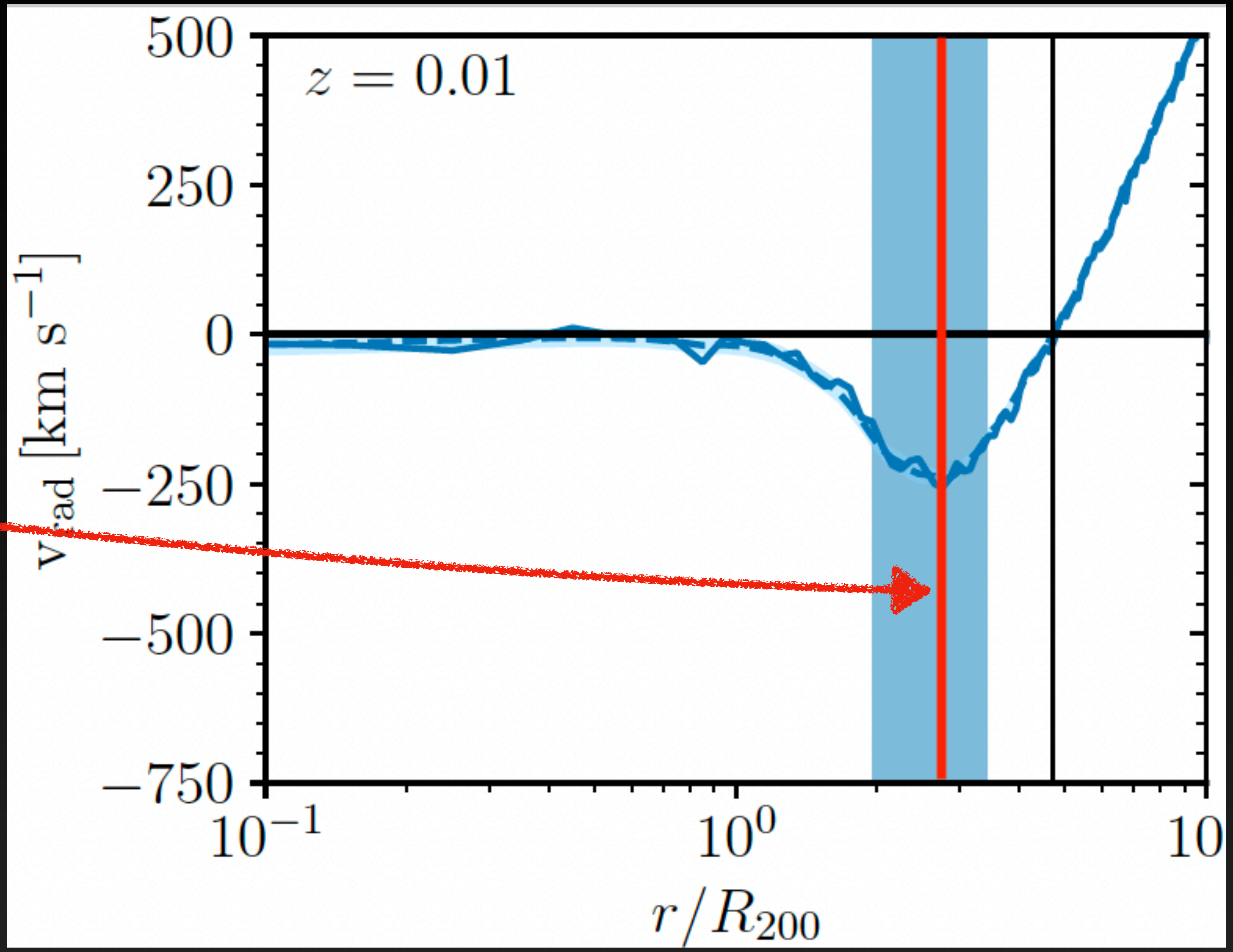

If $\Delta R = \mathrm{d}r$

$$\mathrm{MAR} = \underbrace{\mathcal{K}}_{=1} \frac{\overbrace{M_{\mathrm{shell}}}^{= 4\pi\rho(R_{v_{\min}})R^2_{v_{\min}}}}{\underbrace{t_{\mathrm{inf}}}_{= \mathrm{d}r/v_{\min}}}$$

The accretion model

$\mathrm{MAR_t} = 4\pi\rho(R_{v_{\min}})R^2_{v_{\min}}\, v_{\min}$

Not observable!

If $\Delta R = \mathrm{d}r$ $\quad = \quad$

$$\mathrm{MAR} = \underbrace{\mathscr{K}}_{=1}\, \frac{\overbrace{M_{\mathrm{shell}}}^{= 4\pi\rho(R_{v_{\min}})R^2_{v_{\min}}}}{\underbrace{t_{\mathrm{inf}}}_{= \mathrm{d}r/v_{\min}}}$$

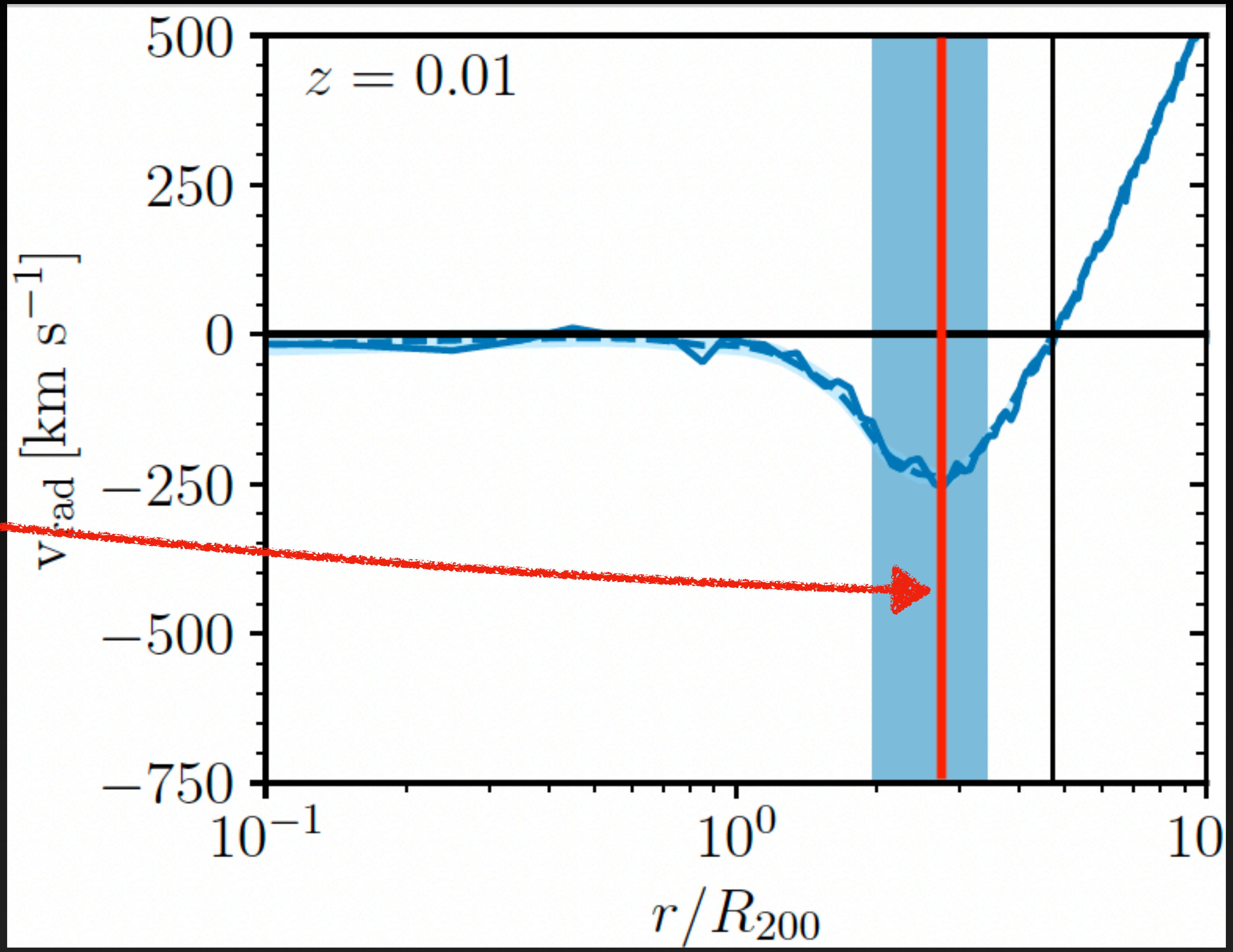

The accretion model

$$\mathrm{MAR_t} = 4\pi\rho(R_{v_{\min}})R^2_{v_{\min}}v_{\min}$$

Not observable!

If $\Delta R = \mathrm{d}r$ $=$

$$\mathrm{MAR} = \mathscr{K}\frac{M_{\mathrm{shell}}}{t_{\mathrm{inf}}}$$

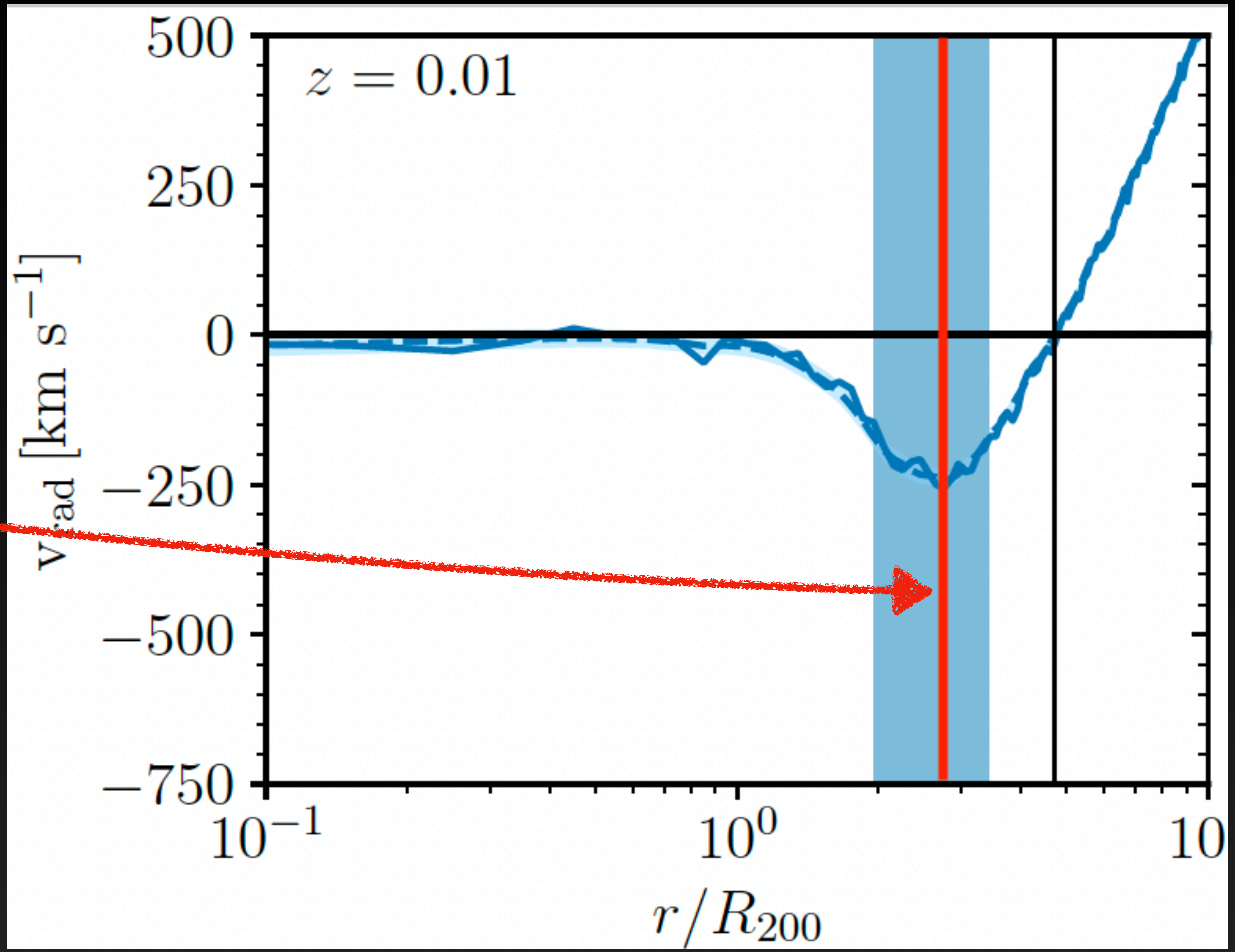

The accretion model

$\mathrm{MAR_t} = 4\pi\rho(R_{v_{\min}})R^2_{v_{\min}}v_{\min}$

Not observable!

If $\Delta R = \mathrm{d}r$

$$\mathrm{MAR} = \mathscr{K}\frac{M_{\mathrm{shell}}}{t_{\mathrm{inf}}}$$

MAR suitable for observations

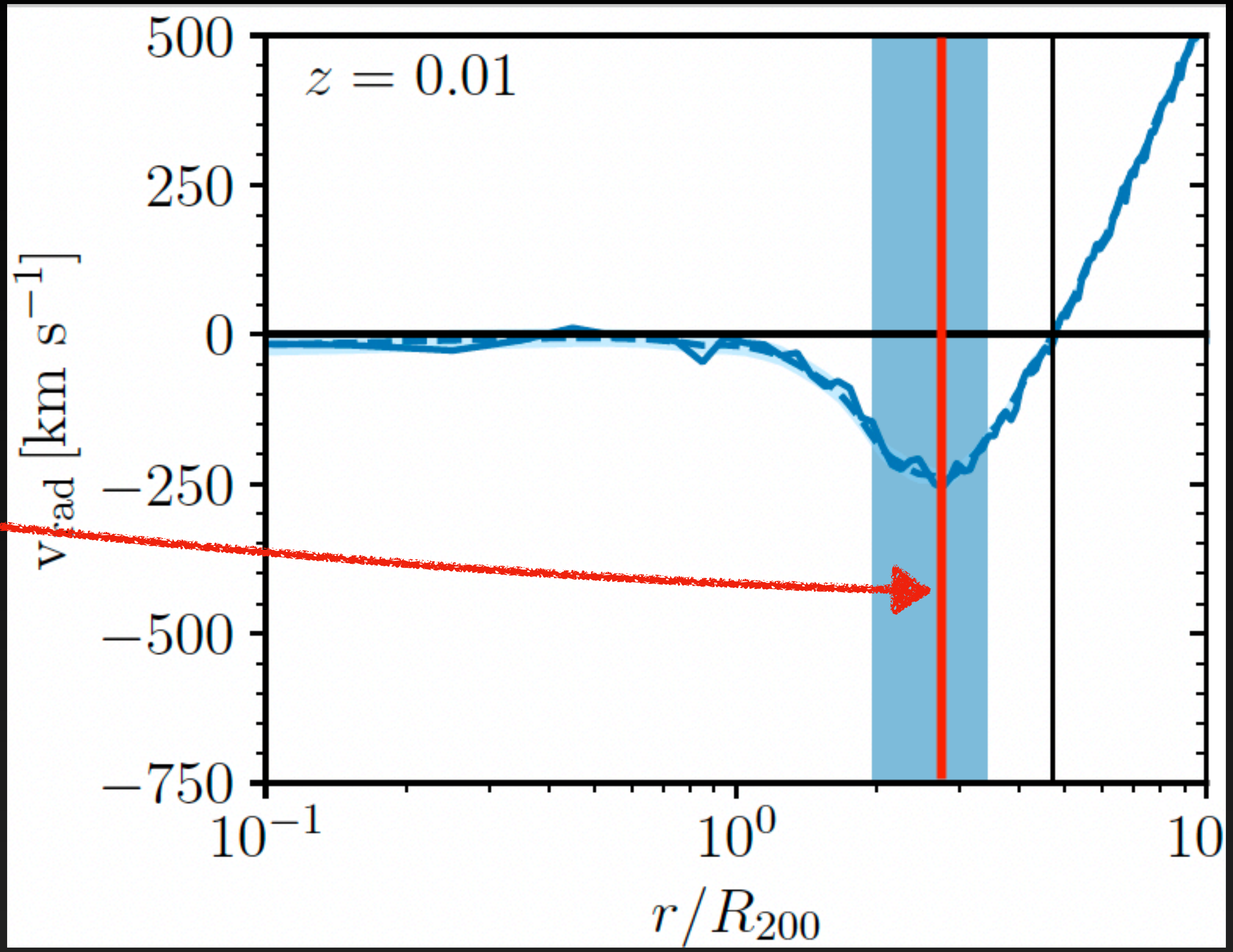

The accretion model

$$\mathrm{MAR_t} = 4\pi\rho(R_{v_\mathrm{min}})R^2_{v_\mathrm{min}}\,v_\mathrm{min}$$

Not observable!

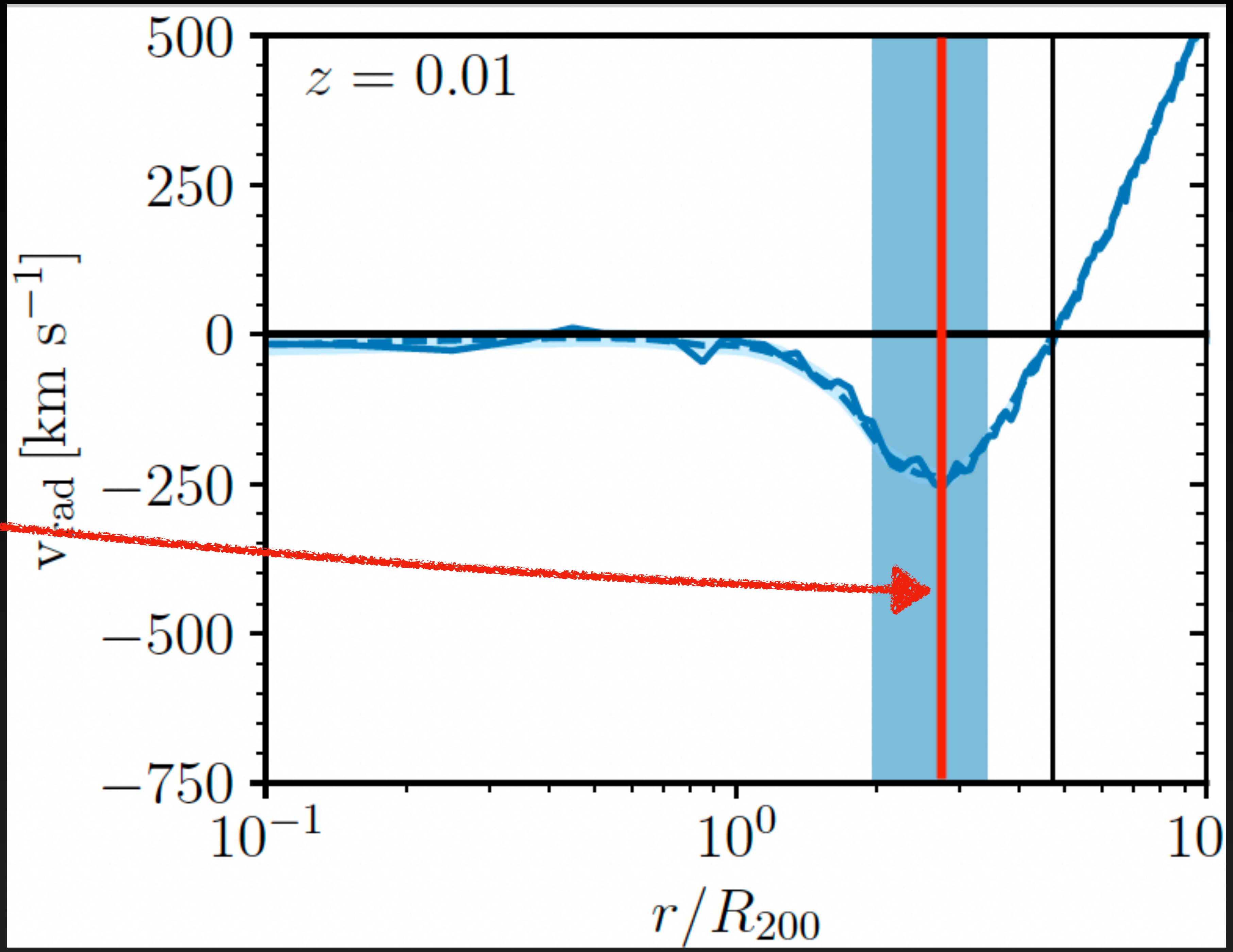

If $\Delta R = \mathrm{d}r$ $=$

$$\mathrm{MAR} = \mathscr{K}\frac{M_\mathrm{shell}}{t_\mathrm{inf}}$$

MAR suitable for observations

M_shell set to ***optimize*** observed versus true $M(r)$

The accretion model

$\mathrm{MAR}_{\mathrm{t}} = 4\pi\rho(R_{v_{\mathrm{min}}})R^2_{v_{\mathrm{min}}}v_{\mathrm{min}}$

Not observable!

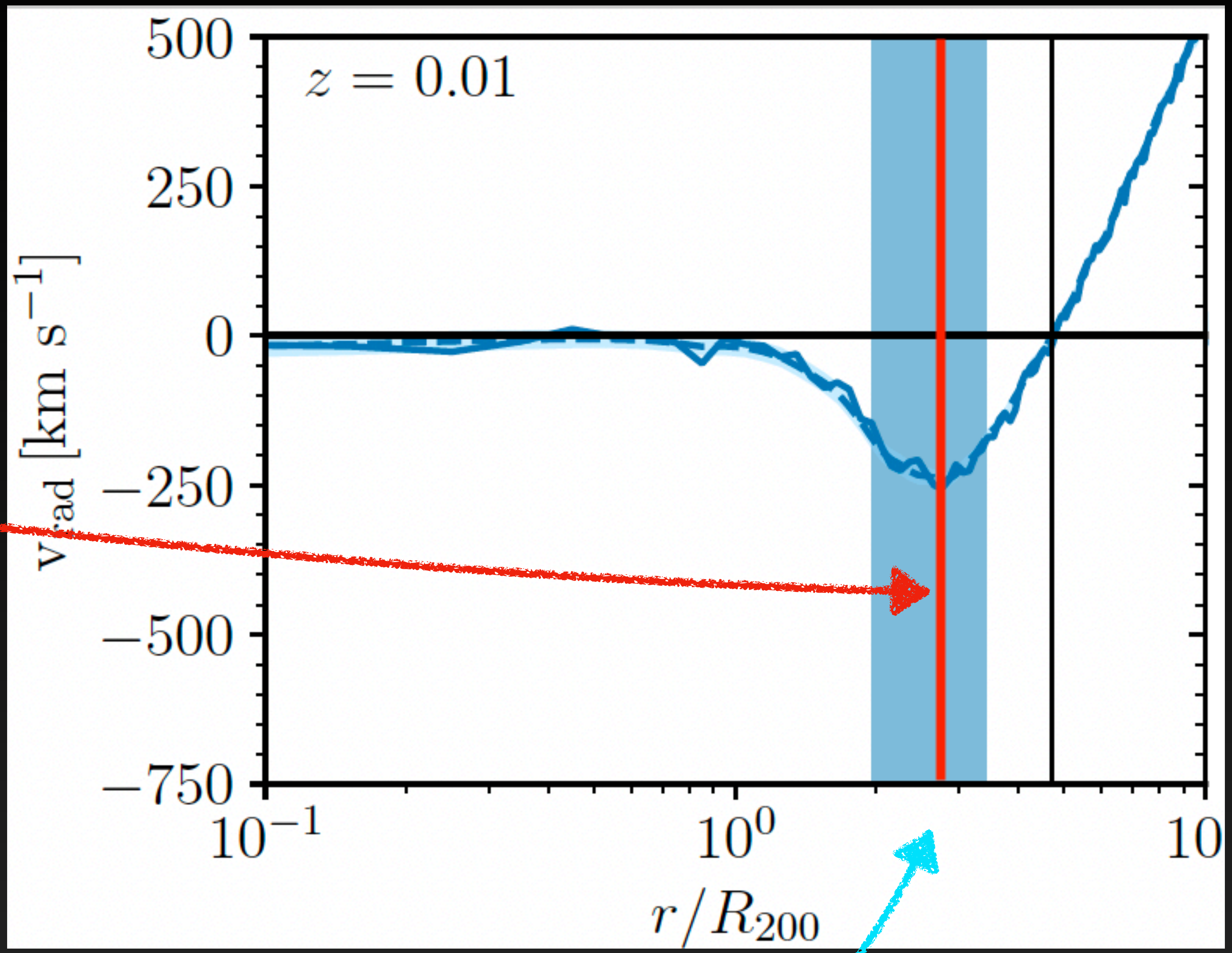

If $\Delta R = \mathrm{d}r$ $=$

$$\mathrm{MAR} = \mathscr{K}\frac{M_{\mathrm{shell}}}{t_{\mathrm{inf}}}$$

MAR suitable for observations

fraction of v_{min}

M_{shell} set to ***optimize*** observed versus true $M(r)$

The accretion model

$\mathrm{MAR_t} = 4\pi\rho(R_{v_{\min}})R^2_{v_{\min}}v_{\min}$

Not observable!

If $\Delta R = \mathrm{d}r$ $=$

$$\mathrm{MAR} = \mathscr{K}\frac{M_{\mathrm{shell}}}{t_{\mathrm{inf}}}$$

MAR suitable for observations

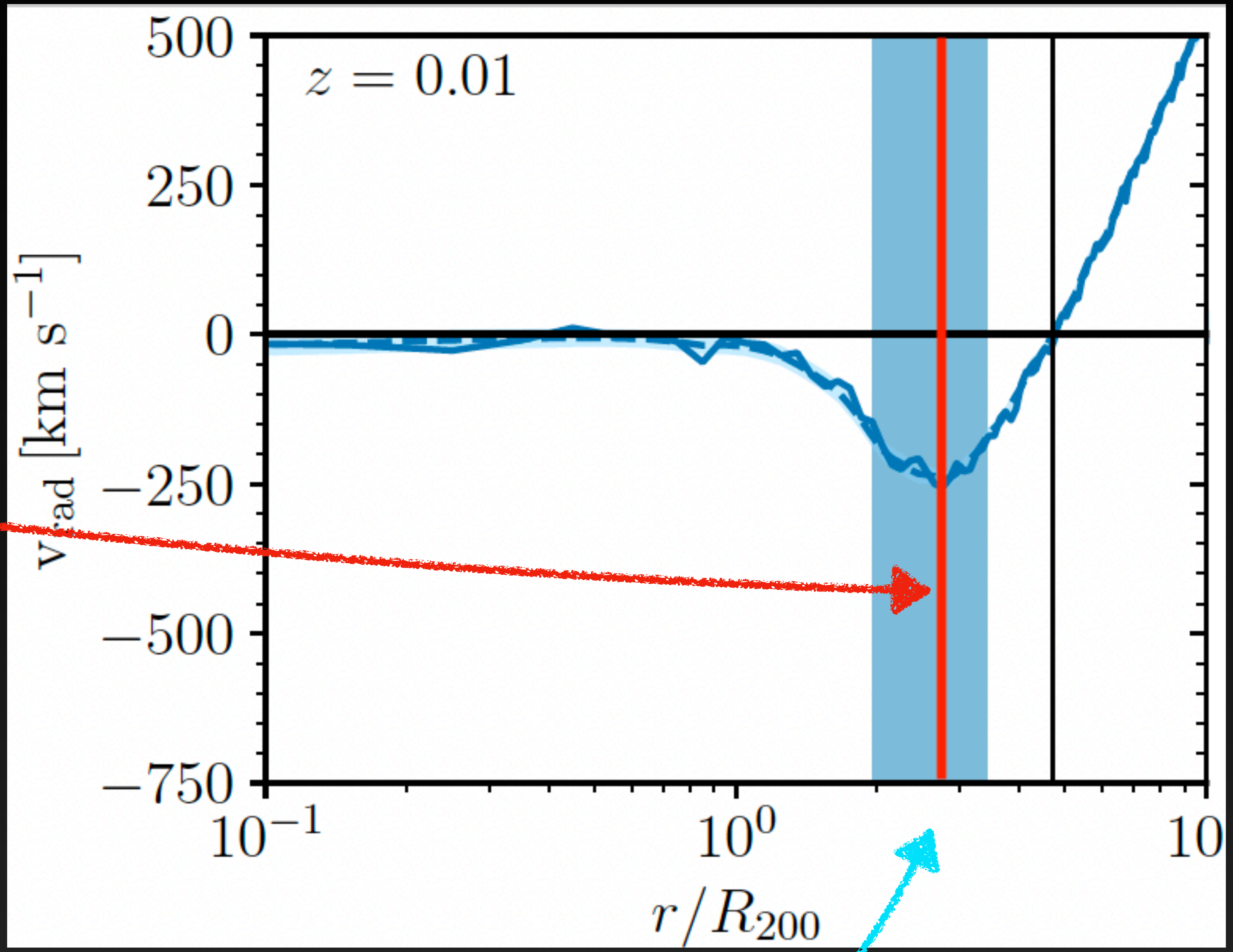

fraction of $v_{\min}$

M_{shell} set to ***optimize*** observed versus true $M(r)$

t_{inf} from linear motion with non-constant acceleration

The accretion model

$\mathrm{MAR_t} = 4\pi\rho(R_{v_{\min}})R^2_{v_{\min}}v_{\min}$

Not observable!

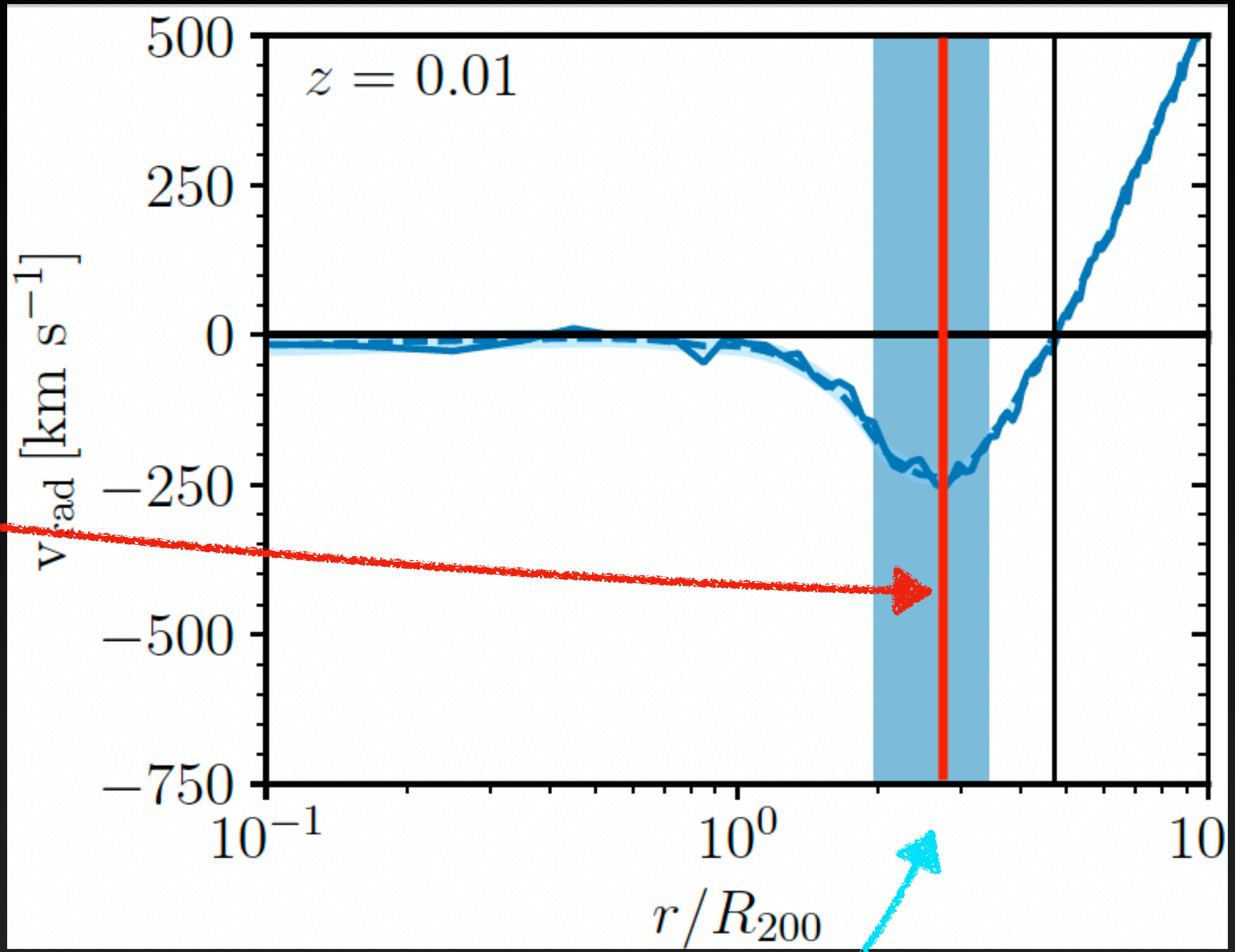

If $\Delta R = \mathrm{d}r$ $=$

$$\mathrm{MAR} = \mathscr{K}\frac{M_{\mathrm{shell}}}{t_{\mathrm{inf}}}$$

MAR suitable for observations

fraction of $v_{\min}$

M_{shell} set to ***optimize*** observed versus true $M(r)$

t_{inf} from linear motion with non-constant acceleration

$\mathscr{K} \neq 1$ links MAR to $\mathrm{MAR_t}$

Infall time: correlation with cluster redshift

Fixed cluster mass

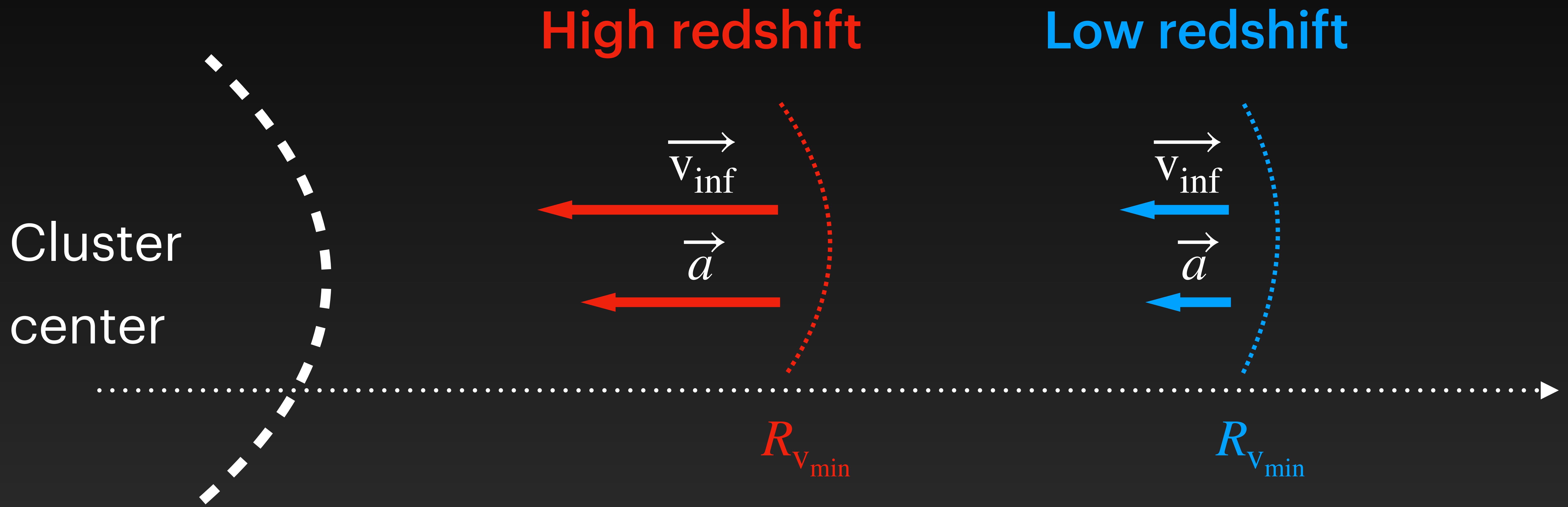

$$t_{\mathrm{inf}} = \sum_n \Delta t_n$$

$$\Delta t_n = \frac{-\mathrm{v}_{\mathrm{inf}} - \sqrt{\mathrm{v}_{\mathrm{inf}}{}^2 - 2a_n\Delta r}}{a_n}$$

- $\Delta t_n < \Delta t_n$
- Lower cluster-centric distance

$$t_{\mathrm{inf}} < t_{\mathrm{inf}}$$

Infall time: cluster mass

Fixed cluster redshift

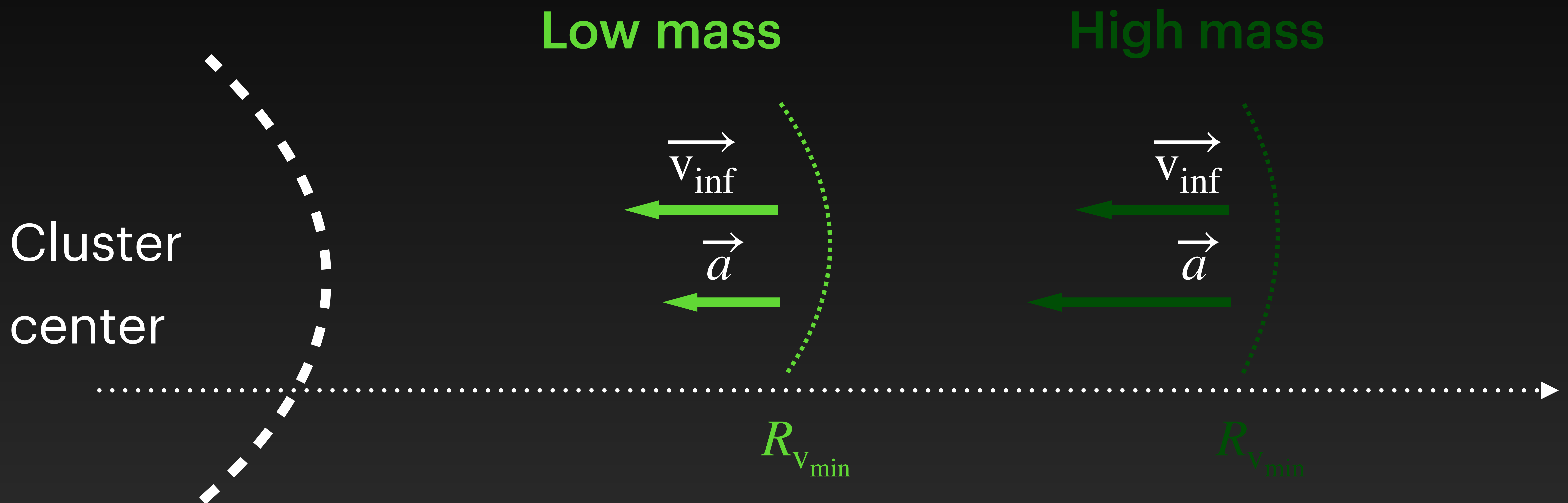

$$t_{inf} = \sum_n \Delta t_n$$

$$\Delta t_n = \frac{-v_{inf} - \sqrt{{v_{inf}}^2 - 2a_n \Delta r}}{a_n}$$

High-mass clusters: deeper gravitational potential, but more extended infall region

No correlation with mass

Infalling shell: cluster redshift

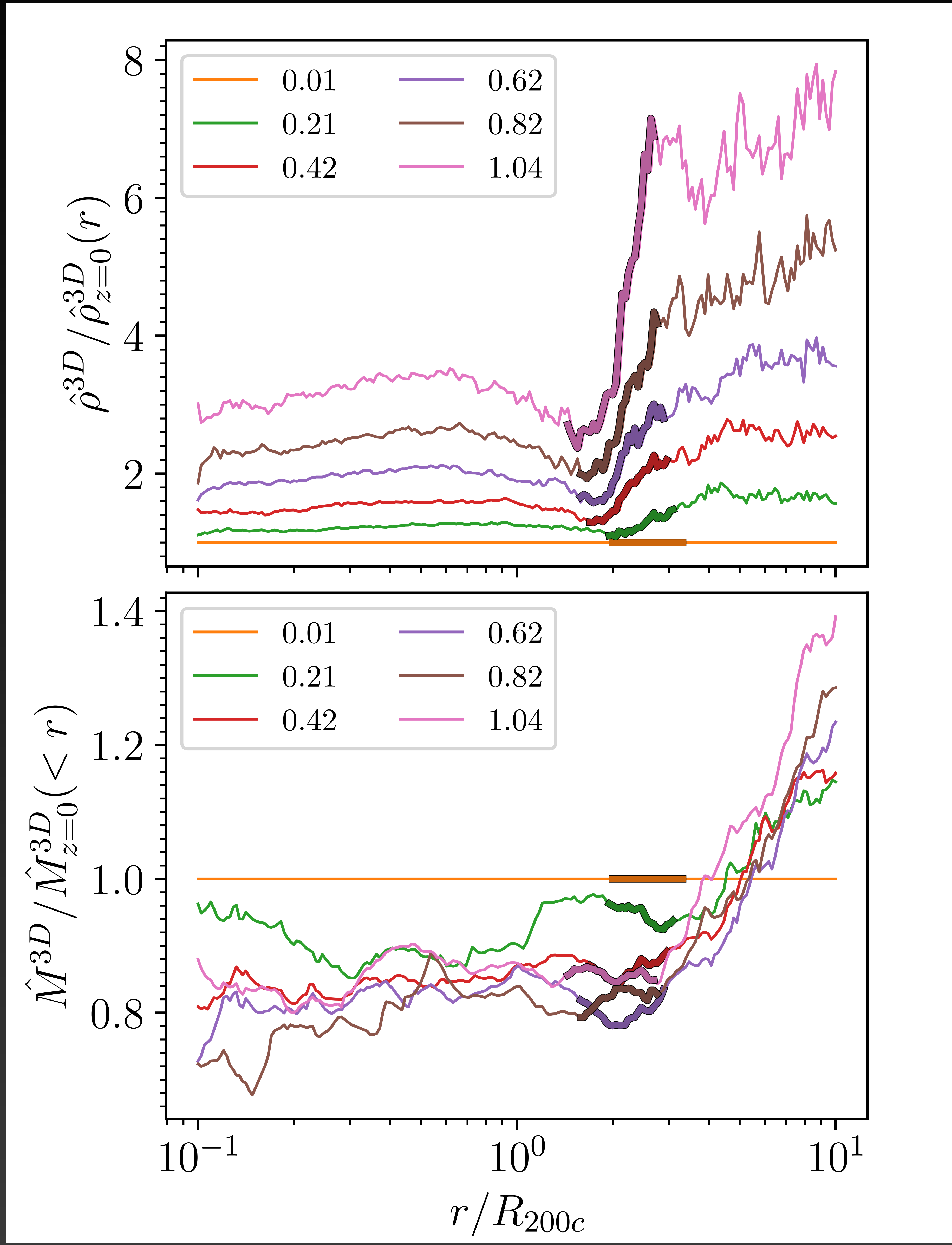

Clusters are denser at higher redshifts, but:

- Physical volume of the shell decreases with increasing redshift
- Mass distributions slightly change with redshift

Weak correlation between shell mass and redshift

Galaxy and Dark Matter based radii

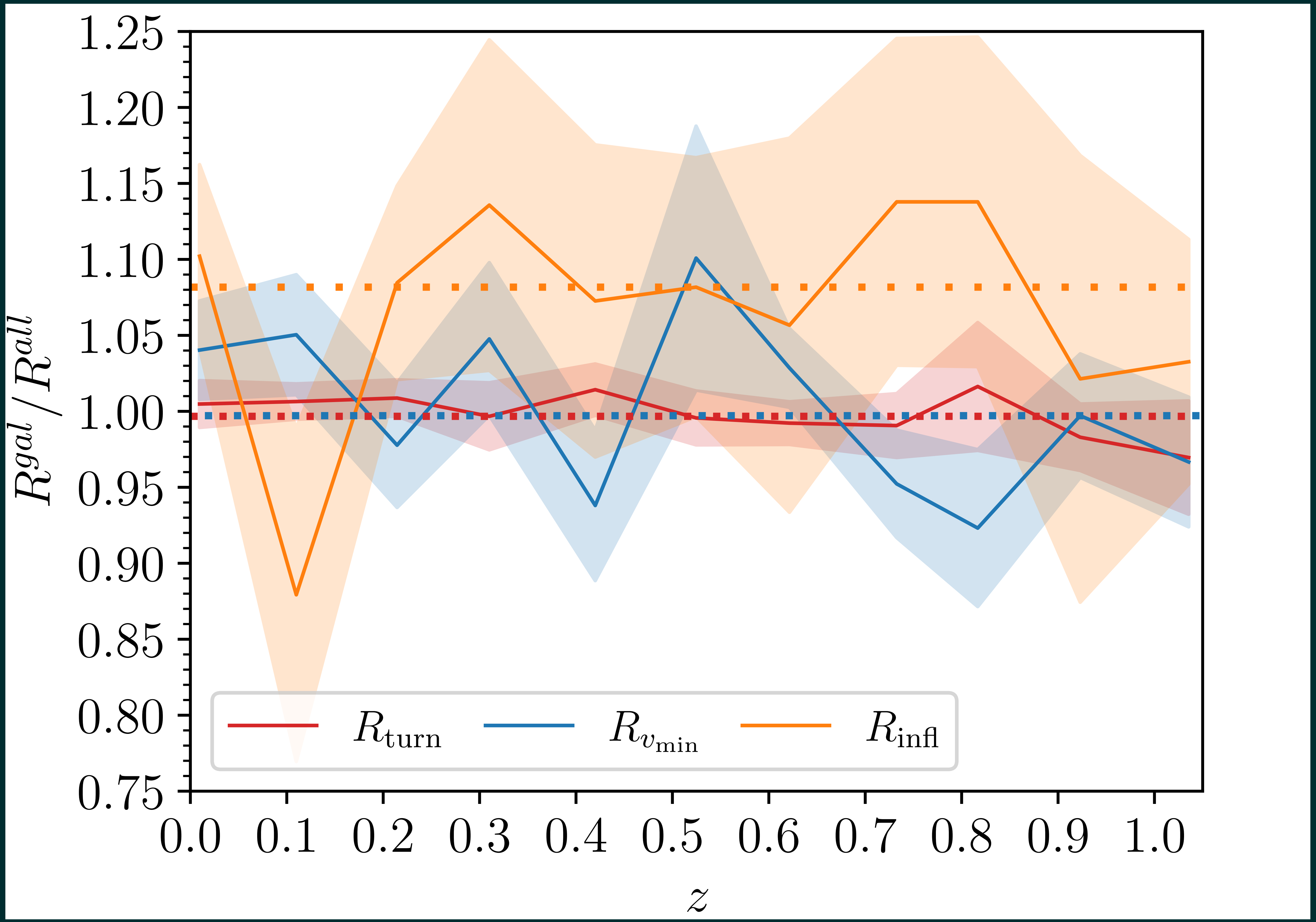

- Small, positive bias between $R_{\mathrm{V_{rad}}}$ from galaxies and total matter
- Consistent with analogous results for R_{spl} *(O'Neil et al. 2021)*
- $R_{v_{\mathrm{min}}}$ and R_{turn} are unbiased

Galaxy and Dark Matter based radii

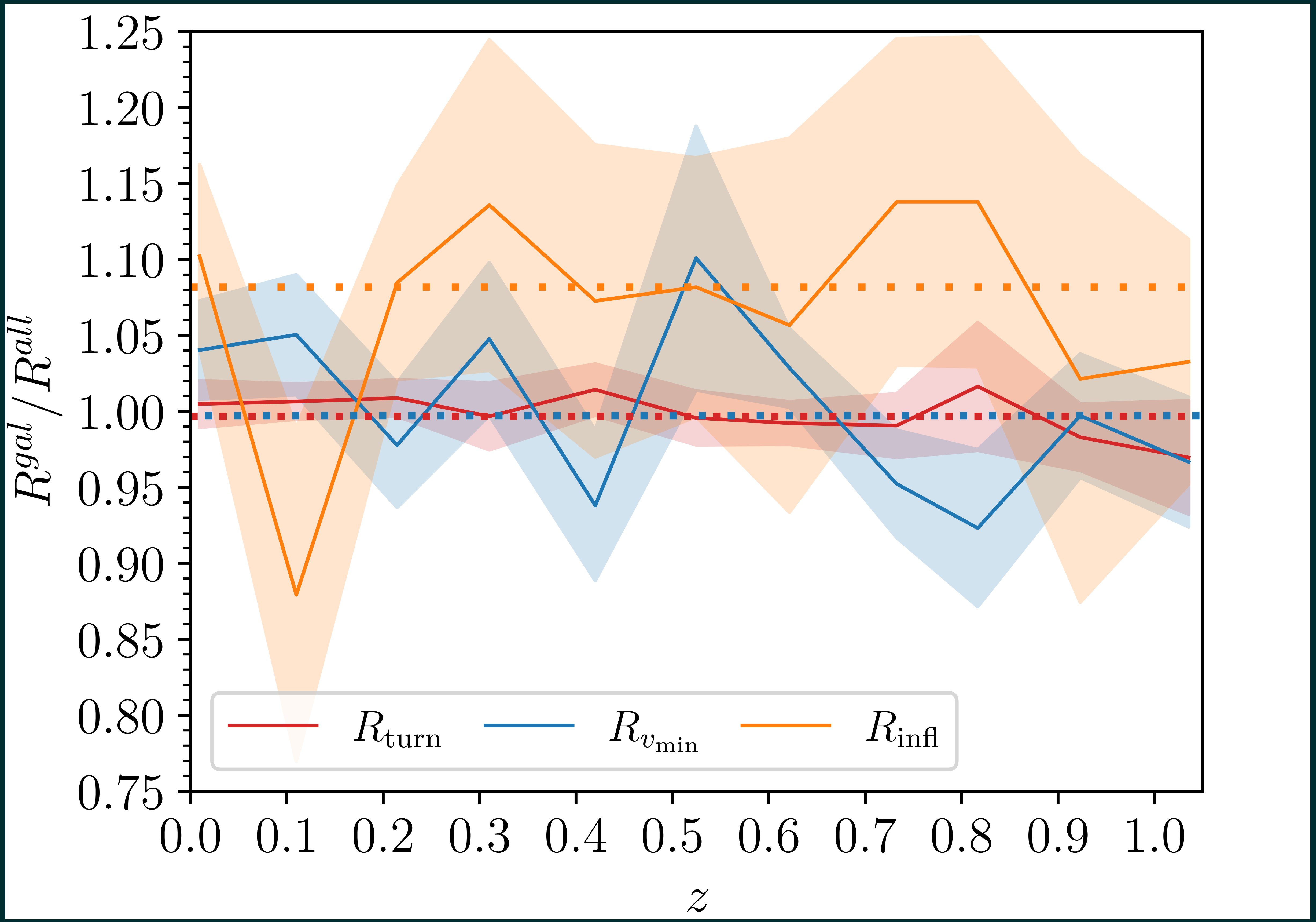

- Small, positive bias between $R_{\mathrm{V_{rad}}}$ from galaxies and total matter
- Consistent with analogous results for R_{spl} *(O'Neil et al. 2021)*
- $R_{v_{\mathrm{min}}}$ and R_{turn} are unbiased